Study on the Profile of Sulfated Glycosaminoglycans, Chondroitin Sulfate/Dermatan Sulfate, in 3T3-L1 Adipocyte Differentiation: Chondroitin Sulfate Potential on Adipogenesis Inhibition

（3T3-L1 脂肪前駆細胞の分化における硫酸化グリコサミノグリカン（コンドロイチン硫酸 / デルマタン硫酸）のプロファイルに関する研究：脂肪細胞分化抑制におけるコンドロイチン硫酸の可能性）

2024

Joint Graduate School of Veterinary Sciences

Tottori University

Danang Dwi Cahyadi

Contents

List of Abbreviations

Actb	beta-actin
ΔHexA	4,5-unsaturated hexuronic acid
APC	adipocyte progenitor cell
B2m	beta 2 microglobulin
Bs-CS	blue shark-derived chondroitin sulfate
C/EBPα	CCATT/enhancer binding protein alpha
C/EBPβ	CCATT/enhancer binding protein beta
C/EBPδ	CCATT/enhancer binding protein delta
C/EBPγ	CCATT/enhancer binding protein gamma
C4ST-1	chondroitin 4-*O*-sulfotransferase 1
C4ST-2	chondroitin 4-*O*-sulfotransferase 2
C4ST-3	chondroitin 4-*O*-sulfotransferase 3
C6ST-1	chondroitin 6-*O*-sulfotransferase 1
Cebpa	CCATT/enhancer binding protein alpha
ChGn-1	chondroitin GalNAc transferase-1
ChGn-2	chondroitin GalNAc transferase-2
CHOP	C/EBP homologous protein
ChPF	chondroitin polymerizing factor
Chpf	chondroitin polymerizing factor
Chst12	carbohydrate sulfotransferase 12
Chst14	carbohydrate sulfotransferase 14
Chst15	carbohydrate sulfotransferase 15
ChSy-1	chondroitin synthase-1
ChSy-2	chondroitin synthase-2
ChSy-3	chondroitin synthase-3
Chsy1	chondroitin sulfate synthase 1
CS	chondroitin sulfate
Csgalnact1	chondroitin sulfate *N*-acetylgalactosaminyltransferase 1
Csgalnact2	chondroitin sulfate *N*-acetylgalactosaminyltransferase 2
CSPG	chondroitin sulfate proteoglycan

Ct	cycle threshold
D4ST-1	dermatan 4-*O*-sulfotransferase 1
DEAE	diethylaminoethyl
DI	differentiated
DS	dermatan sulfate
DS-epi1	glucuronyl C-5 epimerase/dermatan sulfate epimerase 1
DS-epi2	glucuronyl C-5 epimerase/dermatan sulfate epimerase 2
Dse	dermatan sulfate epimerase
Dsel	dermatan sulfate epimerase-like
Fabp4	fatty acid binding protein 4
GAG	glycosaminoglycan
GalNAc	*N*-acetyl-D-galactosamine
GalNAc4S-6ST	GalNAc 4-sulfate 6-*O*-sulfotransferase
GalNAcT-I	GalNAc transferases I
GalNAcT-II	GalNAc transferases II
Gapdh	glyceraldehyde-3-phosphate dehydrogenase
GlcA	D-glucuronic acid
GlcAT-II	GlcA transferase II
GlcNAc	*N*-acetyl-D-glucosamine
HA	hyaluronan
Hmbs	hydroxymethylbilane synthase
HP	heparin
HPLC	high-performance liquid chromatography
HS	heparan sulfate
Hyal1	hyaluronoglucosaminidase 1
Hyal2	hyaluronoglucosaminidase 2
IdoA	L-iduronic acid
KS	keratan sulfate
Lep	leptin
MCE	mitotic clonal expansion
MIQE	minimum information for publication of quantitative real-time PCR experiments
mRNA	messenger ribonucleic acid
Ms-CS	mako shark-derived chondroitin sulfate

Mn	number-average molecular weight
Mw	weight-average molecular weight
ND	non-differentiated
Nono	non-POU domain-containing octamer-binding protein
Pparg	peroxisome proliferator-activated receptor gamma
PPARγ	peroxisome proliferator-activated receptor gamma
Ppia	peptidylprolyl isomerase A
Rn18s	18S ribosomal RNA
RNA	ribonucleic acid
Rpl13a	ribosomal protein L13A
RT-qPCR	reverse transcription quantitative real-time polymerase chain reaction
SEC	size exclusion chromatography
Sp-CS	sharpspine-derived chondroitin sulfate
St-CS	stingray-derived chondroitin sulfate
Tbp	TATA box-binding protein
Tfrc	transferrin receptor
UST	uronyl 2-*O*-sulfotransferase/uronyl 2-sulfotransferase
Ust	uronyl-2-sulfotransferase

General Introduction

Obesity and adipose tissue development

Obesity is one of the conditions which frequently visible to the general population. Due to its rising incidence (Blüher, 2019) and ability to raise the risk of metabolic disorders (Anandacoomarasamy et al., 2008; Czernichow et al., 2011; Sarma et al., 2021), obesity has gained serious attention worldwide. Obesity is simply defined as the accumulation of excessive adipose tissue in the body to the degree to which it might be risky to an individual's health (Diament et al., 2003). Therefore, studies on the fundamental processes of adipocyte formation and possible treatments for obesity have been the subject of investigations. Adipose tissue development can occur via two different mechanisms: hypertrophy, an increase in the size of existing adipocytes, or hyperplasia, an increase in the number of adipocytes (Arner et al. 2010). In adipose tissue development, the process includes the adipocyte formation and development known as adipogenesis. Since mature adipocytes are post-mitotic cells that become incapable of division (Pairault and Green, 1979), differentiation of the preadipocytes or adipocyte progenitor cells (APCs) is required for adipose tissue to develop new adipocytes (Berry and Rodeheffer, 2013).

Over decades, a significant number of research has been conducted in an attempt to clarify the mechanisms behind adipose tissue development. Preadipocytes undergo a morphological rounding during early differentiation, followed by the transformation into mature lipid-storing adipocytes in the terminal differentiation stage. The latter stage involves the synthesis and transport of lipids, metabolic activation related to insulin, and secretion of adipocyte-specific proteins (Farmer, 2006). The coordination of adipocyte differentiation is controlled by a transcriptional cascade, including nuclear receptor peroxisome proliferator-activated receptor gamma (PPARγ) and the CCATT/enhancer binding protein (C/EBP)

family of transcription factors. PPARγ is essential for differentiation and maintenance, while C/EBP members, namely C/EBPα, C/EBPβ, C/EBPδ, C/EBPγ, and C/EBP homologous protein (CHOP) are essential for total adipocyte differentiation. C/EBPβ expression is essential in early differentiation stages, while C/EBPα is required for adipogenesis alongside PPARγ (Esteve Ràfols, 2014). Transcriptional regulation in adipogenesis and the different stages involved in the change from preadipocyte to mature adipocyte are schematically illustrated in Figure GI.1. It is well-known that the differentiation of preadipocytes into adipocytes requires complex regulation of numerous key transcription factors, including two master regulators, PPARγ and C/EBPα (Rosen and MacDougald, 2006; Tang and Lane, 2012), whose coexpression necessarily controls adipocyte gene program (Madsen et al., 2014). PPARγ, one of the PPARs that is most specific to adipose tissue, is induced before the transcriptional activation of the majority of adipocyte genes (Braissant et al., 1996; Evans et al., 2004). In more detail, of the PPARγ isoforms, PPARγ2 is an adipocyte-specific transcription factor (Tontonoz et al., 1994), although PPARγ1 is also reported to be compensatory and capable of promoting adipogenesis (Mueller et al., 2002; Zhang et al., 2004). Moreover, mature adipocytes express PPARγ at its maximum level, with expression rising rapidly during early differentiation (Brun et al., 1996; Chawla and Lazar, 1994).

A study revealed that PPARγ is the proximal effector of adipogenesis since C/EBPα cannot promote adipogenesis in the absence of PPARγ (Rosen et al., 2002). However, previous studies showed that C/EBPα is critical for insulin sensitivity and required to maintain the PPARγ expression in mature adipocytes (El-Jack et al., 1999; Wu et al., 1999). This evidence highlights that the PPARγ and C/EBPα cross-regulation has a crucial role in the transcriptional regulation of adipocytes.

Roles of sulfated glycosaminoglycan, chondroitin sulfate/dermatan sulfate, in cell biology

Glycosaminoglycans (GAGs) are the main glycans commonly found on animal cell surfaces, construct the extracellular matrix, and are involved in many physiological functions (Amendum et al., 2021; Mikami and Kitagawa, 2017; Puri et al., 2020). GAGs are large complex carbohydrate molecules that contain repeating disaccharide units, with molecular masses of about 10–100 kDa, including chondroitin sulfate (CS), dermatan sulfate (DS), keratan sulfate (KS), heparin (HP), and heparan sulfate (HS) that are classified as the sulfated GAGs, whereas hyaluronan (HA) is classified as a non-sulfated GAG (Gandhi and Mancera, 2008). Those GAG members are typically constructed of repeating disaccharides with variable sulfation patterns. The alternating disaccharide units D-glucuronic acid (GlcA) or L-iduronic acid (IdoA) and *N*-acetyl-D-galactosamine (GalNAc) constitute the CS or DS, respectively, while GlcA and *N*-acetyl-D-glucosamine (GlcNAc) are the constituent of HA (Yamada et al., 2011).

Many studies have demonstrated the crucial role of CS in maintaining cell proliferation and differentiation, such as in mouse embryonic stem cells (Izumikawa et al., 2014), mouse neural stem cells (Sirko et al., 2007), and U-937 cell line (Volpi et al., 1993). Moreover, studies have revealed that the specific potential function of the CS/DS compound is determined by distinct sulfation patterns of the CS/DS chains. For example, CS-A chains consist mostly of A-unit [GlcA-GalNAc(4S)], acting as a cell surface receptor in *Plasmodium falciparum*-infected erythrocyte adhesion to the placenta during pregnancy-associated malaria (Achur et al. 2000; Gowda 2006). The CS that contains the C-unit [GlcA-GalNAc(6S)] plays a crucial role in brain neuroplasticity and memory during aging (Miyata et al. 2012; Yang et al. 2021). Previous studies have demonstrated that CS-D, derived from shark cartilage containing D-unit [GlcA(2S)-GalNAc(6S)], can promote neurite outgrowth

(Clement et al. 1998; Nadanaka et al. 1998; Shida et al. 2019). The CS-E compound derived from squid cartilage, which is mainly made up of E-unit [GlcA-GalNAc(4S,6S)], has exhibited a variety of beneficial effects in scientific studies, including promoting osteoblast differentiation (Koike et al., 2012), stimulating neurite outgrowth and providing neuroprotective effects in vitro (Clement et al., 1999; Sato et al., 2008), acting as an antiviral agent against several viruses (Bergefall et al., 2005; Kato et al., 2010), and inhibiting cancer cell migration and metastasis (Li et al., 2008; Willis and Kluppel, 2014).

Chondroitin sulfate in adipocyte development

What is the correlation between CS/DS and adipocyte development? Although there are several pieces of evidence about the critical roles of CS/DS in cell proliferation and differentiation as described above, the detailed phenomena that occurred during adipogenesis still need to be clearly understood. Previous studies reported decreased chondroitin sulfate proteoglycans (CSPGs) during the 3T3-L1 differentiation (Musil et al., 1991; Zizola et al., 2007). On the contrary, Han et al. (2020) reported an increase in the large aggregating CSPGs, versican and biglycan, in obesity. Thus, my study here shows not only that the CS/DS levels are decreasing during 3T3-L1 adipogenesis but also that the CS/DS composition changes in adipogenesis.

This study aims to determine the dynamic of the CS/DS profile during adipocyte differentiation and which CS/DS type is mainly present in the 3T3-L1 cell line. Additionally, the study also evaluates if CS is possibly involved in the regulation of adipocyte differentiation. This study has objectives to facilitate the achievement of these aims, including (1) analyzing the CS/DS composition in non-differentiating and differentiating 3T3-L1 cells and (2) analyzing the effect of exogenous CS treatment on the 3T3-L1 cell differentiation.

Since gene expression analyses by using reverse transcription-quantitative real-time polymerase chain reaction (RT-qPCR) is one of the methods used in this study, validation of the reference genes that are suitable for our 3T3-L1 experimental design was done and will be discussed in detail in **Chapter 1** "**Reference gene expression variability in differentiating and non-differentiating 3T3-L1 cells**". Briefly, this chapter describes the reference gene with the most stable expression among the ten candidates used throughout the study. In **Chapter 2**, "**Qualitative and quantitative analyses in sulfated glycosaminoglycans, chondroitin sulfate/dermatan sulfate, during 3T3-L1 adipocytes differentiation**", CS/DS disaccharides amount and composition during 3T3-L1 adipocyte differentiation were analyzed to reveal the dynamic changes and trends of CS/DS profile during adipocyte differentiation. Moreover, Chapter 2 describes the sulfation pattern of the CS/DS contained in the non-differentiating and differentiating 3T3-L1 cells, as well as depicts the major CS/DS disaccharide in the 3T3-L1 cell line through the compositional analysis done by using a high-performance liquid chromatography (HPLC) system. Furthermore, this chapter provides information on whether CS/DS levels change following adipocyte differentiation or whether CS/DS biosynthesis controls adipocyte differentiation.

In addition to the changes in the CS/DS profile that occurred during adipocyte differentiation, therefore, in the **Chapter 3**, "**Cartilaginous fishes-derived chondroitin sulfate suppresses 3T3-L1 adipocyte differentiation**", the effect of the exogenous CS treatment on the 3T3-L1 cell differentiation was examined. This chapter describes the inhibitory potential of CS substrates on the 3T3-L1 adipocyte differentiation, mainly by decreasing the lipid droplet accumulation.

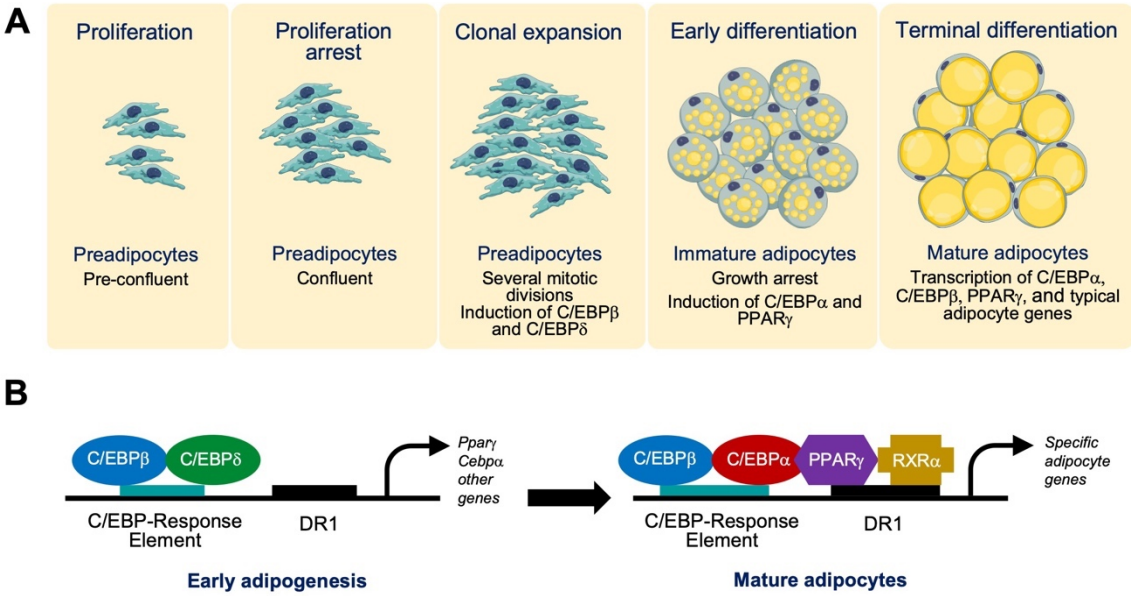

Figure GI.1 Preadipocyte differentiation into mature adipocyte. (**A**) Schematic illustration of the different stages involved in the change from preadipocyte to mature adipocyte and (**B**) the transcriptional regulation during adipogenesis (Esteve Ràfols, 2014).

Chapter 1

Reference gene expression variability in differentiating and non-differentiating 3T3-L1 cells

1.1 Introduction

Obesity has become a global concern owing to its increasing prevalence (Blüher, 2019) and its potential to increase the risk of metabolic diseases (Anandacoomarasamy et al., 2008; Czernichow et al., 2011; Sarma et al., 2021). Consequently, the number of studies on obesity has increased worldwide (Coronado-Ferrer et al., 2022; Zhao et al., 2019). Numerous studies have been conducted to understand the underlying mechanisms of adipocyte development and discover potential therapies for obesity. Various mouse-derived cell lines such as 3T3-L1 and its sublines 3T3-F442A (Green and Kehinde, 1976; Green and Meuth, 1974), Ob17 (Négrel et al., 1978), C3H10T1/2 (Taylor and Jones, 1979), AP-18 (Doi et al., 2005), OP9 (Wolins et al., 2006), and mouse embryonic fibroblasts (MEFs) (Huang et al., 2012) have been established as alternatives to primary cultures and animal models to study adipogenesis. Among these cell lines, 3T3-L1 is the most widely used for adipogenesis studies (Dufau et al., 2021). Adipogenesis, the process of adipocyte differentiation, is regulated at the molecular level by several key transcription factors, including peroxisome proliferator-activated receptor gamma (PPARγ) and CCAAT/enhancer binding protein alpha (CEBPα) (Rosen and MacDougald, 2006). Because multiple molecular events occur during adipogenesis, it is essential to evaluate the expression of various genes that underlie this process, which may be affected by adipogenesis.

Reverse transcription-quantitative polymerase chain reaction (RT-qPCR) has been widely utilized for mRNA quantification in gene expression analysis because of its high

sensitivity and accuracy, as well as its ability to perform real-time analysis (Bustin, 2000; Smith and Osborn, 2009). However, some technical issues must be considered, including RNA extraction, handling, storage, reverse transcription, and amplification efficiency. Therefore, appropriate normalization of the data against a valid reference gene, which could control possible experimental errors throughout the process (Huggett et al., 2005), should be considered to ensure the reliability of the qPCR data, as described in the Minimum Information for Publication of Quantitative Real-Time PCR Experiments (MIQE) guidelines (Bustin et al., 2009).

Several genes such as beta-actin (*Actb*), glyceraldehyde-3-phosphate dehydrogenase (*Gapdh*), and 18S ribosomal RNA (*Rn18s*) are commonly used as reference genes; however, their use has decreased as the utilization of other potential reference genes has increased since the publication of the MIQE guidelines (Chapman and Waldenström, 2015). There is no universal reference gene because it cannot be guaranteed that such a gene will be suitable for every experimental condition (Derks et al., 2008). Thus, validating suitable reference genes is an essential step in gene expression studies using RT-qPCR. Although some studies have reported stable reference genes for RT-qPCR analysis in various 3T3-L1 adipocyte differentiation studies (Anbazhagan et al., 2019; Arsenijevic et al., 2012; Ferguson et al., 2010; Zhang et al., 2014), validation of reference genes suitable for 3T3-L1 adipocyte studies that directly compare differentiating and non-differentiating conditions has not yet been performed. The expression levels of reference genes in 3T3-L1 cells may be altered throughout the experimental timeline under these two conditions; thus, normalizing the expression levels of target genes using unvalidated reference genes will lead to misinterpreting gene expression data.

In this study, we evaluated the expression patterns of genes that have been used or recognized as relatively stable in various experimental designs for 3T3-L1 cell

differentiation studies (Anbazhagan et al., 2019; Arsenijevic et al., 2012; Zhang et al., 2014; Asano et al., 2014), including *Rn18s*, hydroxymethylbilane synthase (*Hmbs*), peptidylprolyl isomerase A (*Ppia*), beta 2 microglobulin (*B2m*), and TATA box-binding protein (*Tbp*). In addition, the gene expression stability of the transferrin receptor (*Tfrc*), non-POU domain-containing octamer-binding protein (*Nono*), ribosomal protein L13A (*Rpl13a*), and two commonly used reference genes, *Actb* and *Gapdh,* were evaluated. Our study focused on evaluating the stability of gene expression and validating the most suitable reference genes for 3T3-L1 adipocyte studies under both differentiation and non-differentiation conditions.

1.2 Materials and Methods

Cell culture and differentiation

Mouse 3T3-L1 preadipocytes (JCRB9014, RRID: CVCL_0123) were obtained from the Japanese Collection of Research Bioresources Cell Bank (JCRB Cell Bank, Osaka, Japan). Cells were seeded at 5×10^4 cells/mL/well in 12-well plates at the same passage number (5) for all triplicate samples. Cells were cultured in Dulbecco's modified Eagle's medium (DMEM, 4.5 g/L glucose; FUJIFILM Wako Pure Chemical Corporation, Osaka, Japan) supplemented with 10% fetal bovine serum (FBS; Biosera, Ringmer, UK) and 1% penicillin and streptomycin (FUJIFILM Wako Pure Chemical Corporation) at 37°C under 5% CO_2. The cells were treated with or without differentiation induction media and divided into five time-based groups: (i) control, day 0; (ii) non-differentiated (ND), day 5; (iii) ND, day 10; (iv) differentiated (DI), day 5; and (v) DI, day 10. Two days post-confluence (day 0), differentiation induction was started for the DI groups by replacing the medium with a differentiation medium containing 10 µg/mL insulin, 2.5 µM dexamethasone, and 0.5 mM 3-isobutyl-1-methylxanthine (AdipoInducer Reagent, Takara Bio, Shiga, Japan). The medium was replaced every 2 days with a medium containing 10 g/mL insulin. The cells

were cultured according to the manufacturer's instructions. The medium was replaced with DMEM containing 10% FBS in the ND group. Cells were collected for RNA extraction on day 0 (control) and days 5 and 10 for the ND and DI groups. Cell cultures were prepared for Oil Red O (ORO) staining at the aforementioned time points. All cell culture experiments were performed in triplicate.

Oil red O staining

The cells were processed for ORO staining to verify lipid droplet accumulation and adipocyte differentiation. The cultured cells were washed with phosphate-buffered saline (pH 7.4) and fixed in 10% neutral-buffered formalin (pH 7.4; FUJIFILM Wako Pure Chemical Corporation) at a temperature ranging from 22°C to 24°C overnight. ORO staining solution (Lipid Assay Kit; Cosmo Bio, Tokyo, Japan) was freshly prepared by mixing the solution with distilled water (dH_2O) at a ratio of 3:2. The working solution was filtered and stained according to the manufacturer's protocol. The cells were then washed thrice with dH_2O and air-dried. ORO solution was added to the culture plates, and the cells were incubated at room temperature for 1 h on an orbital shaker. After the ORO solution was removed, the stained cells were washed three times with dH_2O, and images of the cells were captured using an inverted light microscope (Olympus IX71; Olympus, Tokyo, Japan). A semi-quantitative method was employed to determine lipid droplet accumulation. Isopropanol was used to extract the dye from the stained lipid droplets, and the absorbance of the dye was measured at 492 nm using a microplate reader (Sunrise Remote; Tecan Austria GmbH, Grödig, Austria).

RT-qPCR

Total RNA was isolated from the cells using the ISOSPIN Cell & Tissue RNA kit (Nippon Gene, Tokyo, Japan), and 500 ng of RNA with an A260/280 ratio ranging from 2.08 to 2.13 was reverse transcribed for cDNA synthesis using ReverTra Ace® qPCR RT Master Mix with gDNA Remover (Toyobo, Osaka, Japan) according to the manufacturer's instructions. FastStart Essential DNA Green Master reaction mix (Roche Diagnostics GmbH, Mannheim, Germany), with a final volume of 20 μL for each sample, was used for qPCR analysis, which was performed on a LightCycler® Nano Real-Time PCR Instrument (Roche Diagnostics GmbH). The following 10 reference genes were analyzed: *Actb*, *Gapdh*, *Rn18s*, *Hmbs*, *Ppia*, *B2m*, *Tbp*, *Tfrc*, *Nono*, and *Rpl13a*. We ensured that the primer efficiencies followed those in the LightCycler® Real-Time PCR Systems-Application Manual, which stipulates that PCR efficiency should be at least 85%. The PCR efficiencies of all primer sets used in this study varied between 87.6% (*Gapdh*) and 102.2% (*Tfrc*), which were within the acceptable range (Voss and Ceder, 2023). Moreover, the standard curves showed strong linearity with r^2 values, ranging from 0.9838 (*B2m*) to 0.9999 (*Gapdh*), which is within the acceptable values for RT-qPCR reactions ($r^2 \geq 0.98$) (Broeders et al., 2014; Taylor et al., 2010). Detailed information, including sequences, accession numbers, product sizes, and efficiencies of the primer sets for the 10 reference genes used for RT-qPCR, are presented in Table 1.1. The following primers were used for Leptin (*Lep*) expression analysis: forward, 5'-TCCCTGCCTCAGACCAGTG-3' and reverse, 5'-TAGAGTGAGGCTTCCAGGACG-3' (Zeigerer et al., 2008). Two adipogenic transcription factors, *Pparg* and *Cebpa,* were evaluated. The following primers were used for the target genes: *Pparg* forward, 5'-CAAGAATACCAAAGTGCGATCAA-3' and reverse, 5'-GAGCAGGGTCTTTTCAGAA TAATAAG-3' (Kanda et al., 2009); *Cebpa* forward, 5'-CTAGGAGATTCCGGTGTGGC-3' and reverse, 5'-CCCGAGAGGAAGCAGGAATC-3' (Li et al., 2019). The expression levels

of all genes provided in the present study were automatically determined using the LightCycler® Nano Real-Time PCR System (Roche Diagnostics) based on the calibration curve from each qPCR. As previously mentioned, it is important to normalize gene expression to account for possible technical factors. Therefore, the expression of each gene in the analysis was referred to as a non-normalized expression.

Creation of a heatmap for gene expression levels and the evaluation of 10 reference genes using five algorithms

Heatmap images of the expression of the 10 genes included in the analysis of the ND and DI groups were generated using Heatmapper (Babicki et al., 2016). Z scores for the expression levels of each gene were calculated, and genes with higher and lower than the average expression levels are marked in red and green, respectively. The Average Linkage clustering and Pearson distance measurement methods were used. The expression stability of each gene was evaluated using the geNorm (http://www.qbaseplus.com/) (Vandesompele et al., 2002), NormFinder (https://www.moma.dk/normfinder-software) (Andersen et al., 2004), BestKeeper (http://www.gene-quantification.de/bestkeeper.html) (Pfaffl et al., 2004), and RefFinder (https://www.heartcure.com.au/reffinder/) (Xie et al., 2012). In the ΔCt approach, the stability level was manually calculated using the comparative ΔCt method proposed by Silver et al. (2006).

Data analysis

For the expression levels of reference genes and the determination of target gene expression levels normalized against the reference genes, the data are presented as the mean ± standard deviation (SD). Comparisons between the reference gene mRNA expression levels in each group on days 5 and 10 (both ND and DI groups) and those on day 0 (control

group) were performed using Dunnett's test. For the semi-quantitative analysis of oil droplet accumulation and *Lep*, *Pparg,* and *Cebpa* expression analyses, comparisons between means were performed using the Bonferroni test. Microsoft Excel add-in statistical software (Bell Curve for Excel version 4.02; Social Survey Research Information, Tokyo, Japan) was used to perform the statistical analyses. Differences were considered statistically significant at *P < 0.05 and **P < 0.01.

1.3 Results

Verification of adipocyte differentiation after adipogenic induction

In the present study, 3T3-L1 cells from the DI group exhibited morphological changes to adipocyte-like structures, with lipid droplet accumulation observed on days 5 and 10 after adipogenic induction. In contrast, cells in the ND group did not show lipid droplet accumulation, similar to those in the control group (Figure 1.1A). Semi-quantitative measurements showed that the DI group had 6.2-fold higher lipid droplet accumulation than the control group on day 5, and 15.1-fold higher accumulation on day 10 (Figure 1.1B). Additionally, *Lep* mRNA expression was higher in the DI group on days 5 and 10, indicating the presence of mature adipocytes (Figure 1.1C). Induction of differentiation triggers deep phenotypic changes in preadipocytes as they transition into mature adipocytes. In contrast, the cells that were not subjected to differentiation induction maintained their fibrocyte-like phenotypes.

Different reference gene expression levels in non-differentiating and differentiating 3T3-L1 cells

The cycle threshold (Ct) values of the 10 reference genes and their gene expression levels, as calculated from the calibration curves, are provided in Tables 1.2 and 1.3, respectively. The candidate reference genes showed a wide range of Ct values of 10 reference genes across all five sample groups, ranging from 13.11–26.07. *Rn18s* and *Gapdh* exhibited the highest expression levels, with median Ct values of 13.38 and 17.93, respectively. In contrast, *Tbp* showed the lowest expression, with a median Ct value of 25.85 (Figure 1.2). In addition, *Ppia* and *Tbp* exhibited relatively smaller ranges of Ct values than other candidate genes. We observed fluctuations in the expression levels of the 10 reference genes at different time points (0, 5, and 10 days), regardless of their exposure to

differentiation induction, as shown in the Z-score heatmap (Figure 1.3A). Furthermore, these results show for the first time that the expression levels of reference genes vary at different time points in non-differentiated 3T3-L1 cells as well as in differentiation-induced cells.

Validation of suitable reference genes using five algorithms

The stability of the expression levels of the 10 candidate reference genes was analyzed to determine the most suitable reference genes for 3T3-L1 adipocyte studies under both non-differentiating and differentiating conditions. The results of the gene expression stability ranking analysis using the five algorithms are presented in Table 1.4. geNorm evaluates the reference gene stability (*M*), defined as the average pairwise variation in the expression levels of a certain gene and all candidate genes (Vandesompele et al., 2002). A lower *M* value obtained using the geNorm algorithm indicates more stable gene expression. The genes that exhibited the most stable expression in both non-differentiating and differentiating 3T3-L1 cells (days 0, 5, and 10) were *Ppia* and *Tbp*. The expression stabilities of the remaining candidate genes, from highest to lowest, were *Rn18s*, *Nono*, *Actb*, *Rpl13a*, *Hmbs*, *Tfrc*, *B2m*, and *Gapdh* (Figure 1.3B, Table 1.4).

NormFinder automatically determines the stability values for all candidate reference genes analyzed in any number of samples arranged into any number of experimental groups (Andersen et al., 2004). The NormFinder algorithm-derived stability values of the 10 reference genes shown in Figure 1.3B and Table 1.4 demonstrate that *B2m* had the least stable gene expression, with a stability value three times higher than that of the second most unstable gene, *Gapdh*. The gene expression stability ranking of the 10 reference genes from NormFinder showed that *Ppia* and *Tbp* had the most stable gene expression (Table 1.4). Although the expression of the middle-ranked reference genes varied slightly, the genes with

the most and least stable expression identified using NormFinder were consistent with the results obtained using geNorm, as mentioned previously.

BestKeeper evaluates the expression stability of reference genes by calculating the SD of Ct values and the coefficient of variation, followed by a pairwise correlation analysis of the BestKeeper index and an analysis of the correlation between the expression levels of each candidate gene (Pfaffl et al., 2004). Based on the analysis performed using the other three algorithms and the comparative ΔCt method, RefFinder provides geomean ranking values (Xie et al., 2012). As shown in Figure 1.3B, the results generated by the BestKeeper and RefFinder programs validate the results of the other algorithms. According to these algorithms, the gene with the most stable expression was *Tbp*, followed by *Ppia*, whereas the genes with the most unstable expression were *Gapdh* and *B2m*. Manual calculations using the comparative Ct method gave results similar to those generated by the other four algorithms, with *Ppia* and *Tbp* as the genes with the most stable expression and *Gapdh* and *B2m* with the least stable expression (Figure 1.3B). Moreover, the ranking of gene expression stabilities obtained using the Ct method was the same as that obtained using the geNorm method (Table 1.4).

The ranking of the expression stability of the reference genes analyzed in this study is shown in Table 1.4. The geometric means of the ranks calculated from these five algorithms indicated that *Ppia* and *Tbp* had the highest ranks for expression stability, whereas *Gapdh* and *B2m* had the least stable expression. Thus, *Ppia* and *Tbp* could be considered the most suitable reference genes for gene expression studies under both non-differentiating and differentiating conditions. However, *Gapdh* and *B2m* might not be suitable for studying gene expression in 3T3-L1 cells.

Impact of reference gene selection on the interpretation of the expression levels of target genes

In the present study, gene expression levels calculated from the calibration curve were used to prepare graphs. Our results showed that the expression patterns of the reference genes in 3T3-L1 cells might be altered not only in differentiating cells owing to adipogenic induction but also in non-differentiating cells (Figure 1.4A). *Ppia* was the gene with the most stable expression in 3T3-L1 cells. *Rn18s* expression increased on day 5 and decreased slightly on day 10, regardless of adipogenic induction. The expression levels of *Hmbs* increased in a day-dependent manner and accelerated in the DI group. In addition, the expression levels of *Tfrc* were relatively stable in the ND group; however, their expression levels increased with adipogenic induction on day 5 and then slightly decreased on day 10. The expression patterns of the other six reference genes are shown in Figure 1.5. *Tbp*, the gene with the second most stable expression, exhibited a stable expression pattern, in addition to *Ppia*. On day 10, *Nono*, *Actb*, and *Rpl13a* showed decreased expression levels. Despite the significance levels in comparison with the control group, their expression was relatively lower in the DI group than in the ND group. *B2m* expression levels were lower in the ND group on day 5, followed by a significant increase on day 10, whereas its expression level remained consistently lower in the DI group. *Gapdh*, the gene with the least stable expression, showed an increase in gene expression in a day-dependent manner, which was more significant in the DI group.

In the present study, we normalized two adipogenesis-related transcription factors, *Pparg* and *Cebpa* (Madsen et al., 2014), against four selected reference genes, *Ppia*, *Rn18s*, *Hmbs*, and *Tfrc*, which have expression patterns with different stabilities ranging from more to less stable (Figure 1.4B,C). This was performed to demonstrate how the selection of reference genes affected the gene expression analysis results. The expression of PPARγ and

CEBPα cooperatively induces adipogenesis (Madsen et al., 2014). These genes exhibit similar expression patterns. The expression level of *Pparg* in the DI group was significantly increased on days 5 and 10 after adipogenic induction. Specifically, the raw expression level of *Pparg* was 1.35-fold higher on day 10 than on day 5 after induction. When the expression level of *Pparg* was normalized to that of *Ppia* and *Rn18s*, *Pparg* expression increased by 1.38- and 1.55-fold, respectively. These expression patterns are consistent with the raw expression patterns (Figure 1.4B). However, the magnitude of *Pparg* expression on day 10 in the DI group, when normalized to *Hmbs* expression levels, did not increase, unlike the raw expression profile. Generally, *Pparg* expression levels were markedly increased compared to the raw expression levels when normalized to *Tfrc,* whose expression levels were relatively low. Moreover, *Pparg* expression levels in the DI group were 3.08-fold higher on day 10 than on day 5 after induction. These consistent and inconsistent expression patterns compared to the raw expression pattern were also observed for *Cebpa* (Figure 1.4C). *Pparg* and *Cebpa* expression levels normalized to those of *Tbp*, *Nono*, *Actb*, *Rpl13a*, *B2m*, and *Gapdh* are presented in Figure 1.6. On day 10, the DI group showed a 1.31-fold increase in *Pparg* expression levels normalized to *Tbp* compared to day 5, which was similar to the non-normalized expression level. Additionally, *Pparg* expression levels normalized to *Nono*, *Actb*, and *Rpl13a* in the DI group were 1.81-, 2.03-, and 1.83-fold higher, respectively, on day 10 than on day 5 after adipogenic induction. Normalizing *Pparg* expression against the genes with the least stable expression, *B2m* and *Gapdh*, resulted in distinctive expression patterns compared to non-normalized expression. As *Pparg* and *Cebpa* mRNA levels were similar in 3T3-L1 cells, the correct and incorrect patterns of *Cebpa* normalized against *Tbp*, *Nono*, *Actb*, *Rpl13a*, *B2m*, and *Gapdh* were similar to those of *Pparg* (Figure 1.6).

1.4 Discussion

The strategy for normalizing the expression levels of a gene of interest against appropriate reference genes in RT-qPCR gene expression analysis is based on the assumption that reference genes are expressed at constant levels across various treatments and experimental conditions (Thellin et al., 1999). However, an ideal reference gene does not exist (Huggett et al., 2005; Vandesompele et al., 2002; Zhang et al., 2015). Disparities in gene expression levels were observed at different time points for all housekeeping genes analyzed in this study, regardless of adipogenic induction, as shown in the Z-score heatmap (Figure 1.3A). The most common reference genes, such as *Gapdh*, *Actb*, and *Rn18s* are often used to normalize gene expression data in RT-qPCR analysis. Commonly used reference genes, such as *Gapdh* and *Actb,* are acceptable for qualitative or semi-quantitative assays, including conventional RT-PCR (Huggett et al., 2005). However, several studies have demonstrated that some commonly used reference genes such as *Actb*, *Rn18s*, and *Gapdh* are unstable in different tissues under various experimental conditions (Adachi et al., 2015; Svingen et al., 2015).

In a previous study of 3T3-L1 differentiation, *Rn18s* and *Hmbs* were the most stable reference genes (Zhang et al., 2014). *Hmbs* and *B2m* are the most stable reference genes for 3T3-L1 adipocyte differentiation under hypoxic and normoxic conditions (Anbazhagan et al., 2019). Other research groups have recommended normalization against *Atp5b*, *Nono,* and *Hprt* as the most suitable reference genes during the mitotic clonal expansion (MCE) phase of 3T3-L1 differentiation, whereas *Actb*, *Nono, Rpl13a*, and *Ywhaz* have been reported as the best reference genes during the terminal differentiation phase (Arsenijevic et al., 2012). From our perspective, appropriate reference genes may differ between studies depending on the experimental design. However, the use of commonly used reference genes without validation before gene expression analyses has yielded unreliable results. Therefore,

the normalization of gene expression levels against inappropriate reference genes may have a major impact on the conclusions of the study owing to false statistical analysis results and misinterpretation of data (Ferguson et al., 2010).

Unlike previous validations, the present study evaluated the expression of 10 candidate reference genes, not only in adipogenic-induced 3T3-L1 cells but also in non-differentiated cells during the culture period. A comparison of gene expression between differentiating and non-differentiating cells, which were maintained for the same culture period, is necessary to determine whether the alteration in gene expression was caused by adipogenic induction or whether it was naturally altered during the culture period (day 0–10). In the present study, all five algorithms showed that *Gapdh* and *B2m* were unsuitable because their expression levels were unstable across the experimental groups. Despite its common utilization as a reference gene in gene expression analysis, *Gapdh* mRNA is stimulated by insulin on 3T3-Ll and 3T3-F442A cell lines (Alexander et al., 1985; Alexander et al., 1988), as well as upregulated during rat brown adipocytes differentiation (Barroso et al., 1999). This suggests that *Gapdh* must be avoided in in vitro adipogenesis studies because insulin is frequently used in adipocyte culture media (Dufau et al., 2021).

Our study also validated *Ppia* and *Tbp* as the most suitable reference genes for 3T3-L1 adipogenesis studies comparing differentiating and non-differentiating cells. As shown in Figure 1.4B,C), we demonstrated the importance of selecting an appropriate reference gene. Normalization against *Ppia* resulted in consistent *Pparg* and *Cebpa* expression levels compared with their non-normalized expression levels (Figure 1.3B,C). Similar results were obtained when expression levels were normalized to those of *Tbp* (Figure 1.6). In addition to the top-ranked reference genes *Ppia* and *Tbp*, we demonstrated that normalization to *Rn18s* was acceptable for determining *Pparg* and *Cebpa* expression levels. Although *Rn18s* expression is not the most stable, the results of this study are consistent with those of a

previous study (Zhang et al., 2014). The difference in *Pparg* and *Cebpa* expression levels between differentiated and non-differentiated cells was extremely significant, and the surge in gene expression levels was also significantly different between the time points. Therefore, normalization to unstable reference genes may not detect any changes in the gene expression patterns. This result emphasized that reference gene suitability may also affect target gene expression patterns. The present study showed that the expression of the unstable reference gene *Hmbs,* increased in a day-dependent manner, regardless of the presence or absence of differentiation induction, whereas Zhang *et al*. (2014) revealed consistent expression of *Hmbs* during differentiation. Normalization of *Pparg* and *Cebpa* expression against *Hmbs* showed no difference in expression levels between undifferentiated and differentiated cells, resulting in incorrect expression patterns (Figure 1.4B,C). In the determination of *Pparg* and *Cebpa* expression levels, normalization against *Tfrc* showed extremely high gene expression levels with a similar statistical justification; however, this resulted in incorrect data (Figure 1.4B,C). Moreover, normalization against other unstable reference genes, namely, *Nono*, *Actb*, *Rpl13a*, *B2m*, and *Gapdh*, resulted in inaccurate expression levels (Figure 1.6). Taken together, these data highlight that normalizing gene expression levels to those of an inappropriate reference gene can lead to misinterpretation of data.

Gene expression variability may be affected by various factors, including glucose concentration (Mohammadi-Farani et al., 2014; Nishitani et al., 2019), FBS supplementation (Bieback et al., 2010; Kwon et al., 2016), pH (Lemma et al., 2018; Rauschner et al., 2021), and temperature (Vergara et al., 2014; Torres et al., 2018). In addition, gene expression variability is caused by the cell passage number (Chang-Liu and Woloschak, 1997; O'Driscoll et al., 2006), culture duration (Yang et al., 2012; Emam et al., 2015), cell cycle synchronization (Mukhitov et al., 2019), and experimental treatments (Choi et al., 2006; Schreiber et al., 2017; Brzeszczyńska et al., 2020). Among these factors, the

physicochemical environment (pH and temperature) is accurately controlled. The biochemical conditions of the cellular environment in this study were maintained using the same cell culture medium throughout the experiments. A constant glucose concentration, a single batch of FBS contained in the culture media, and the implementation of a routine media replacement protocol eliminated the possibility of these factors causing gene expression variability. Cells at the same passage number were used to ensure homogeneity of the physical characteristics of the cells among all experimental groups. However, in this study, we did not synchronize the cell cycle before day 0. Therefore, an unsynchronized cell cycle might affect gene expression, especially in the ND groups. Nonetheless, our study revealed that some reference genes were stably expressed across the different treatments and throughout the experimental period. Gene expression variability was likely caused by treatment with adipogenic induction reagents and the experimental duration, rather than by a lack of synchronization.

We showed that the expression levels of reference genes may be affected over time, even in non-differentiating cells, and that *Ppia* and *Tbp* were stable reference genes throughout 10 days in both undifferentiated and differentiated 3T3-L1 cells. The expression of these housekeeping genes remained stable in both the undifferentiated and differentiated 3T3-L1 cells after 10 days. One limitation of this study is that it focused on only 10 reference genes; thus, reference genes other than those analyzed in this study may be suitable under a similar experimental design. Notably, the expression of known reference genes was altered in non-differentiating cells throughout the experiment.

1.5 Summary

Since gene expression analysis requires proper normalization to obtain reliable data, validation of the reference genes before the gene expression analysis is important. In this study, the stability of the expression of 10 reference genes in the 3T3-L1 cell line, which is the most widely used cell line in adipogenesis studies, with and without adipogenic induction, was evaluated. These 10 reference genes were subjected to RT-qPCR analysis and the evaluation of expression stability was performed using the following five algorithms: geNorm, NormFinder, BestKeeper, RefFinder, and the ΔCt method. The findings of the study revealed that (1) the expression levels of the reference genes changed over time, even in non-differentiating cells, and (2) peptidylprolyl isomerase A (*Ppia*) and TATA box-binding protein (*Tbp*) were stable reference genes for 10 days in both undifferentiated and differentiated 3T3-L1 cells. In addition, glyceraldehyde-3-phosphate dehydrogenase (*Gapdh*) and beta 2 microglobulin (*B2m*) were found to be the least stable genes. Notably, the expression of known reference genes in non-differentiating cells was altered throughout the experiment. This study highlights that the validation of reference genes prior to the RT-qPCR analysis is crucial for adipogenesis studies.

Table 1.1 Mouse cDNA primer sequences of the 10 reference genes used for RT-qPCR

Gene symbol	Primer sequences (5'-3')	Accession number	Product size (bp)	Primer efficiency (%)	r^2 value	References of primer sequences
Actb	F:AGCCATGTACGTAGCCATCC R:TTTGATGTCACGCACGATTT	NM_007393.5	250	93.1	0.9987	-
Gapdh	F:AGGTCGGTGTGAACGGATTTG R:TGTAGACCATGTAGTTGAGGTCA	NM_001289463.1	123	87.6	0.9999	-
Rn18s	F:GCAATTATTCCCCATGAACG R:GGCCTCACTAAACCATCCAA	NR_003278.3	123	90.3	0.9856	Anbazhagan et al. (2019)
Hmbs	F:ATGAGGGTGATTCGAGTGGG R:TTGTCTCCCGTGGTGGACATA	NM_001110251.1	134	88.9	0.9864	Zhang et al. (2014)
Ppia	F:CAGGTCCATCTACGGAGAGA R:CATCCAGCCATTCAGTCTTG	NM_008907.2	146	90.3	0.9990	Muñoz et al. (2021)
B2m	F:ATACGCCTGCAGAGTTAAGC R:TCACATGTCTCGATCCCAGT	NM_009735.3	70	87.9	0.9838	Muñoz et al. (2021)
Tbp	F:CCAATGACTCCTATGACCCCTA R:CAGCCAAGATTCACGGTAGAT	NM_013684.3	104	98.8	0.9998	Asano et al. (2014)
Tfrc	F:GTTTCTGCCAGCCCCTTATTAT R:GCAAGGAAAGGATATGCAGCA	NM_011638.4	152	102.2	0.9994	Zhang et al. (2014)
Nono	F:TGCTCCTGTGCCACCTGGTACTC R:CCGGAGCTGGACGGTTGAATGC	NM_023144.2	170	94.5	0.9995	Arsenijevic et al. (2012)
Rpl13a	F:GGCTGCCGAAGATGGCGGAG R:GCCTTCACAGCGTACGACCACC	NM_009438.5	131	93.8	0.9995	Arsenijevic et al. (2012)

Table 1.2 The Ct values of non-differentiated and differentiation induced 3T3-L1 cell line

Gene	*Actb*	*Gapdh*	*Rn18s*	*Hmbs*	*Ppia*	*B2m*	*Tbp*	*Tfrc*	*Nono*	*Rpl13a*
Control, Day 0 (1)	18.748	19.930	13.636	25.199	19.166	19.023	25.843	25.177	21.871	22.348
Control, Day 0 (2)	18.982	20.800	13.868	25.354	19.105	19.033	26.072	25.380	22.017	22.653
Control, Day 0 (3)	18.812	19.631	13.813	25.306	19.200	18.802	25.950	25.226	22.119	22.703
ND Day 5 (1)	18.004	19.884	13.209	24.990	18.968	19.656	25.879	25.313	21.664	22.623
ND Day 5 (2)	18.129	19.488	13.200	24.937	18.789	19.363	25.804	25.310	21.844	22.255
ND Day 5 (3)	18.088	19.576	13.304	24.951	18.998	19.467	25.815	25.344	21.588	22.384
ND Day 10 (1)	18.741	17.647	13.560	24.949	19.026	18.169	25.958	25.253	21.705	22.510
ND Day 10 (2)	18.333	17.618	13.532	24.718	18.889	17.933	25.801	24.976	21.624	22.648
ND Day 10 (3)	18.558	17.441	13.442	24.856	18.946	18.022	25.957	25.199	21.685	22.573
DI Day 5 (1)	18.520	17.932	13.195	24.553	19.113	20.396	25.763	23.642	22.304	23.140
DI Day 5 (2)	18.595	17.828	13.215	24.577	18.824	20.428	25.928	23.746	21.869	22.659
DI Day 5 (3)	18.443	19.642	13.109	24.450	18.980	20.201	25.860	23.588	21.566	22.625
DI Day 10 (1)	19.092	16.472	13.319	24.026	18.970	20.194	25.805	24.810	22.480	23.294
DI Day 10 (2)	19.154	16.392	13.383	24.076	19.123	20.315	25.848	24.855	22.346	23.355
DI Day 10 (3)	19.190	16.230	13.479	24.067	18.979	20.153	25.788	24.838	22.366	23.257

Table 1.3 The gene expression levels calculated from calibration curves

Gene	*Actb*	*Gapdh*	*Rn18s*	*Hmbs*	*Ppia*	*B2m*	*Tbp*	*Tfrc*	*Nono*	*Rpl13a*
Control, Day 0 (1)	0.140	0.011	0.090	0.066	0.092	0.361	0.123	0.028	0.144	0.202
Control, Day 0 (2)	0.120	0.006	0.077	0.059	0.096	0.359	0.105	0.024	0.131	0.165
Control, Day 0 (3)	0.135	0.013	0.080	0.061	0.090	0.416	0.114	0.027	0.122	0.160
ND Day 5 (1)	0.229	0.011	0.118	0.075	0.105	0.242	0.120	0.026	0.165	0.168
ND Day 5 (2)	0.211	0.014	0.119	0.077	0.117	0.292	0.126	0.026	0.147	0.215
ND Day 5 (3)	0.217	0.014	0.111	0.077	0.103	0.273	0.125	0.025	0.174	0.197
ND Day 10 (1)	0.141	0.046	0.094	0.077	0.101	0.620	0.113	0.027	0.161	0.181
ND Day 10 (2)	0.185	0.047	0.096	0.089	0.110	0.719	0.126	0.032	0.170	0.166
ND Day 10 (3)	0.159	0.052	0.102	0.082	0.106	0.680	0.113	0.028	0.163	0.174
DI Day 5 (1)	0.163	0.038	0.119	0.099	0.095	0.152	0.130	0.083	0.108	0.120
DI Day 5 (2)	0.155	0.041	0.118	0.097	0.115	0.149	0.116	0.077	0.144	0.164
DI Day 5 (3)	0.172	0.013	0.126	0.106	0.104	0.172	0.121	0.086	0.176	0.168
DI Day 10 (1)	0.112	0.096	0.110	0.138	0.105	0.173	0.126	0.037	0.096	0.108
DI Day 10 (2)	0.107	0.101	0.106	0.134	0.095	0.160	0.122	0.035	0.105	0.104
DI Day 10 (3)	0.105	0.112	0.099	0.135	0.104	0.177	0.127	0.036	0.104	0.111

Table 1.4 Gene expression stability ranking by five different algorithms on non-differentiated and differentiation-induced 3T3-L1 cells

Gene symbol	Geometric mean of ranks	geNorm		NormFinder		BestKeeper		RefFinder		ΔCt method	
		M value	Rank	Stability value	Rank	Std Dev [± CP]	Rank	Geomean of ranking values	Rank	Mean SD	Rank
Ppia	1.320	0.121	1	0.018	1	0.094	2	1.4	2	0.532	1
Tbp	1.516	0.126	2	0.019	2	0.069	1	1.2	1	0.549	2
Rn18s	3.178	0.145	3	0.027	4	0.187	3	3.0	3	0.567	3
Nono	3.776	0.227	4	0.023	3	0.268	4	4.0	4	0.587	4
Actb	5.697	0.267	5	0.038	8	0.312	6	5.5	5	0.649	5
Rpl13a	5.966	0.283	6	0.036	7	0.281	5	6.0	6	0.650	6
Hmbs	6.787	0.368	7	0.034	6	0.356	7	6.4	7	0.727	7
Tfrc	7.282	0.456	8	0.030	5	0.479	8	8.0	8	0.895	8
B2m	9.192	0.589	9	0.156	10	0.737	9	9.0	9	1.151	9
Gapdh	9.791	0.791	10	0.039	9	1.322	10	10.0	10	1.600	10

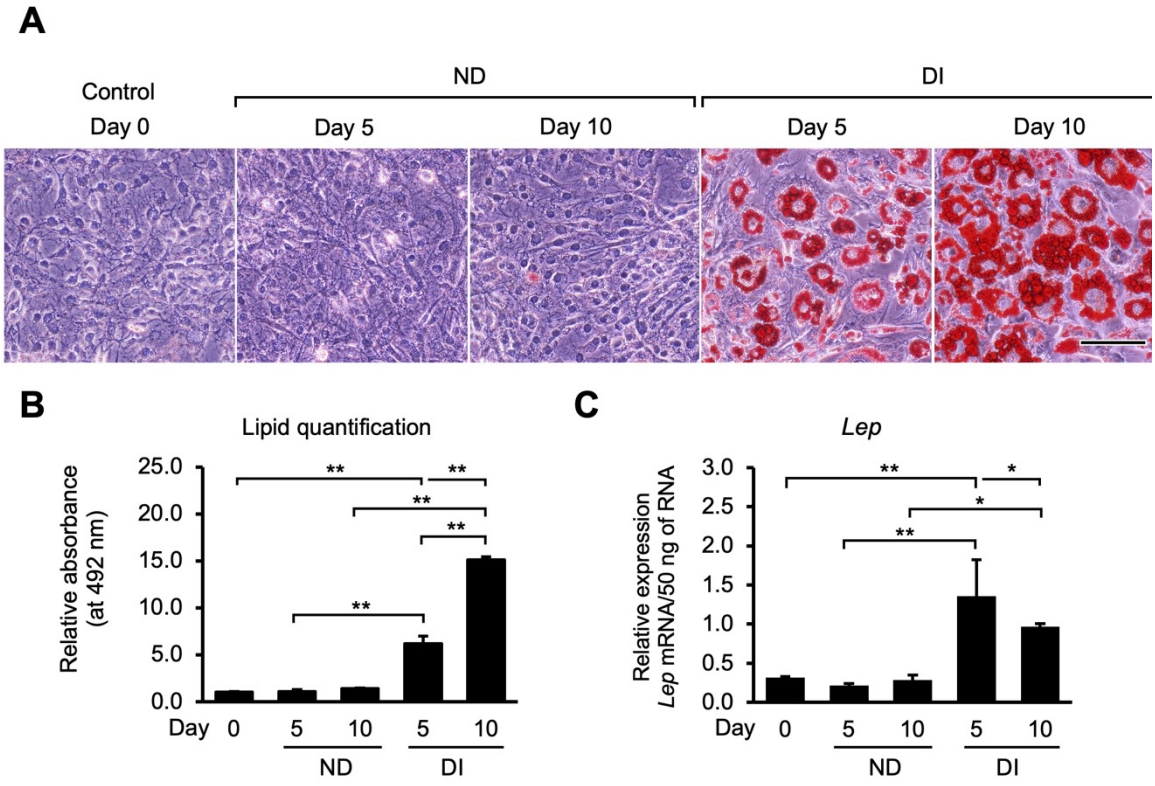

Figure 1.1 Oil red O (ORO) staining and quantification of accumulated lipid droplets in non-differentiated (ND) and differentiated (DI) 3T3-L1 cells on days 0, 5, and 10. (**A**) Accumulation of lipid droplets was observed in the DI groups by staining with ORO, at days 5 and 10 after differentiation induction. Scale bar = 100 µm. (**B**) Quantification of lipid droplet accumulation in 3T3-L1 cells. The absorbance of the eluted ORO obtained from the stained oil droplets was measured using a microplate reader at 492 nm. *P < 0.05 and **P < 0.01 using Bonferroni test. (**C**) Relative *Lep* mRNA expression per 50 ng of RNA in all five groups. *Lep* expression was higher in the DI groups than in the ND groups, indicating the stage of mature adipocytes in the DI groups. *P < 0.05 and **P < 0.01 using Bonferroni test. Data are presented as the mean ± standard deviation (SD) of triplicate samples.

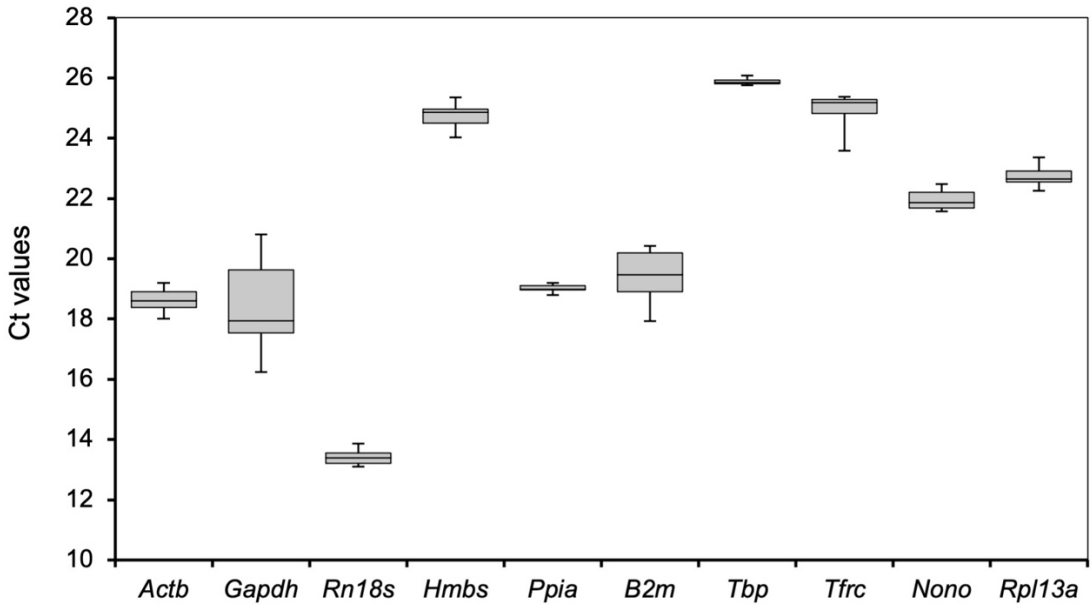

Figure 1.2 Distribution of cycle threshold (Ct) values of each candidate reference gene across all sample groups. A line within each box indicates the median Ct values, whereas the lower and upper boundaries of each box indicate the first and third quartiles of the data, respectively. Minimum and maximum values are indicated by the lower and upper ends of the whiskers, respectively.

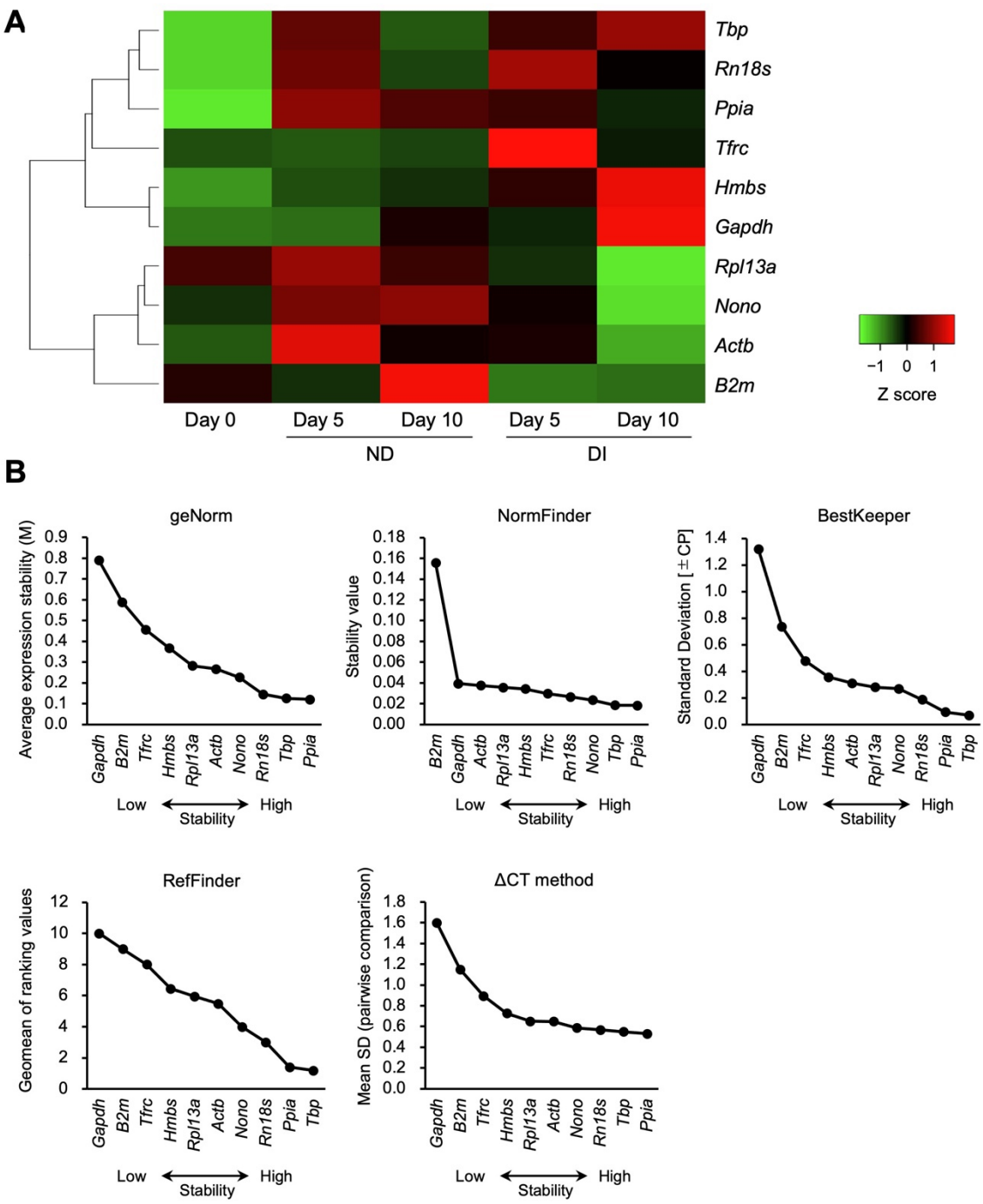

Figure 1.3 Heatmap of the gene expression levels of 10 reference genes and the gene expression stability levels evaluated using five algorithms. (**A**) Heatmap image for each gene expression level in the Control, non-differentiated (ND), and differentiated (DI) groups. The colors in the heatmap show the Z scores of gene expression levels in the triplicate samples. Gene expression levels higher than the mean are indicated in red and those lower than the mean are indicated in green. (**B**) The expression levels of 10 reference genes were analyzed using geNorm, BestKeeper, NormFinder, RefFinder, and the ΔCt method in the Control, ND, and DI groups. A lower value (right side of the horizontal axis) indicates a reference gene with a more stable expression.

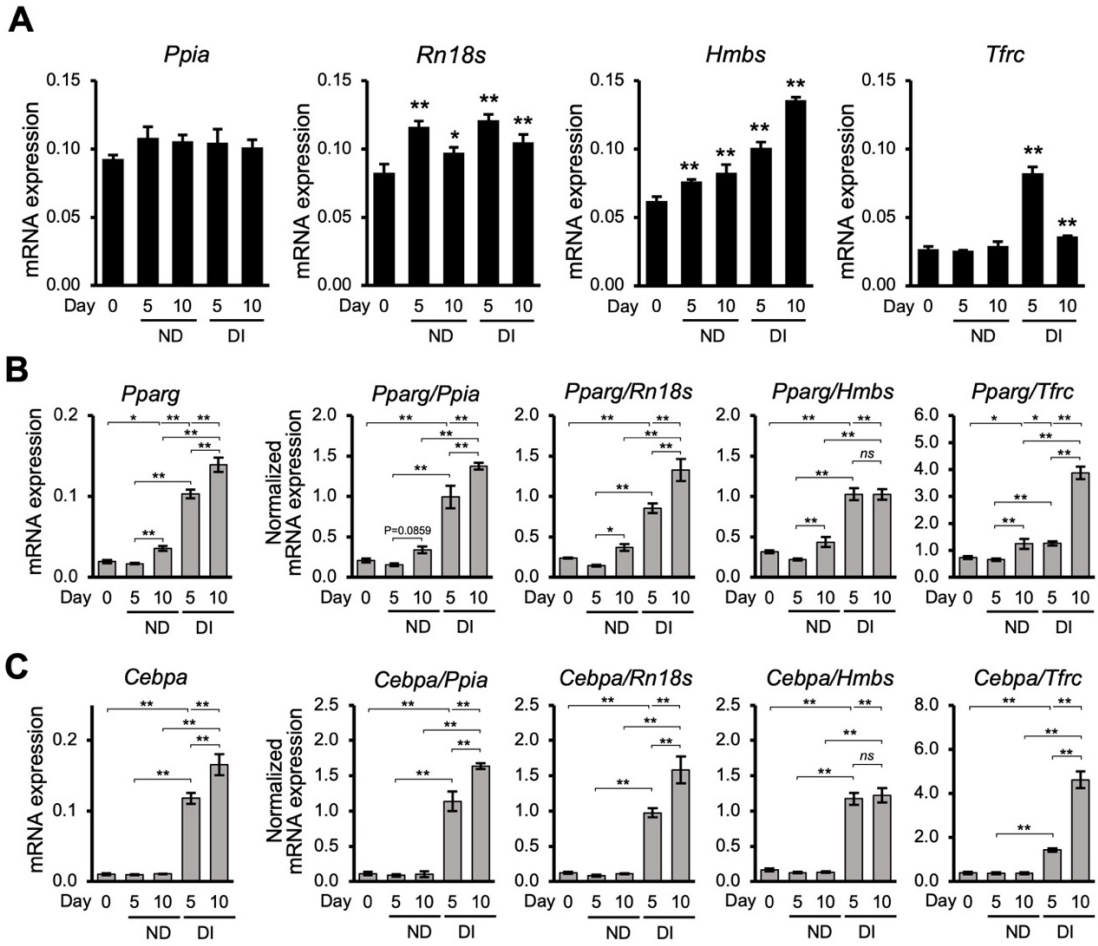

Figure 1.4 Selection of reference genes affects the expression pattern of the target genes. (**A**) Expression pattern of representative stable and unstable reference genes in non-differentiating and differentiating 3T3-L1 cells. The non-normalized expression levels of *Ppia*, *Rn18s*, *Hmbs*, and *Tfrc* show different patterns indicating that the gene expression levels differed among the groups. Differences were considered statistically significant at *P < 0.05 and **P < 0.01 compared to the Control group using Dunnett's test. (**B**) Comparative gene expression levels of *Pparg* in non-differentiated (ND) and differentiated (DI) groups against the representative gene expression levels. *P < 0.05 and **P < 0.01 using Bonferroni test. (**C**) *Cebpa* expression levels in non-differentiated (ND) and differentiated (DI) groups normalized to the selected reference genes. *P < 0.05 and **P < 0.01 using Bonferroni test. Data for all graphs are presented as the mean ± standard deviation (SD) of triplicate samples.

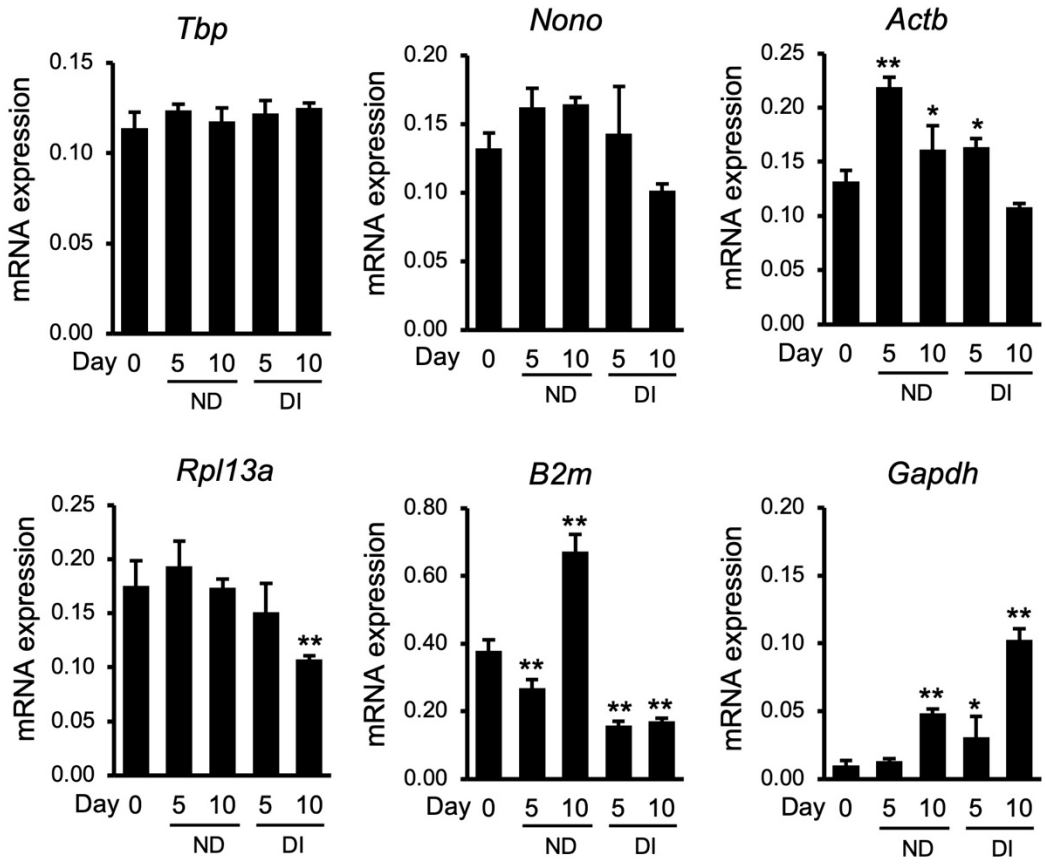

Figure 1.5 Expression pattern of stable and unstable reference genes in non-differentiating and differentiating 3T3-L1 cells. The expression levels (non-normalized) of *Tbp*, *Nono*, *Actb*, *Rpl13a, B2m*, and *Gapdh* show different patterns, indicating that the gene expression levels differed among the groups. Data are presented as the mean ± standard deviation (SD) of triplicate samples. *P < 0.05 and **P < 0.01 compared to the Control group using Dunnett's test.

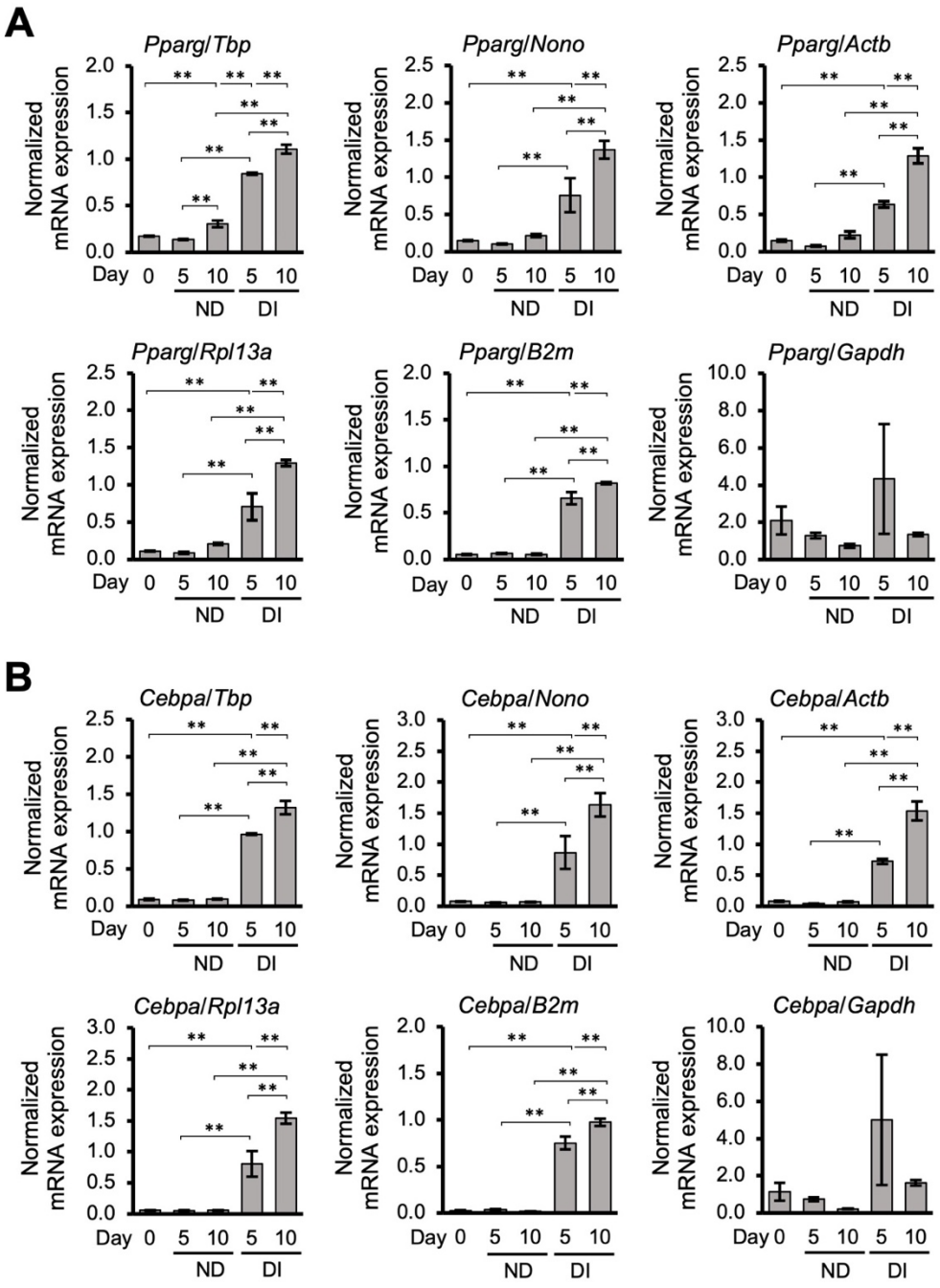

Figure 1.6 Comparative gene expression levels of the adipogenesis-related transcription factors, (**A**) *Pparg* and (**B**) *Cebpa*, in non-differentiated (ND) and differentiated (DI) groups against *Tbp*, *Nono*, *Actb*, *Rpl13a, B2m*, and *Gapdh*. Data are shown as the mean ± standard deviation (SD) obtained from triplicate samples. The Bonferroni test was used to evaluate the significance of differences between means (**, $P < 0.01$).

Chapter 2

Qualitative and quantitative analyses in sulfated glycosaminoglycans, chondroitin sulfate/dermatan sulfate, during 3T3-L1 adipocytes differentiation

2.1 Introduction

Chondroitin sulfate/dermatan sulfate (CS/DS) is a type of sulfated glycosaminoglycans (GAGs) that construct the extracellular matrix in various vertebrates and invertebrates' tissues (Yamada et al., 2011) in the form of CS proteoglycans (CSPGs), which are involved in various biological events (Mizumoto et al., 2015). Chondroitin sulfate contains repeating disaccharide structures of D-glucuronic acid (GlcA) and *N*-acetyl-D-galactosamine (GalNAc), in the form of 4)GlcAβ(1→3)-GalNAcβ(1 structure (Miyachi et al., 2015; Mizumoto et al., 2015; Zhang et al., 2019). Structural variations associated with the position of sulfation construct the major CS subclasses, such as O [GlcA-GalNAc], A [GlcA-GalNAc(4S)], C [GlcA-GalNAc(6S)], D [GlcA(2S)-GalNAc(6S)], and E [GlcA-GalNAc(4S6S)] units (Sugahara and Mikami, 2007; Sugiura et al., 2012). The epimerization of the uronic acid, D-GlcA into L-iduronic acid (IdoA), results in the formation of DS chains, which are indicated as iO, iA, iC, iD, and iE units according to the coding system proposed by Sugahara and Mikami (Sugahara and Mikami, 2007). The detailed structure of the repeating disaccharides of CS and DS is presented in Figure 2.1A.

Biosynthesis of the CS repeating disaccharide region involves several enzymes known as glycosyltransferases. Chondroitin GalNAc transferase-1 (ChGn-1) and ChGn-2 which possess both GalNAc transferases I (GalNAcT-I) and GalNAcT-II activities, respectively, catalyze the chain initiation and elongation of CS backbone (Gulberti et al., 2012; Sato et

al., 2003; Uyama et al., 2003). Other glycosyltransferases, chondroitin synthase-1 (ChSy-1), ChSy-2, ChSy-3, and chondroitin polymerizing factor (ChPF), that possess GlcA transferase II (GlcAT-II) and GalNAcT-II activities, respectively, are involved in the chondroitin polymerization (Izumikawa et al., 2007; Kitagawa et al., 2003; Yada et al., 2003). Moreover, formation of the structural variation of CS/DS chains is catalyzed by sulfotransferases and epimerases: chondroitin 4-*O*-sulfotransferase 1 (C4ST-1), C4ST-2, C4ST-3, chondroitin 6-*O*-sulfotransferase 1 (C6ST-1), GalNAc 4-sulfate 6-*O*-sulfotransferase (GalNAc4S-6ST), uronyl 2-*O*-sulfotransferase (UST), dermatan 4-*O*-sulfotransferase 1 (D4ST-1), and glucuronyl C-5 epimerases (DS-epi1 and DS-epi2) (Mizumoto and Yamada, 2021). A schematic diagram of the CS/DS biosynthesis and sulfation pathways, as well as the related enzyme-encoding genes, are shown in Figure 2.1B.

Study on the content and composition of GAGs, especially CS/DS, in animal tissues has been carried out for decades on various species from both vertebrates and invertebrates (Cahyadi et al., 2022; Higashi et al., 2015; Muthusamy et al., 2004; Okazaki et al., 1992; Sundaresan et al., 2018; Suzuki et al., 2019; Takeda-Okuda et al., 2019; Takeda et al., 2016; Toledo et al., 1977; Vasan et al., 1983; Volpi, 2004; Yamada et al., 2011). In addition, investigations of their biological roles at the cellular and molecular levels have also been carried out progressively. CS/DS is essential for the maintenance of cell proliferation and differentiation (Izumikawa et al., 2014; Mizumoto and Yamada, 2021; Mizumoto and Yamada, 2022; Ogura et al., 2021; Sirko et al., 2007; Volpi et al., 1993). Furthermore, the fluctuation of CS levels during cell differentiation may provide essential information for a better understanding of cell and tissue development. Interestingly, such basic knowledge could provide a potential tool in controlling cells' commitment to differentiate by manipulating the CS abundance. For example, in a previous study, Mikami et al. (2012) revealed that CS amount is reduced during myogenesis, and its enforced suppression of CS

promotes myogenic differentiation. Thus, in other words, factors controlling CS levels may provide therapeutic potential for muscle degeneration.

In adipose tissue development, a serial process of adipogenesis, which includes preadipocyte proliferation and differentiation, occurs and is followed by the enlargement of the lipid droplet. During adipogenesis, transcription factors such as peroxisome proliferator-activated receptor gamma (PPARγ), CCAAT-enhancer-binding protein alpha (C/EBPα), and fatty acid binding protein 4 (FABP4) express to regulate adipogenesis (Rosen and MacDougald, 2006). In addition to the study in C2C12 myoblast (Mikami et al., 2012), studies on GAG and gene expression profiles during tissue stem cell differentiation have been conducted in MC3T3-E1 osteoblast (Haupt et al., 2009), human bone marrow mesenchymal stromal cells (hBMSCs, toward hepatocytes) (Mikael et al., 2019), and murine embryonic stem cells (mESCs, toward embryoid bodies and extraembryonic endodermal cells) (Nairn et al., 2007, 2012). Moreover, analysis of CSPG expression in adipose tissue and 3T3-L1 cells adipogenesis, which is our focus in this study, has also been reported in several studies (Calvo et al., 1991; Han et al., 2020; Musil et al., 1991; Zizola et al., 2007).

However, information on the detailed composition of CS types and expression profiles of CS-related genes in the 3T3-L1, the most used cell line in adipogenesis studies, is still limited. Given the role of CS in tissue stem cell proliferation and differentiation, we believe that understanding the changes in CS/DS content and composition during adipogenesis is essential to elucidate the role of CS/DS in the regulation of adipogenesis. Adipocyte biology has been studied in animal sciences for decades, involving studies related to the enhancement of carcass composition by reducing fat deposition (Etherton, 2000) or the improvement of intramuscular fat deposition as it enhances meat quality and provides sensory benefits (Albrecht et al., 2015; Guan et al., 2017). Similarly, numerous studies on adipocyte development and the discovery of potential therapies for obesity have been conducted for

decades (Ambele et al., 2016; Calvo et al., 1991; Choi et al., 2006; Guan et al., 2017; Han et al., 2020). Since CS/DS is thought to be important in adipocyte differentiation, the present study aims to profile the amount and composition of CS/DS in adipogenesis, as well as gene expression associated with their synthesis and degradation. Of note, the significance of this study is to provide a better understanding of the quantitative and qualitative changes in CS/DS profiles in adipocyte differentiation, which potentially contribute to the control of adipose tissue development.

2.2 Materials and Methods

Cell culture and differentiation

The 3T3-L1 mouse preadipocytes cell line (JCRB9014, RRID:CVCL_0123) was obtained from the Japanese Collection of Research Bioresources Cell Bank (JCRB Cell Bank, Osaka, Japan). Cells were cultured at 37°C under 5% CO_2 condition in the Dulbecco's modified Eagle's medium (DMEM; FUJIFILM Wako Pure Chemical Corporation, Osaka, Japan), supplemented with 10% fetal bovine serum (FBS; Biosera, Ringmer, UK) and 1% commercial mixture of antibiotic containing penicillin and streptomycin (FUJIFILM Wako Pure Chemical Corporation), hereinafter referred to as basic culture medium. Two days after reaching the confluency, the cells proceeded without or with adipogenic induction for non-differentiated (ND) and differentiated (DI) groups, respectively. For the DI group, differentiation was started (day 0) by adding the differentiation medium, which was the basic culture medium supplemented with AdipoInducer Reagent containing 10 μg/mL insulin, 2.5 μM dexamethasone, and 0.5 mM 3-isobutyl-1-methylxanthine (Takara Bio, Shiga, Japan), for two days. The medium was then replenished with maintenance medium (basic culture medium supplemented with 10 μg/mL insulin) every two consecutive days, until day 10. A

standard culture medium added with phosphate-buffered saline (PBS, pH 7.4) was used to replenish the medium for the ND group at the same time course.

For studies to determine the CS/DS amount and composition as well as the molecular weight analysis, the 3T3-L1 preadipocytes were cultured in T75 flasks and divided into two groups, ND and DI groups. Cells were harvested for analysis on day 10. For gene expression analysis using reverse transcription quantitative real-time polymerase chain reaction (RT-qPCR), cells were seeded in 12-well plates and divided into five groups at three different time courses as follows: (i) Control, confluent preadipocytes on day 0, (ii) ND and (iii) DI groups on day 5, and (iv) ND and (v) DI groups on day 10.

Oil red O staining

Oil Red O (ORO) staining was performed on the Control group, as well as the ND and DI groups on days 5 and 10, to determine the progression of adipocyte differentiation, which was shown by lipid droplet accumulation. Cells were washed with PBS and fixed with 10% neutral-buffered formalin (pH 7.4; FUJIFILM Wako Pure Chemical Corporation) overnight at room temperature. Further, cells were stained with a freshly prepared ORO staining solution (Lipid Assay Kit; Cosmo Bio, Tokyo, Japan) according to the manufacturer's instructions. Briefly, after staining for at least 15 minutes at room temperature, the ORO staining solution was removed, and the stained cells were washed with distilled water (dH_2O) three times. Images of the cells were captured using an inverted light microscope (Olympus IX71; Olympus, Tokyo, Japan). Isopropanol was used to extract the dye from the stained lipid droplets. Semi-quantitative approach by measuring the absorbance of the dye extraction using a microplate reader (Tecan Sunrise Remote, Grödig, Austria) at 492 nm was performed to quantify the amount of oil droplets.

Isolation of GAGs from the 3T3-L1

On day 10, the culture medium was aspirated from the flasks, and the cells were washed with PBS to completely remove the remaining culture medium. The PBS was then aspirated, and 3 mL of absolute ethanol (EtOH) was added to each flask. The cells were harvested by using a cell scrapper. The EtOH and the precipitates were moved to the sample tubes and dried in a desiccator equipped with a vacuum pump for 2 h. These dried samples were weighed and then proteolyzed, concisely, distilled water (8 mL/g dried sample) was added into the tube containing the dried sample and this suspension was incubated at 55°C, followed by the addition of borate buffer (0.5 M, pH 7.0, 10 mL/g dried sample) and 5% protease (PROTIN NY100, Amano Enzyme, Nagoya, Japan) (50 mg/g dried sample). After completing the incubation for 5 days, each suspension was cooled on ice and quenched by adding the trichloroacetic acid (5%, w/v), followed by centrifugation. Sodium acetate (5%, w/v) and 4 times the volume of EtOH were added. The samples were then spined down and the EtOH was removed. To each sample, 0.5 mL of purified water was added, and the suspension was freeze-dried overnight.

Compositional analysis of CS/DS

Prior to the compositional analysis of CS/DS, 300 µL of dH_2O was added to the dried samples. The enzymatic digestion was performed by adding 100 µL of the sample substrate in a mixture of bovine serum albumin (BSA) solution (0.01 mg/µL), 250 mM Tris-HCl buffer (10 µL, pH 8.0), and chondroitinase ABC (1 mU/µL) (EC 4.2.2.4, Sigma Aldrich, Tokyo, Japan) or chondroitinase AC (1 mU/µL) (EC 4.2.2.5, IBEX Pharmaceuticals, Montreal, Canada) for 8 h at 37°C or 30°C, respectively. Chondroitinases, enzymes that have been used for CS/DS disaccharides compositional analysis (Yoshida et al. 1989), create a double bond between carbons 4 and 5 in the uronic acid residue at the cleavage site, resulting

in unsaturated disaccharides. Therefore, the CS/DS disaccharides we analyzed in this study were in the form of unsaturated disaccharides rather than in the form of CS/DS oligosaccharides. A schematic diagram of the enzymatic digestion of GAGs is presented in Figure 2.2. Unsaturated disaccharides obtained from the enzymatic digestion were filtered with centrifugal filter units (Millipore Ultrafree-MC-HV, Durapore-PVDF 0.45 μm, Merck Millipore, Carrigtwohill, Ireland). CS/DS amount and type were analyzed using a high-performance liquid chromatography (HPLC) system as previously described by Yoshida et al. (1989). In the present study, the analysis was performed using HPLC Waters 616 Pump with Waters 600s Controller and Waters 2487 Dual λ Absorbance Detector (Waters Corporation, Milford, MA, USA). A volume of 25 μL of sample was injected onto a YMC-Pack PA-G column (4.6 × 250 mm, 5 μm; YMC, Kyoto, Japan) and the analysis was performed under the following conditions: isocratic conditions with eluent 16 mM NaH_2PO_4 buffer for the first 10 min followed by a linear gradient from NaH_2PO_4 buffer to 800 mM NaH_2PO_4 buffer at 25 °C, flow rate of 1 mL/min, UV absorbance at 232 nm. To distinguish the hyaluronic acid (HA) from the CS/DS hybrid chains, the 4,5-unsaturated hexuronic acid (ΔHexA)-GalNAc and ΔHexA-GlcNAc were detected by using an HPLC system (ÄKTA Purifier, General Electric Healthcare, Boston, MA, USA), according to the method described in the previous study (Hjerpe et al., 1982). Briefly, analysis on 50 μL of sample was carried out on the Hypersil APS-2 columns (100×4.6 mm+250×4.6 mm, 5 μm; Thermo Scientific, Waltham, MA, USA) in combination with the Shodex OHpak SB-G 6B guard column (6.0 ×50 mm, Showa Denko K. K., Kanagawa, Japan), under the following conditions: isocratic at 35 °C, using 9 mM of NaH_2PO_4 (pH 2.55), flow rate of 0.8 mL/min, UV absorbance at 231 nm. Calculation of the amounts of CS/DS hybrid chains and their sulfation patterns was performed by using a calibration curve based on the HPLC peak area of the standard unsaturated disaccharide (Seikagaku Corporation, Tokyo, Japan). In short, as previously

described by Akatsu et al. (2011), the total amount of disaccharide from chondroitinase AC digests subtracted from chondroitinase ABC digests to estimate the IdoA-containing disaccharides.

Determination of molecular weight of the GAGs

The molecular weight of the crude glycans was estimated by using size exclusion chromatography (SEC). A concentration of 1 mg/mL glycan solution in dH_2O was prepared and analyzed in a system consisting of a Shodex OHpak SB-G 6B guard column (6.0×50 mm, Showa Denko K. K.) followed by the Shodex OHpak SB-805 HQ analytical column (8.0×300 mm, Showa Denko K. K.) using 0.1 M $NaNO_3$ buffer at a flow rate 1 mL/min. This HPLC analysis was performed over an 18-min period and monitored with a refractive index (RI) indicator. For this measurement, the result obtained from pullulan standards (Shodex Standard Pullulan Kit P-82, Showa Denko K. K.) was used to generate the molecular weight calibration curve.

RT-qPCR

The total RNA was extracted from the cells by using ISOSPIN Cell & Tissue RNA (Nippon Gene, Tokyo, Japan) and quantified by using NanoDrop 2000c Spectrophotometer (Thermo Fisher Scientific, Wilmington, DE, USA). An aliquot of each total RNA (500 ng) sample was reverse transcribed for cDNA synthesis using ReverTra Ace qPCR RT Master Mix with gDNA Remover (Toyobo, Osaka, Japan). The RT-qPCR experiments were carried out on a LightCycler® Nano Real-Time PCR Instrument using FastStart Essential DNA Green Master (Roche Diagnostics GmbH, Mannheim, Germany). Adipogenesis transcription factors, peroxisome proliferator-activated receptor gamma (*Pparg*) and fatty acid binding protein 4 (*Fabp4*), were examined to verify the adipogenic induction, in

addition to the ORO staining quantitative approach. Furthermore, the following gene expression levels were analyzed: chondroitin sulfate *N*-acetylgalactosaminyltransferase 1 (*Csgalnact1*), chondroitin sulfate *N*-acetylgalactosaminyltransferase 2 (*Csgalnact2*), chondroitin sulfate synthase 1 (*Chsy1*), chondroitin polymerizing factor (*Chpf*), hyaluronoglucosaminidase 1 (*Hyal1*), hyaluronoglucosaminidase 2 (*Hyal2*), carbohydrate sulfotransferase 12 (*Chst12*), carbohydrate sulfotransferase 15 (*Chst15*), uronyl-2-sulfotransferase (*Ust*), carbohydrate sulfotransferase 14 (*Chst14*), dermatan sulfate epimerase (*Dse*), and dermatan sulfate epimerase-like (*Dsel*). Each gene expression level was normalized to that of a previously validated suitable reference gene, peptidylprolyl isomerase A (*Ppia*) (Cahyadi et al., 2023). Detailed information about the primer sets used in RT-qPCR reactions is presented in Table 2.1.

Data analysis

All data are presented as mean ± standard deviation (SD). A significant difference between the two groups was determined using an unpaired two-tailed *t*-test, while the comparisons among the means in multiple groups were performed using a one-way analysis of variance (ANOVA) followed by a Bonferroni *post hoc* test. A P-value less than 0.05 was considered statistically significant. Statistical analyses were performed using the Microsoft Excel add-in statistical software (BellCurve for Excel version 4.02; Social Survey Research Information, Tokyo, Japan).

2.3 Results

Confirmation of the status of adipocyte differentiation

The ORO staining confirmed that 3T3-L1 cells in the DI group transformed into adipocyte-like structures and accumulated lipid droplets on days 5 and 10 after being induced to differentiate. However, cells in the ND group, like those in the control group, maintained their fibroblast-like phenotype and did not accumulate lipid droplets (Figure 2.3A). This result was confirmed by a semi-quantitative analysis of the absorbance for lipid droplet accumulation (Figure 2.3B). In addition, as many studies revealed the cellular events that occurred during adipogenesis, we have also confirmed the surge of the mRNA expression of the adipogenesis transcription factors, *Pparg* and *Fabp4*, in the DI group on days 5 and 10 (Figure 2.3C,D).

Quantitative analysis of CS/DS contents

Representative chromatograms of GAG peptides after digestion with chondroitinases are shown in Figure 2.4A. The amount of unsaturated CS/DS and HA disaccharides, as well as their compositions calculated from the HPLC analysis, are summarized in Figure 2.4B,C, and in Table 2.2. In this study, the compositional analysis of CS/DS was performed only on the 3T3-L1 cells that underwent 10 days of adipogenic differentiation. This was done to highlight the difference between the ND and DI groups, as on day 10 of the DI group, the cells were considered almost completely differentiated. The amount of the unsaturated disaccharides of CS/DS from the 3T3-L1 cell cultures was significantly decreased in the DI group compared to the ND group ($P<0.01$). A measured amount of CS+DS in the cells from ND and DI groups was 0.48 ± 0.13 mg and 0.10 ± 0.03 mg, respectively. In addition to the CS/DS detected in our analysis, the HA amount in the cells from the DI group was about

90% less (0.04 ± 0.00 mg) than that of the ND group (0.46 ± 0.15 mg) (P<0.01) (Figure 2.4B).

Molecular weight of the GAGs contained in 3T3-L1 cells

In addition to the GAG compositional analysis, the present study investigated its molecular weight. The molecular weight revealed in this study corresponds with the chain length of the GAGs. However, the estimation of this molecular weight should be considered as from the mixture of the CS/DS and HA. Lower weight-average molecular weight (Mw; 3.1 ± 0.3 kDa) was detected in the samples from the differentiating 3T3-L1 cells (DI group) with a low degree of dispersion indicated as Mw and number-average molecular weight (Mn) ratio (Mw/Mn; 2.2 ± 0.1). Contrarily, the GAGs contained in the cells from the ND group possessed the Mw value 10.3 ± 1.0 kDa with a higher degree of dispersion (Mw/Mn; 5.2 ± 0.1). Representative HPLC chromatograms and the comparative Mw between ND and DI groups are shown in Figure 2.4D,E.

Decreased expression of Csgalnact1, Csgalnact2, and Chpf in differentiated cells

To investigate the functional analysis of the CS synthesis in 3T3-L1 cells, the mRNA expressions of genes encoding glycosyltransferases that are involved in the CS biosynthesis, *Csgalnact1*, *Csgalnact2*, *Chsy1,* and *Chpf,* were examined. In the DI group, regardless of the time course, our results showed the remarkably low expression of *Csgalnact1* and *Chpf,* and considerably lower expression of both *Csgalnact2* on day 10, but not *Chsy1,* which was not altered during the differentiation compared to that of non-differentiated cells, as well as the control group (Figure 2.5A–D).

CS degradation-associated Hyal1 expression

In addition to the glycosyltransferases-encoded genes expression, we also investigated the expression of CS hydrolases-related genes, *Hyal1* and *Hyal2*. Our results showed that *Hyal1* expression in the ND group was significantly decreased on day 10. Although *Hyal1* expression on day 10 in the DI group was not different compared to those of the ND and DI groups on day 5 and the control group, the expression was considerably higher compared to that of the ND group on day 10 ($P = 0.074$). On the other hand, the expression level of *Hyal2* was not altered over the time course and by the adipogenic induction, except for its decreased expression in the DI group on day 10 compared to that of on day 5 (Figure 2.5E,F).

Decrease in Dsel expression in the differentiated cells

The DI group showed a difference in the composition of the GlcA and IdoA residues of CS/DS compared to the ND group. This led us to investigate the expression of DS-epimerases-encoding genes, *Dse* and *Dsel*, which promote the formation of IdoA in the CS/DS chain (Akatsu et al., 2011; Maccarana et al., 2009; Pacheco et al., 2009a). Our study revealed that the *Dse* expression in the DI group on day 5 was decreased compared to that in the ND group, but there was no difference between both groups on day 10 (Figure 2.6A). On the other hand, the DI group on day 10 exhibited a significantly lower *Dsel* expression compared to the ND group (Figure 2.6B).

Composition of CS/DS types and sulfotransferases gene expression

The composition of the unsaturated disaccharides of CS/DS in 3T3-L1 preadipocytes was revealed in our study, demonstrating the ΔA unit [GlcA-GalNAc(4S) and IdoA-GalNAc(4S)] (calculated from A+iA units) as the major CS/DS disaccharides in 3T3-L1 cell line that reached 89% and 86% in ND and DI groups, respectively (Figure 2.4C). In fact,

compositions of the unsaturated disaccharides in CS vary among the cell lines, but the ΔO unit (ΔDi-0S), ΔA unit (ΔDi-4S), or ΔC unit (ΔDi-6S) are the major three disaccharides (Higashi, 2020). By using the adipogenic-induction medium to promote cell differentiation, our results also showed a significant change in its composition between both groups. The composition of the GlcA residues, A unit [GlcA-GalNAc(4S)], was increased in the DI group (44%), compared to the ND group (27%). Contrarily, the less IdoA residues [IdoA-GalNAc(4S)] were detected in the DI group (42%), compared to the ND one (62%). The GlcA and IdoA residues of ΔO unit, O [GlcA-GalNAc(0S)] and iO [IdoA-GalNAc(0S)] CS/DS disaccharides in non-differentiated 3T3-L1 cells were 8% and 2%, respectively. However, both O and iO units were not detectable in the DI group, suggesting the absence or possibly a very low amount of the ΔO unit presence in the differentiated 3T3-L1 cells. Moreover, only IdoA residues of ΔE unit, iE, were detected in both ND (2%) and DI groups (14%).

We have demonstrated the mRNA expression level of CS/DS sulfotransferase-related genes as shown in Figure 2.6C–F. The mRNA expression level of *Chst12* was increased significantly in the DI group on day 10, supporting the result that the composition of the A unit of CS was increased. Our study also revealed that the *Chst15* expression level on day 10 was substantially higher compared to those on day 5 and the control group. The mRNA expression level of this gene on day 10 was significantly decreased in the DI group compared to the ND group. Another sulfotransferase-encoded gene, *Ust,* was generally expressed higher on day 10 compared to those on day 5 and the control group with no significant difference observed between ND and DI groups.

2.4 Discussion

In this chapter, our study confirms that both the lipid droplet accumulation and expression of the adipogenesis markers increase in a day-dependent manner. A decrease in CSPG levels in various cells has been reported in some studies. Calvo et al. (1991) reported that CSPGs increase during the differentiation of 3T3-L1 cells, but Zizola et al. (2007) confirmed the decrease in large CSPG molecule level after a few days, as observed at 72 h after the initiation of cell differentiation. Previous research showed that the CSPG contents are decreased in the differentiated U-937-4 macrophage-like cells (Kolset et al., 1988) and in the differentiated HL-60 cells toward granulocytes and monocytes (Laskin et al., 1991; Reiss et al., 1985). Although in this study we measured the CS/DS disaccharide under a different experimental design compared to those previous studies, it seems that the decrease in GAGs biosynthesis is a common phenomenon that occurs upon cell differentiation in some cell types including 3T3-L1 adipocytes. Moreover, our results indicate the decrease of CS/DS biosynthesis and/or the increase of their degradation during the 3T3-L1 cell differentiation.

The remarkably low molecular weights of the GAGs detected in our study are still within the range of the CS/DS subclass, which is from 2 to 50 kDa (Leal et al., 2023). The decrease in the GAG molecular weight representing the shorter CS/DS chains supports the results of the decreased CS/DS contents after adipocyte differentiation. Regarding the expression of CS biosynthesis-related genes, a previous study reported a similar result of the decreased expression of the *CSGALNACT1* gene (compared to controls) in human adipose-derived stromal cells (ASCs) at 7 and 21 days after adipogenic induction (Ambele et al., 2016). It is known that some glycosyltransferases, namely ChGn-1, ChGn-2, ChSy-1, ChSy-2, ChSy-3, and ChPF, regulate CS synthesis. These glycosyltransferases are involved in a series of events, including chain initiation and catalyze chondroitin polymerization, forming

the repeating GlcA and GalNAc disaccharide residue (Gulberti et al., 2012; Izumikawa et al., 2007, 2008; Mikami and Kitagawa, 2013; Sato et al., 2003). Moreover, this complex polymerization activity in CS biosynthesis involves various combinations of the above enzymes (Izumikawa et al., 2007, 2008). These phenomena of the decreased expression of the genes encoding glycosyltransferases strongly support the results of CS/DS analysis, in which the content was significantly decreased in the DI group. These findings suggest that during 3T3-L1 differentiation, there is a decrease in glycosyltransferase activity required in the CS biosynthesis.

In conjunction with the results of CS/DS contents, this study evaluates the CS degradation-related genes, *Hyal1* and *Hyal2*. Both *Hyal1* and *Hyal2* encode hyaluronidases, which have degradation activity against CS, as well as HA (Gushulak et al., 2012; Honda et al., 2012; Yamada and Mizumoto, 2022). These results may indicate the involvement of hyaluronidases, mainly HYAL1, in the occurrence of CS degradation in the differentiating cells. However, compared to the glycosyltransferase reduction, the change in *Hyal1* expression is thought to be insignificant. Thus, we suggest that the decrease in the molecular weight, as well as the amount of CS/DS, is predominantly caused by the decrease in their biosynthesis.

DS-epi1 and DS-epi2 encoded by *Dse* and *Dsel*, respectively, facilitate the epimerization of the GlcA residue into IdoA residue resulting in the formation of a DS chain (Pacheco et al., 2009a). Stachtea et al. (2015) reported that double knockout of both DS-epi1 and DS-epi2 mice showed no epimerase activity due to the complete absence of IdoA residue. However, a study in the DS-epi1-null mice showed that epimerase activity is mainly regulated by DS-epi1 in several organs but the brain, which is suggested to be regulated by DS-epi2 (Maccarana et al., 2009). *Dsel* expression in the mouse brain is higher than that of *Dse* and is suggested to be mainly responsible for the IdoA residue (Akatsu et al., 2011).

Suppression of *Dsel* is linked to the decrease of DS-epi2 activity, which may contribute to the decrease in the proportion of IdoA residue compared to GlcA residue. Here we also suggest that epimerase activity in adipose tissue is mainly regulated by DS-epi2.

Sulfotransferase encoded by the *Chst12* gene, C4ST-2, is known to catalyze the sulfate transfer of chondroitin and desulfated dermatan sulfate to position 4 of the GalNAc (Hiraoka et al., 2000), and is involved in CS-A formation. The increased *Chst12* expression in the DI group on day 10 may contribute to the increased ratio of CS-A in the DI group. In addition, an absence of non-sulfated (ΔO unit) CS/DS in the DI group suggests that sulfation at GlcA-GalNAc residues occurred and the CS/DS types were formed; it is reasonable to assume that the increase in *Chst12* promoted the formation of non-sulfated CS/DS to A unit CS/DS. In contrast, the significantly lower expression level of *Chst14* was observed in the same group on day 5 and day 10. The decreasing expression level of another sulfotransferase-encoding gene, *Chst14,* that encodes D4ST-1, is consistent with the genome-wide analysis in human ASCs previously reported, in which the *CHST14* gene was down-regulated on days 7, 14, and 21 post-adipogenic induction (Ambele et al., 2016). Previous studies showed that a lack of D4ST-1 activity due to the *CHST14* gene mutation causes a substantial reduction in the number of IdoA residues (Miyake et al., 2010; Pacheco et al., 2009b). The significant decrease in *Chst14* expression in the DI group probably promotes the substantial reduction of IdoA residue, especially DS-A.

The formation of highly sulfated CS/DS, E units, is facilitated by GalNAc4S-6ST, encoded by *Chst15,* which catalyzes the transfer of sulfates to positions 4 and 6 of their GalNAc residue (Ito and Habuchi, 2000; Ohtake et al., 2003). This lower expression of *Chst15* in the DI group compared to the ND group on day 10, is consistent with the previous research that showed the downregulated *CHST15* gene expression in human ASCs on day 14 of post-adipogenic induction compared to the control group (Ambele et al., 2016). As

previously mentioned, only iE, the IdoA residue of ΔE unit, was detected in the DI group. However, on the contrary, *Chst15* expression was decreased in the DI group compared to the ND group, regardless of its relatively high expression on day 10. Thus, we suggest that the decrease of this *Chst15* expression might occurred in correlation to the decreased CS/DS amount revealed by HPLC analysis, but was not at the level of reducing GalNAc4S-6ST activity. UST, encoded by *Ust*, transfers a sulfate group to position 2 of GlcA and IdoA residues in CS/DS (Kobayashi et al., 1999). However, the absence of its product, ΔD unit, in the present study, suggests that the content of the ΔD unit was very low in 3T3-L1 cells and may have been below the minimum threshold detected by HPLC analysis.

After accounting for the CS biosynthesis-related gene expression trends and the CS/DS contents in both differentiating and non-differentiating cells, we highlight that a decrease in glycosyltransferase activities is the primary cause of the decreased CS/DS contents that occurred during adipogenesis. These findings are graphically illustrated in Figure 2.7. The trend should remain consistent, but we cannot exclude the possibility that fluctuations in the relative amounts of each CS/DS type could occur as a result of the cell culture conditions.

In this study, we showed that the A unit (ΔDi-4S) is the predominant disaccharide in CS/DS from the 3T3-L1 cell line, both in differentiated and non-differentiated cells. The present findings also confirm that the amount of CS/DS was reduced in cells undergoing differentiation. However, it was still unclear whether the CS/DS levels change along with adipocyte differentiation or whether this CS/DS biosynthesis controls adipocyte differentiation. The details of these cause-and-effect relations remain an issue to be elucidated in future studies to support the potential strategies for controlling fat development. Nonetheless, these qualitative and quantitative changes in CS/DS before and after adipocyte differentiation revealed in our study may provide important molecular information for a detailed understanding of adipocyte differentiation.

2.5 Summary

In this study, a high-performance liquid chromatography (HPLC) system was used to reveal the chondroitin sulfate/dermatan sulfate (CS/DS) contents, average molecular weight (Mw), and sulfation pattern in 3T3-L1 during adipogenesis. Additionally, CS/DS synthesis/degradation- and sulfotransferase-related gene expression was also analyzed by reverse transcription real-time PCR (RT-qPCR). The results showed that the CS/DS amount was significantly decreased in the differentiated (DI) group compared to the non-differentiated (ND) group, along with a lower expression of CS biosynthesis-related genes, chondroitin sulfate *N*-acetylgalactosaminyltransferase 1, chondroitin sulfate *N*-acetylgalactosaminyltransferase 2, and chondroitin polymerizing factor. The glycosaminoglycans (GAGs) in the DI group also showed lower Mw than those of the ND group. Furthermore, it was revealed that the A unit (ΔDi-4S) is the predominant disaccharide in CS/DS from the 3T3-L1 cell line, both in differentiated and non-differentiated cells, with a proportionally higher CS-A ratio in the DI group. This was consistent with the expression of carbohydrate sulfotransferase 12 that encodes chondroitin 4-O-sulfotransferase, for CS-A formation. Unlike the ND group, both GlcA and IdoA residues in the O unit of CS/DS from the DI group were absent. Overall, the findings of the study confirm that the CS/DS biosynthesis was reduced in cells undergoing differentiation. It was still unclear whether the CS/DS levels change along with adipocyte differentiation or whether this CS/DS biosynthesis controls adipocyte differentiation. Nonetheless, these qualitative and quantitative changes in CS/DS and CS/DS-synthases/hydrolases before and after adipocyte differentiation reveal valuable insights into adipocyte development.

Table 2.1 Mouse cDNA primer sequences of the various genes used for RT-qPCR

Gene symbol	Primer sequences	Accession number	Product size (bp)	References of primer sequences
Pparg	5'-CAAGAATACCAAAGTGCGATCAA-3' 5'-GAGCAGGGTCTTTTCAGAATAATAAG-3'	NM_001127330.3	69	Kanda et al. (2009)
Fabp4	5'-TGGAAGCTTGTCTCCAGTGA-3' 5'-AATCCCCATTTACGCTGATG-3'	NM_024406.4	121	Kanda et al. (2009)
Csgalnact1	5'-TCTCTGGTTCCTGCTCACTGAAATA-3' 5'-TCTGCTTGGTCTGAGACTTTGGTAG-3'	NM_001252623.1	144	Ogawa et al. (2012)
Csgalnact2	5'-TCTGCCTGGTACCTGTGTTCTGA-3' 5'-TATCTGCCTGAACATTTCGACCAA-3'	NM_001362149.1	115	Ogawa et al. (2012)
Chsy1	5'-AACTTTCTCTTCGTGGGAGTCA-3' 5'-GGAATTGTCTTGGACCATGT-3'	NM_001081163.2	89	Lyu et al. (2022)
Chpf	5'-TTCGTCCCTCTCCGCTAGCTGACG-3' 5'-AAGGCGGCCGCTGTCCGACGTGTC-3'	NM_001001566.3	83	Ogawa et al. (2012)
Hyal1	5'-TACACAGCATGCTCAGAAAG-3' 5'-AGTGTCTCCATTCCAAACAG-3'	NM_008317.6	193	Myung et al. (2019).
Hyal2	5'-CGAGGACTCACGGGACTGA-3' 5'-GGCACTCTCACCGATGGTAGA-3'	NM_010489.3	57	Jadin et al. (2008)
Chst12	5'-ATCAGCATCACCAGCAACA-3' 5'-TTGGTCATGCTGCCCTG-3'	NM_021528.3	138	Koike et al. (2015)
Chst14	5'-CCAAAGTGGCCTGCTCTAACTG-3' 5'-AAGTCACTGCGGTGGTCCAT-3'	NM_028117.3	100	Yoshizawa et al. (2018)
Chst15	5'-TATGACAACAGCACAGACGG-3' 5'-TGCAGATTTATTGGAACTTGCGAA-3'	NM_029935.6	153	Mizumoto et al. (2013)
Ust	5'-TCGTACCGTGGTCTTGCTTC-3' 5'-TAAATAGGGCTGTTCGGCGG-3'	NM_177387.3	148	Hosaka et al. (2022)
Dse	5'-AGCACATTGCAGCTCGGCTTAC-3' 5'-GCTGCCATCCTCTCCATGTAGTC-3'	NM_172508.3	211	Stachtea et al. (2015)
Dsel	5'-ACGTGGTCAAATGGCTTCAT-3' 5'-GCTGTGAAATCCAGGTGACAT-3'	NM_001081316.2	274	Stachtea et al. (2015)
Ppia	5'-CAGGTCCATCTACGGAGAGA-3' 5'-CATCCAGCCATTCAGTCTTG-3'	NM_008907.2	146	Muñoz et al. (2021)

Table 2.2 Amount type of disaccharides, and ratio of disaccharides members contained in non-differentiated and differentiated 3T3-L1 cells

Sample	Defatted dry weight (mg)	Concentration (g/100 g defatted dry cells)		Actual concentration (whole cultured cells) (mg)		CS, DS composition (%)								
		CS+DS	HA	CS+DS	HA	O	iO	A	iA	C	iC	D+iD	E	iE
Non-differentiated (ND)														
ND (1)	17.3	3.57	3.51	0.62	0.61	7	4	25	62	0	0	0	0	3
ND (2)	10.1	3.59	4.65	0.36	0.47	7	1	34	55	0	0	0	0	2
ND (3)	10.2	4.52	3.08	0.46	0.31	10	0	20	68	0	0	0	0	2
			Mean	0.48	0.46	8	2	27	62	0	0	0	0	2
			SD	0.13	0.15	1	2	7	7	0	0	0	0	0
Differentiated (DI)														
DI (1)	24.0	0.39	0.15	0.09	0.04	0	0	49	37	0	0	0	0	14
DI (2)	24.5	0.26	0.15	0.06	0.04	0	0	47	39	0	0	0	0	13
DI (3)	27.7	0.46	0.14	0.13	0.04	0	0	36	50	0	0	0	0	14
			Mean	0.10	0.04	0	0	44	42	0	0	0	0	14
			SD	0.03	0.00	0	0	7	7	0	0	0	0	1

Abbreviations of disaccharides: O, -GlcA-GalNAc-; iO, -IdoA-GalNAc; A, -GlcA-GalNAc4S-; iA, -IdoA-GalNAc4S; C, -GlcA-GalNAc6S-; iC, -IdoA-GalNAc6S; D, -GlcA2S-GalNAc6S-; iD, -IdoA2S-GalNAc6S; E, -GlcA-GalNAc4S6S; iE, -IdoA-GalNAc4S6S

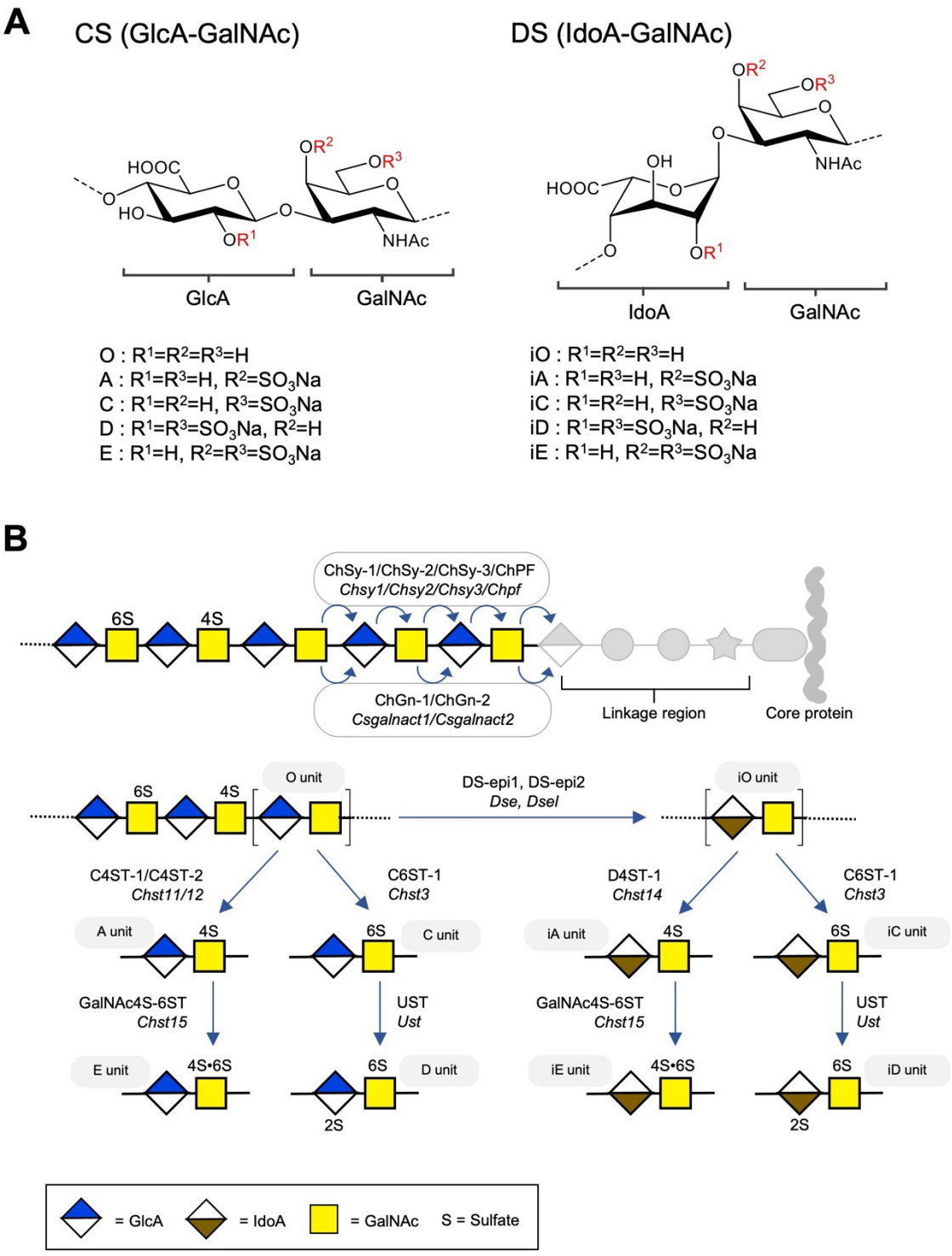

Figure 2.1 Structure and biosynthesis of CS and DS. (**A**) The chemical structure of CS and DS disaccharides repeating units comprise GlcA or IdoA, and GalNac. (**B**) Schematic diagram of CS/DS biosynthesis. A number of glycosyltransferases catalyze chain initiation and elongation, as well as participate in chondroitin polymerization. Several sulfotransferases catalyze the sulfation at various positions in CS/DS, resulting in the formation of different CS/DS types. Abbreviation: GlcA, glucuronic acid; GalNAc, *N*-acetylgalactosamine; IdoA , iduronic acid; ChSy, chondroitin synthase; ChPF, chondroitin polymerizing factor; ChGn, chondroitin GalNac transferase; C4ST, chondroitin 4-*O*-

sulfotransferase; C6ST, chondroitin 6-*O*-sulfotransferase; GalNAc4S-6ST, GalNAc 4-sulfate 6-*O*-sulfotransferase; UST, uronyl 2-*O*-sulfotransferase; D4ST, dermatan 4-*O*-sulfotransferase; DS-epi, glucuronyl C-5 epimerase; *Chsy*, chondroitin sulfate synthase; *Chpf*, chondroitin polymerizing factor; *Csgalnact*, chondroitin sulfate *N*-acetylgalactosaminyltransferase; *Chst*, carbohydrate sulfotransferase; *Ust*, uronyl-2-sulfotransferase.

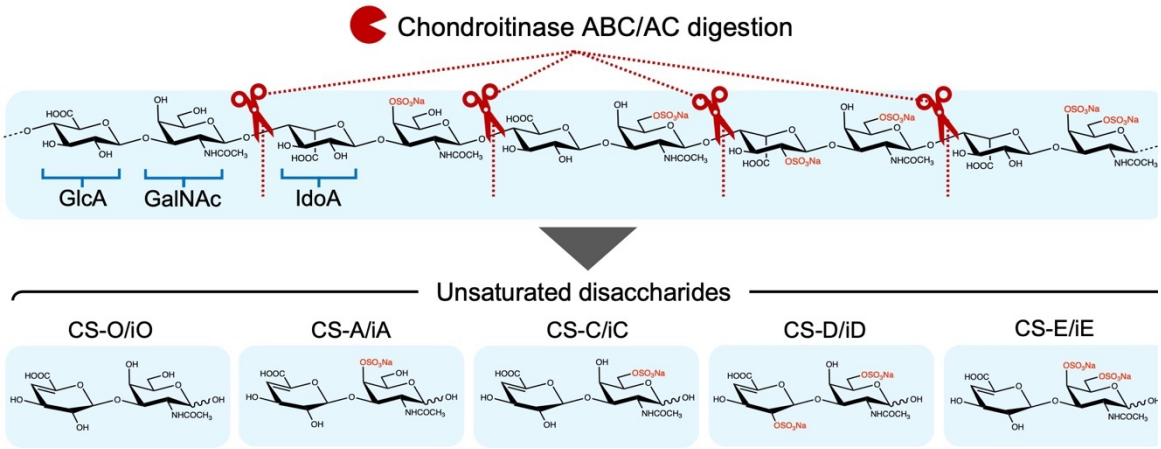

Figure 2.2 Enzymatic digestion of the GAGs using chondroitinase ABC and AC. Chondroitinases produce an unsaturated compound that possesses double carbon-carbon bonds in the uronic acid (GlcA and IdoA) residues at the cleavage site. CS/DS types of these unsaturated disaccharides are determined by using an HPLC system. Abbreviation: GlcA, glucuronic acid; GalNAc, *N*-acetylgalactosamine; IdoA, iduronic acid.

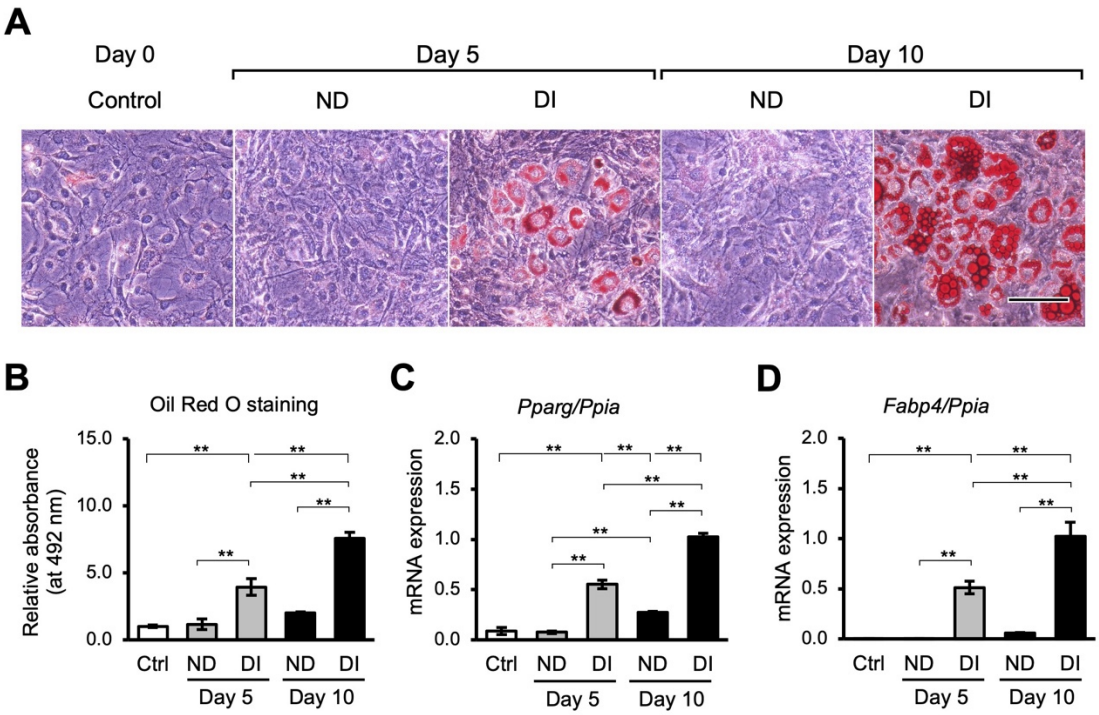

Figure 2.3 Semi-quantitative Oil Red O (ORO) staining and adipogenesis transcription factors-related gene expression analysis confirms the adipocyte differentiation. (**A**) Lipid droplet accumulation was observed in the differentiated (DI) groups, on days 5 and 10 post-differentiation induction. Scale bar = 100 µm. (**B**) Accumulation of lipid droplets was observed in the differentiated 3T3-L1 cells of the DI groups. The absorbance of the eluted ORO obtained from the stained oil droplets was measured using a microplate reader at 492 nm. **P < 0.01 using Bonferroni test. (**C**) *Pparg* and (**D**) *Fabp4* expression per 50 ng of total RNA in all experimental groups. The mRNA expression of both *Pparg* and *Fabp4* in the DI groups was higher than in the ND groups. **P < 0.01 using Bonferroni test. Data are presented as the mean ± standard deviation (SD) of triplicate samples.

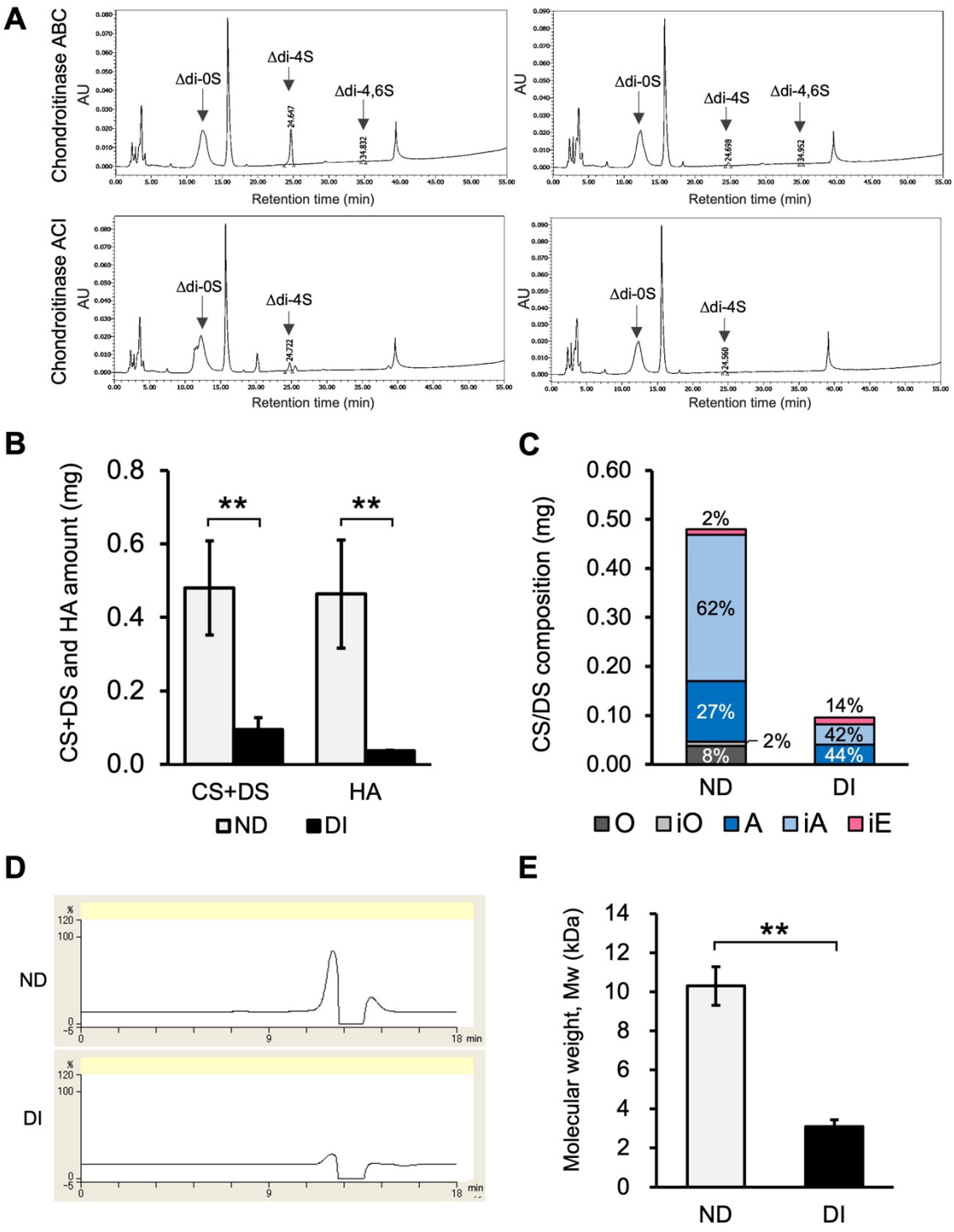

Figure 2.4 Glycosaminoglycans (GAGs) contents, composition of CS/DS types, and its molecular weight. (**A**) Representative chromatograms of the unsaturated disaccharides obtained from the chondroitinase digestion detected in the 3T3-L1 cells of the non-differentiated (ND) and differentiated (DI) groups. The elution positions of unsaturated disaccharides are indicated: Δdi-0S, ΔHexAα1-3GalNAc (ΔO unit); Δdi-4S, ΔHexAα1-3GalNAc(4S) (ΔA unit); Δdi-4,6S, ΔHexAα1-3GalNAc(4S,6S) (ΔE unit). (**B**) CS+DS and HA contents were reduced in the DI group compared to the ND group. **P < 0.01 using an unpaired two-tailed *t*-test. (**C**) Composition of the CS/DS types in the ND and DI

groups. ΔA unit was the major CS/DS disaccharide found in 3T3-L1 cells, although the alteration of the CS/DS types composition was observed in the DI group compared to the ND group. (**d**) Representative chromatograms of the non-differentiating and differentiating 3T3-L1 cells-derived GAGs molecular weight measurement. (**e**) The molecular weight of the GAGs in the ND and DI groups. The results indicate a reduction in the chain length of GAGs in the DI group. **$P < 0.01$ using an unpaired two-tailed *t*-test. Data are presented as the mean ± standard deviation (SD) of triplicate samples.

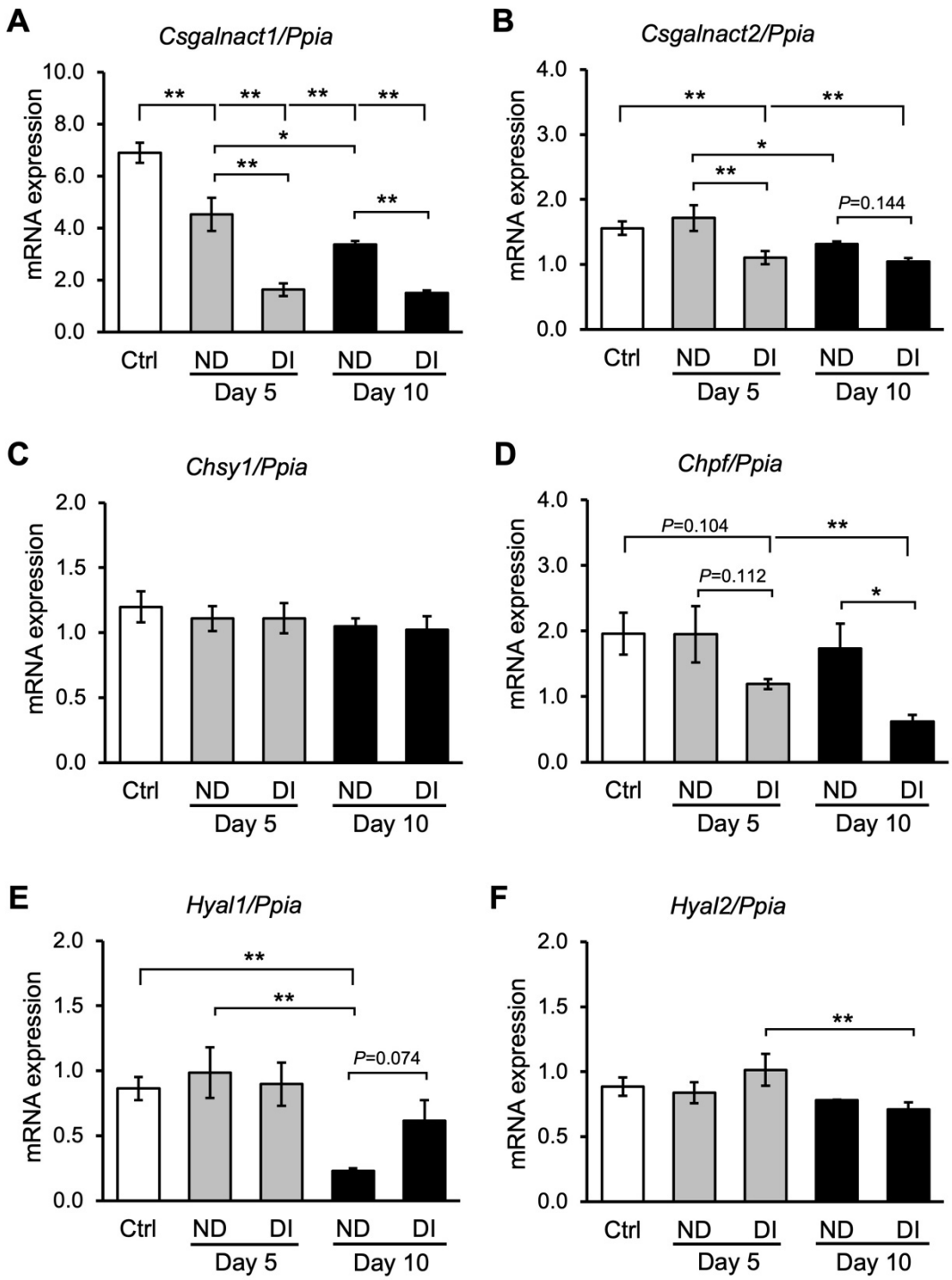

Figure 2.5 Decreased mRNA expression encoding ChGn-1 and -2 (*Csgalnact1* and *Csgalnact2*) and ChPF (*Chpf*) in the DI group compared to the ND and control group. The mRNA expression of glycosyltransferases-encoding genes (**A**) *Csgalnact1*, (**B**) *Csgalnact2*, (**C**) *Chsy1*, (**D**) *Chpf*; and CS hydrolases-encoding genes (**E**) *Hyal1* and (**F**) *Hyal2*. *P < 0.05 and **P < 0.01 using Bonferroni test. Data are presented as the mean ± standard deviation (SD) of triplicate samples.

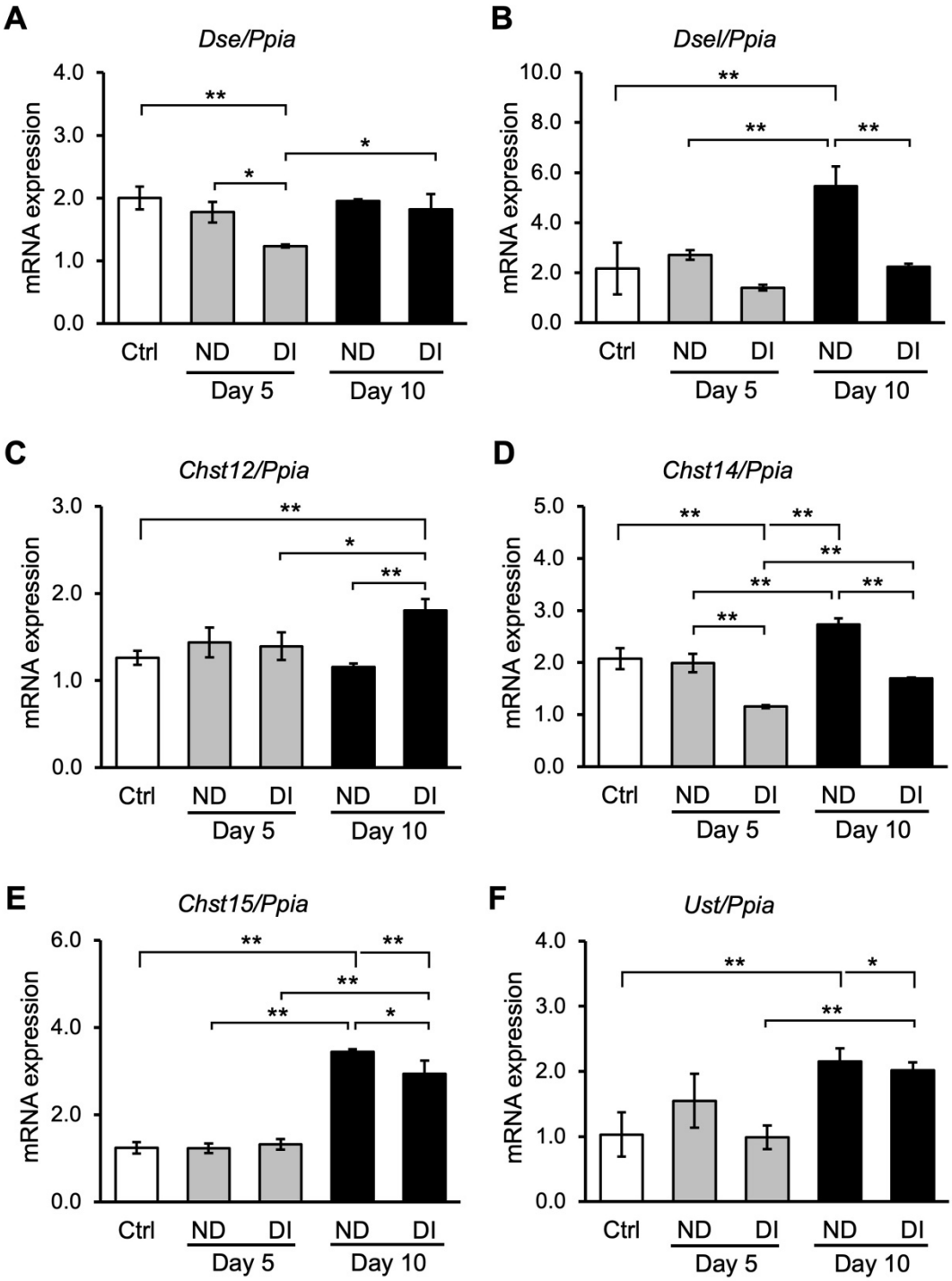

Figure 2.6 mRNA expression levels of genes encoding DS epimerases and sulfotransferases in the non-differentiating and differentiating 3T3-L1 cells. The mRNA expression of (**A**) *Dse*, (**B**) *Dsel*, (**C**) *Chst12*, (**D**) *Chst14*, (**E**) *Chst15*, (**F**) *Ust*. *P < 0.05 and **P < 0.01 using Bonferroni test. Data are presented as the mean ± standard deviation (SD) of triplicate samples.

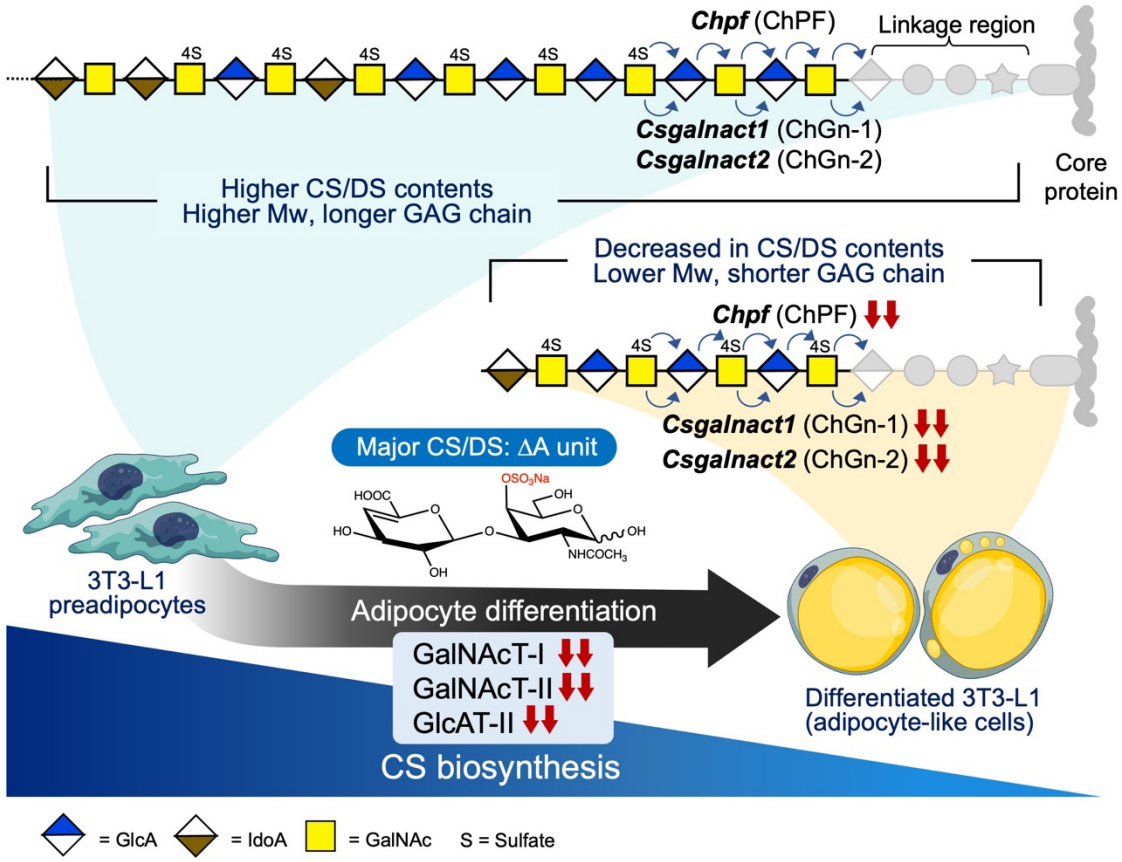

Figure 2.7 Graphical illustration of the changes in the CS/DS contents and its related gene expression, during 3T3-L1 differentiation. In general, a decrease in CS/DS contents in the differentiated 3T3-L1 cells is caused by decreased expression of glycosyltransferase genes. *Csgalnact1* and *Csgalnact2* are associated with the GalNAcT-I and GalNAcT-II activities, respectively, while *Chpf* is associated with both GlcAT-II and GalNAcT-II activities. Abbreviation: GlcA, glucuronic acid; GalNAc, *N*-acetylgalactosamine; IdoA, iduronic acid; ChPF, chondroitin polymerizing factor; ChGn, chondroitin GalNac transferase; *Chpf*, chondroitin polymerizing factor; *Csgalnact*, chondroitin sulfate *N*-acetylgalactosaminyltransferase; GalNAcT, GalNAc transferase; GlcAT, GlcA transferase.

Chapter 3

Cartilaginous fishes-derived chondroitin sulfate suppresses 3T3-L1 adipocyte differentiation

3.1 Introduction

Chondroitin sulfate (CS), a sulfated glycosaminoglycan (GAG), is found at the cell surface and plasma membranes to construct the extracellular matrix (ECM) in most animal tissues (Haylock-Jacobs et al., 2011; Yamada et al. 2011). Currently, animal-derived CSs are widely used in biomedical applications, particularly in treating osteoarthritis in humans and animals (Henrotin et al., 2010). Currently, CS is obtained from natural resources due to the difficulty of chemical synthesis, resulting in variations in composition, chain length, and sulfation patterns based on origin (Martel-Pelletier et al., 2015). Bovine and porcine cartilage are among the main sources of commercial CS (Schiraldi et al., 2010). In addition to the terrestrial animal tissue-derived CS, a variety of tissues or parts, including scales, skin, bones, cartilage, heads, gills, fins, and eyeballs from both marine and freshwater fish species, have been utilized for the extraction of chondroitin sulfate (Gavva et al., 2020; Novoa-Carballal et al., 2017; Valcarcel et al., 2017). However, the yield, purity, composition, and sulfation patterns may vary based on the source and methods used for isolation.

It is known that the potential bioactivity of CS/DS depends on their sulfation patterns and different sources of CS provide distinct biological functions (Volpi, 2019). For example, sturgeon cartilage-derived CS mainly contains the A unit [GlcA-GalNAc(4S)], which enhances cell adhesion and induces proliferation and migration in fibroblasts (Im et al., 2010); C unit [GlcA-GalNAc(6S)]-rich CS disaccharide from ray cartilage increases neurite outgrowth through the hepatocyte growth factor signaling pathway (Hashiguchi et al., 2011).

Nadanaka et al. (1998) reported that shark cartilage-derived CS-D, which contains D-unit [GlcA(2S)-GalNAc(6S)], has been found to promote neurite outgrowth. In addition, exogenous CS-E from squid cartilage, composed mainly of E-unit [GlcA-GalNAc(4S,6S)], promotes osteoblast differentiation (Koike et al., 2012) and exhibits neuroprotective potential in vitro (Sato et al., 2008).

For decades, the processes involved in the adipocyte development have been studied. During early differentiation, preadipocytes undergo a morphological change, which is followed by their transformation into mature adipocytes that store lipids in the terminal differentiation stage. The adipocyte differentiation process is complex and involves the regulation of numerous transcription factors, including two key regulators, peroxisome proliferator-activated receptor gamma (PPARγ) and the CCATT/enhancer binding protein (C/EBPα). These factors control the adipocyte gene program and their coexpression is necessary to differentiate preadipocytes into adipocytes (Madsen et al., 2014; Rosen and MacDougald, 2006; Tang and Lane, 2012). Other potential activities of the CS polysaccharide chain on adipocyte development have also been studied. The anti-obesity potential of salmon nasal CS has been reported to inhibit lipase activity in vitro and has a fat-storage-lowering effect in vivo (Han et al., 2000). Xu et al. (2015) also reported the anti-adipogenic activity of fucosylated CS isolated from the sea cucumber (*Acaudina molpadioides*). Recently, the inhibitory effect of chondroitin sulfate oligosaccharides from mottled skate (*Raja pulchra*) on lipid accumulation in vitro has been previously reported (Li et al., 2019).

Alternative to the mammalian cartilage, the preference for cartilaginous fishes (Chondrichthyes) as the source of CS seems reasonable since cartilaginous fishes possess a higher ratio of cartilage per total body weight (Lee and Langer, 1983). In the previous chapter, our study demonstrated a significant decrease in the CS/DS content during 3T3-L1

adipogenesis, thus, we hypothesize that the exogenous CS treatment would suppress the adipocyte differentiation. This study examined the effect of high-purity CSs extracted from cartilaginous fish of different origins (mako shark, *Isurus oxyrinchus*; blue shark, *Prionace glauca*; sharpspine skate, *Okamejei acutispina*; and stingray, *Dasyatis akajei*) on 3T3-L1 adipocyte differentiation using the same isolation method. The study presents a novel finding about chondroitin sulfate derived from certain marine species, which can potentially inhibit the differentiation of adipocytes.

3.2 Materials and Methods

Preparation of CS from cartilaginous fishes

Cartilaginous fishes-derived CS polysaccharides used in the study were isolated from specific tissues of some species: mako shark (*Isurus oxyrinchus*, spine part), blue shark (*Prionace glauca*, spine part), sharpspine skate (*Okamejei acutispina*, head and tail parts) and stingray (*Dasyatis akajei*, head part). The CS substrates were obtained from previous research samples on the analysis of contents and sulfation patterns of the CS/DS hybrid chain described in Takeda et al. (2016). The contents and sulfation patterns of the cartilaginous fishes-derived CS/DS are summarized in Table 3.1.

To facilitate the CS treatment in vitro, the pure glycans obtained from each cartilaginous fish were subjected to further purification using diethylaminoethyl (DEAE)-cellulose chromatography to get a high purity of glycans. Briefly, a portion of 100 mg crude glycans was diluted with a small volume of 0.15 M LiCl/0.05M acetic acid at pH 4.0. This mixture was applied to a DEAE-cellulose column (size $\phi 2.2 \times 15$ cm). Using 160 mL of buffer containing 0.5, 1.0, and 2.0 M LiCl, the column was gradually washed. Fractions with carbazole-positive properties were subjected to dialysis and further desalted through a column for gel permeation (LH-20, H2O, $\phi 1.1 \times 80$ cm).

Cell culture

The mouse 3T3-L1 preadipocyte cell line from the Japanese Collection of Research Bioresources Cell Bank, Osaka, Japan (JCRB9014), was used in this study as an in vitro adipogenesis model. The cells were cultured in 96- or 12-well plates under a 5% CO_2 atmosphere at 37°C. Dulbecco's modified Eagle's medium (DMEM; FUJIFILM Wako Pure Chemical Corporation, Osaka, Japan), with 10% fetal bovine serum (FBS; Biosera, Ringmer, UK) and 1% of antibiotic mixture -containing penicillin and streptomycin (FUJIFILM Wako Pure Chemical Corporation) supplementation was used to grow the cells.

Cell viability assay

Cells were seeded at a density of 1×10^3 cells per well in 96-well plates, with triplicate runs in each group. Cells were treated with 10, 100, and 1000 μg/mL of the four cartilaginous fishes-derived CS, which are mako shark-derived CS (Ms-CS), blue shark-derived CS (Bs-CS), sharpspine skate-derived CS (Sp-CS), stingray-derived CS (St-CS); and PBS only for control in each group. After 72 hours of incubation, the viability assay was measured using Cell Counting Kit-8 (CCK-8, Dojindo, Kumamoto, Japan). CCK-8 solution (10 μL) was added to each well and followed by 2 hours of incubation for a color reaction. Absorbance was measured at 450 nm with a microplate reader (Sunrise Remote; Tecan Austria GmbH, Grödig, Austria).

Cell differentiation

Cells were seeded in 12-well plates at a density of 5×10^4 cells/mL/well with triplicate runs in each group. After two days of confluence, day 0, the cells were induced for differentiation in a medium containing 10 μg/mL insulin, 2.5 μM dexamethasone, and 0.5 mM 3-isobutyl-1-methylxanthine (AdipoInducer Reagent, Takara Bio, Shiga, Japan) for two

days. A basic culture medium containing 10 μg/mL insulin was utilized to culture the cells, with medium replacement every other two days until day 10. Cells were divided into several groups: negative control group (NC), cultured in basic culture medium with DMSO and PBS only; positive control group (PC), adipogenic-induced cells treated with PBS alone; Ms-CS groups, adipogenic-induced cells treated with 10, 100, and 500 μg/mL of mako shark-derived CS; Bs-CS groups, adipogenic-induced cells treated with 10, 100, and 500 μg/mL of blue shark-derived CS; Sp-CS groups, adipogenic-induced cells treated with 10, 100, and 500 μg/mL of sharpspine skate-derived CS; and St-CS groups, adipogenic-induced cells treated with 10, 100, and 500 μg/mL of stingray-derived CS.

Lipid droplet area measurement

Per the manufacturer's instructions, live cell imaging was performed on day 10 using LipiDye staining (Funakoshi, Tokyo, Japan). Briefly, the culture medium was changed to the 1 μM LipiDye-containing medium and incubated at 37°C for 2 hours. Cells were also incubated with a culture medium containing 2 μg/mL Hoechst 33342 (Dojindo) for nuclear staining at 37°C for 20 minutes. Images of the stained nuclei and lipid droplets were captured using an inverted fluorescent microscope (Olympus IX71; Olympus, Tokyo, Japan). The lipid droplet area in each experimental group was measured using ImageJ, an image-processing software (Schneider et al., 2012). In this measurement, five arbitrary visual fields at 200× magnification were chosen for each replicate sample (n = 3 replicates), providing fifteen visual fields for each experimental group. The measured lipid area presented in this study demonstrated the lipid droplet area per total visual field area of 150,692.52 μm^2.

RT-qPCR

To investigate the gene expression in CS-treated cells, we focused on two CS samples, Ms-CS and Sp-CS, which have the strongest effect based on the morphological evaluation. Differentiated 3T3-L1 cells' total RNA was extracted using the ISOSPIN Cell & Tissue RNA kit (Nippon Gene, Tokyo, Japan). The cDNA was synthesized using ReverTra Ace® qPCR RT Master Mix with gDNA Remover (Toyobo, Osaka, Japan) from 250 ng of RNA of each sample with an A260/280 ratio ranging from 1.94 to 2.19, according to the manufacturer's protocol. Gene expression levels were determined by quantitative real-time PCR (qPCR) with FastStart Essential DNA Green Master reaction mix (Roche Diagnostics GmbH, Mannheim, Germany), with a final volume of 20 μL for each sample. qPCR analyses were performed on a LightCycler® Nano Real-Time PCR Instrument (Roche Diagnostics GmbH). All target gene expressions were normalized to the validated reference gene, *Ppia* (Cahyadi et al., 2023).

Mouse cDNA primers used were as follows: *Pparg* (NM_001127330.3) forward, 5'-CAAGAATACCAAAGTGCGATCAA-3' and reverse, 5'-GAGCAGGGTCTTTTCA GAATAATAAG-3' (Kanda et al., 2009); *Cebpa* (NM_007678.4) forward, 5'-CTAGGAGATTCCGGTGTGGC-3' and reverse, 5'-CCCGAGAGGAAGCAGGAATC-3' (Li et al., 2019); *Csgalnact1* (NM_001252623.1) forward 5'-TCTCTGGTTCCTG CTCACTGAAATA-3' and reverse, 5'-TCTGCTTGGTC TGAGACTTTGGTAG-3' (Ogawa et al., 2012); *Csgalnact2* (NM_001362149.1) forward 5'-TCTGCCTGGTA CCTGTGTTCTGA-3' and reverse, 5'-TATCTGCCTGAACATTTCGACCAA-3' (Ogawa et al., 2012); *Chsy1* (NM_001081163.2) forward 5'-AACTTTCTCTTCGTGGGAGTCA-3' and reverse, 5'-GGAATTGTCTTGGACCATGT-3' (Lyu et al., 2022); *Ppia* (NM_008907.2) forward 5'-CAGGTCCATCTACGGAGAGA-3' and reverse, 5'-CATCCAGCCATT CAGTCTTG-3' (Muñoz et al., 2021).

Data analysis

Data are expressed as mean ± standard deviation (SD). Statistical analyses of the data were performed using Dunnett's test following ANOVA, with the Microsoft Excel add-in statistical software (Bell Curve for Excel version 4.02; Social Survey Research Information, Tokyo, Japan). The statistical significance of the differences was set at a P-value of 0.05 or lower and indicated by an asterisk symbol (*$P < 0.05$ and **$P < 0.01$).

3.3 Results

Cartilaginous fish-derived CS stimulated preadipocyte proliferation in 3T3-L1 cells, with varying effects depending on its origin. At a concentration of 1000 μg/mL, Ms-CS, Bs-CS, and Sp-CS significantly increased 3T3-L1 preadipocyte proliferation after 72 hours, compared to each control group, while St-CS showed a tendency to increase proliferation without statistical significance ($P = 0.0714$) as shown in Figure 3.1. Cells with Bs-CS treatment, in particular, showed significantly higher viability in all concentration ranges of 10, 100, and 1000 μg/mL than those of each control group, with P values of 0.0063, 0.0013, and < 0.001, respectively. These results demonstrated that cartilaginous fish-derived CS accelerates cell proliferation in a concentration-dependent manner.

To evaluate the effect of those cartilaginous fishes-derived CS on adipocyte differentiation, cells were stained with LipiDye for lipid droplet visualization. In contrast to the cell proliferation activity, we observed that the high concentration of CS suppressed lipid accumulation in the mouse 3T3-L1 adipocytes during the adipogenic induction for cell differentiation as shown in Figure 3.2. Fluorescent staining of cellular lipid droplets with LipiDye, a fluorescent dye that specifically visualizes lipid droplets, showed the green lipid droplets in the differentiated 3T3-L1 adipocyte-like cells. A decrease in the occurrence of lipid droplets was seen following the cartilaginous fish-derived CS treatment, particularly at a high concentration (500 μg/mL) compared to the cells in the positive control group. To corroborate our finding of inhibition of lipid droplet accumulation in the cells, we used Hoechst dye, a nuclear counterstain, to qualitatively evaluate the cell density. It seemed that a comparable number of the stained nuclei were also observed in high concentrations of CS-treated groups, clearly seen in the Ms-CS and Sp-CS groups (Figure 3.2). Furthermore, quantification of the lipid droplet area showed a significant reduction in the lipid droplet accumulation in all the CS-treated groups, as shown in Figure 3.3. The lipid droplet area of

the cartilaginous fishes-derived CS-treated groups was significantly lower ($P < 0.01$) than that of the control group. Our results demonstrated that Ms-CS and Sp-CS exhibit the most remarkable decrease in the occurrence of lipid droplets. In addition, the treatment of cartilaginous fishes-derived CS at 10, 100, and 500 μg/mL concentrations showed a decrease in the lipid droplet in a concentration-dependent manner.

Following the decrease in the occurrence of lipid droplets observed in the CS-treated groups, we further investigated the gene expression of adipogenesis markers with a focus on the treatment with two CS origins, Ms-CS and Sp-CS. The group treated with Ms-CS showed increased expression of *Pparg* at concentrations of 100 and 500 μg/mL ($P < 0.05$), and increased expression of *Cebpa* at a concentration of 500 μg/mL ($P < 0.05$), compared to the control group (Figure 3.4). On the other hand, although a significant difference was not observed in the Sp-CS treated groups, a decreasing trend in the expression of *Pparg* and *Cebpa* was seen, indicating a reduction in expression in a concentration-dependent manner across the different Sp-CS concentration.

Furthermore, our evaluation of the CS biosynthesis genes, *Csgalnact1*, *Csgalnact2*, and *Chsy1,* showed a relatively consistent expression in the CS-treated groups of Ms-CS and Sp-CS groups, compared to the control group, regardless of the concentration given to the cells (Figure 3.5). We observed a significant increase in the *Csgalnact2* expression in the Sp-CS group at the concentration of 500 μg/mL ($P < 0.01$).

3.4 Discussion

Adipocyte development includes the transition process of undifferentiated fibroblast-like preadipocytes undergoing morphological changes to mature lipid-loaded adipocyte morphology (Butterwith, 1994; Farmer, 2006). In the present study, despite the lipid droplets seen in all CS-treated groups, a decrease in the occurrence of lipid droplets is strong evidence

that CS suppressed adipocyte differentiation by inhibiting lipid droplet formation. Furthermore, with the degree of lipid droplet reduction, we suggest that Sp-CS shows the strongest inhibitory effect on lipid droplet accumulation among four different CS origins. Based on the report by Takeda et al. (2016), the C type of CS disaccharide (CS-C) is the major disaccharide contained in cartilaginous fishes-derived CS used in this study; however, each substrate possesses a different compositional structure. Therefore, it should be noted that the effect on the 3T3-L1 cell proliferation and differentiation is distinct. Unless CS/DS polysaccharides have similar structures, CS/DS samples will not produce the same clinical effects (Yamada and Sugahara, 2008). Furthermore, it is thought that the 4S/6S ratio of CS disaccharides is considered important in determining their bioactivity. Miyata et al. (2012) reported that changes in the abundance of 4S and 6S CS disaccharides (4S/6S ratio) can affect the stability and integrity of perineuronal nets. Among the four cartilaginous fish-derived CSs, Ms-CS and Sp-CS have a higher 4S/6S ratio of 0.24 and 0.21, respectively. The ratio of 4S to 6S of CS disaccharides is likely to influence the potential of CS to inhibit adipocyte differentiation.

In contrast to the reduction in lipid droplet accumulation, Ms-CS and Sp-CS treatment did not suppress the mRNA level of *Pparg* and *Cebpa*. During the course of 3T3-L1 cell differentiation, increases in PPARγ and C/EBPα are important events (Wu et al., 1999). PPARγ expression rapidly increases in early differentiation and is maximally expressed in mature adipocytes (Brun et al., 1996; Chawla and Lazar, 1994). It is suggested that the increase in *Pparg* and *Cebpa* mRNA levels during the inhibition of the 3T3-L1 adipocyte differentiation is due to negative regulation induced by some metabolism-associated factors.

From the gene expression analyses, the results of this study show unaltered expression of most glycosyltransferase genes. However, significantly increased *Csgalnact2* expression in the group treated with the highest Sp-CS concentration indicates CS biosynthesis

stimulation. *Csgalnact2* encodes chondroitin GalNAc transferase-2 (ChGn-2), which possesses GalNAc transferases II (GalNAcT-II) activity, responsible for catalyzing the chain initiation and elongation of glycan backbone of CS (Sato et al., 2003; Uyama et al., 2003). Based on these findings, we suggest that exogenous CS treatment, at a certain concentration, stimulates CS biosynthesis and reduces the lipid accumulation in the differentiated 3T3-L1.

This study has limitations since the purity of the CS products we used in this study might not be precisely 100%, even though we proceeded with the purification steps mentioned earlier. It means some contaminants or other compounds might be contained in those CS products. Given that fact, there is also the possibility that the inhibitory effect on adipocyte differentiation can be observed more significantly when treating the cells with higher-purity CSs.

All in all, our findings show that CS inhibits the 3T3-L1 adipocyte differentiation by suppressing lipid droplet accumulation, although the degree of suppression of the differentiation depends on the CS composition and origin. In addition, our results highlight the role of GAG, particularly CS, in inhibiting adipogenesis. However, further investigation is required to understand the underlying mechanism. The results of this study provide additional information about the bioactivity of CS and its correlation to adipogenesis so that controlling CS abundance may lead to therapeutic potential in lowering adipose tissue development.

3.5. Summary

This study showed that cartilaginous fish-derived CS (Ms-CS, Bs-CS, and Sp-CS) promotes preadipocyte proliferation in 3T3-L1 cells at concentrations of 1000 μg/mL. Additionally, the study also examined the effect of CS on adipocyte differentiation, with lipid droplet visualization showing a decrease in lipid droplet occurrence following the

exogenous CS treatment. The lipid droplet area of the cartilaginous fishes-derived CS-treated groups was significantly lower than that of the control group. The study found that Ms-CS and Sp-CS had the most significant impact on reducing the occurrence of lipid droplets. Moreover, treating cartilaginous fish-derived CS with concentrations of 10, 100, and 500 μg/mL showed a concentration-dependent decrease in the presence of lipid droplets. In contrast to the lipid droplet reduction, the gene expression of adipogenesis markers, *Pparg* and *Cebpa*, stayed at a high level in the CS-treated groups of Ms-CS and Sp-CS, regardless of the concentration given to the cells. It is highly likely that some other factors induced a negative regulation, resulting in unsuppressed mRNA levels of *Pparg* and *Cebpa*. A significant increase in *Csgalnact2* expression in the Sp-CS group at the concentration of 500 μg/mL was observed. This suggests that exogenous CS treatment, at a certain concentration, stimulates CS biosynthesis and reduces lipid accumulation in the differentiated 3T3-L1. Overall, the study shows that CS inhibits 3T3-L1 adipocyte differentiation by suppressing lipid droplet accumulation, although the degree of suppression depends on the CS composition and origin. The results highlight the role of GAG, particularly CS, in inhibiting adipogenesis, but further investigation is required to understand the underlying mechanism.

Table 3.1 Content and sulfation patterns of the CS/DS obtained from various origins used in the study

Species (sample code)	Tissue	Sulfation patterns of disaccharide unit											
		CS+DS type (%)				CS type (%)				DS type (%)			
		A+iA	C+iC	D+iD	E+iE	A	C	D	E	iA	iC	iD	iE
Mako shark (Ms-CS)	Spine	33	48	18	1	11	46	0	0	22	2	18	1
Blue shark (Bs-CS)	Spine	20	67	13	0	5	52	0	0	15	15	13	0
Sharpspine skate (Sp-CS)	Head-tail	28	61	10	1	10	47	0	0	18	14	10	1
Stingray (St-CS)	Head	24	66	10	0	9	55	0	0	15	11	10	0

Data of CS/DS compositional analysis of the cartilaginous fishes used in this study obtained from the previous report (Takeda et al., 2016).

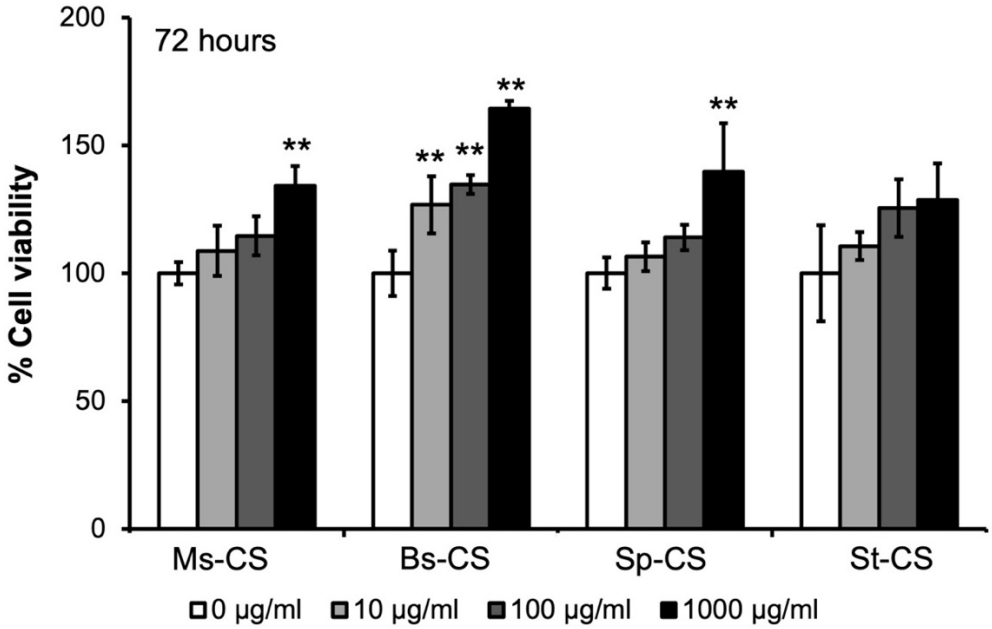

Figure 3.1 Effect of several cartilaginous fishes-derived CS from mako shark (Ms-CS), blue shark (Bs-CS), sharspine skate (Sp-CS), and stingray (St-CS) at various concentrations on 3T3-L1 cell viability. A high concentration of CS at 1000 ug/mL increases the proliferation. The columns and bars show the mean and standard deviation, respectively (n=3). **P < 0.05 compared to the control (0 µg/ml) of each group (Dunnett's test).

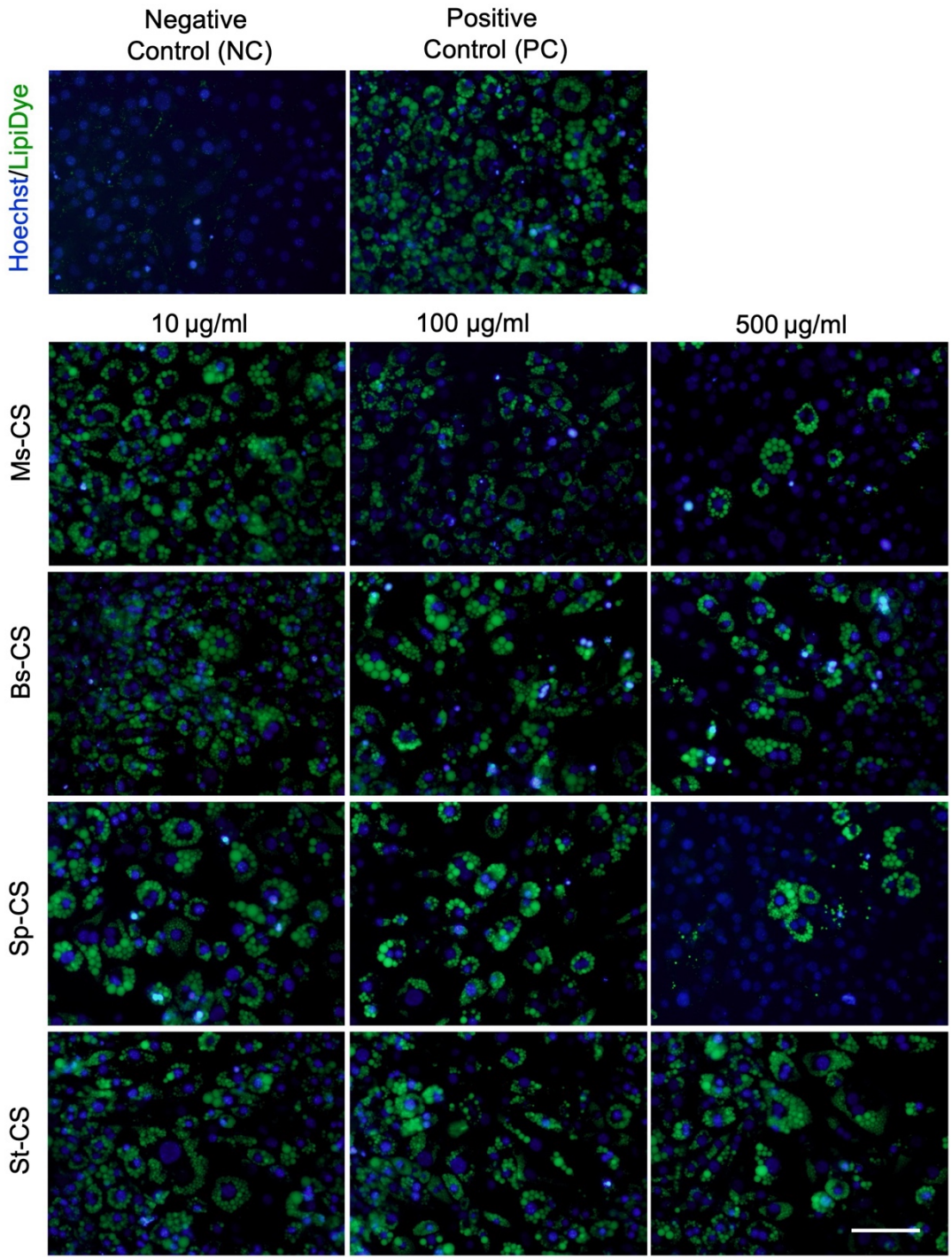

Figure 3.2 CS derived from various cartilaginous fishes -induced morphological changes in the 3T3-L1 adipocyte-like cells. Lipid droplets were accumulated in 3T3-L1 cells following differentiation induction for 10 days. In the positive control (PC) group, abundant lipid droplets were observed. A decrease in lipid droplet accumulation was seen in a high concentration of CS (at 500 μg/mL), especially in the Ms-CS and Sp-CS groups. Lipid droplets and nuclei are shown as green and blue, respectively. Ms-CS, mako shark-derived CS; Bs-CS, blue shark-derived CS; Sp-CS, sharpspine skate-derived CS; St-CS, stingray-derived CS. Scale bar=100μm.

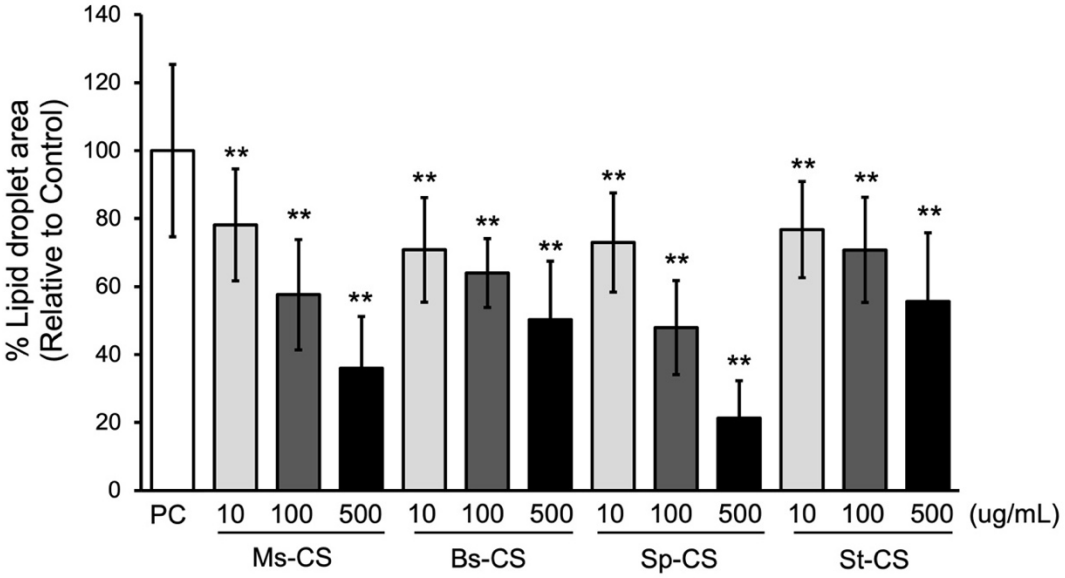

Figure 3.3 CS from several origins inhibit lipid accumulation in a dose-dependent manner. The columns and bars show the mean values and standard deviation, respectively. Ms-CS, mako shark-derived CS; Bs-CS, blue shark-derived CS; Sp-CS, sharpspine skate-derived CS; St-CS, stingray-derived CS. Data were obtained from triplicate of an independent experiment and analyzed with Dunnett's test. **P<0.01 compared to the positive control (PC).

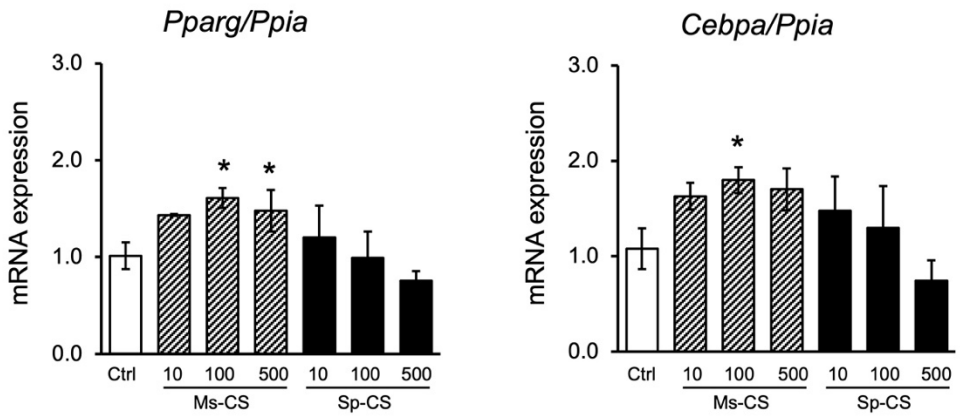

Figure 3.4 Effect of cartilaginous fishes-derived CS on the expression of adipogenesis markers, *Pparg* and *Cebpa*. Ms-CS, mako shark-derived CS; Sp-CS, sharpspine skate-derived CS. Data were obtained from triplicate of an independent experiment and analyzed with Dunnett's test. **P<0.01 compared to the control.

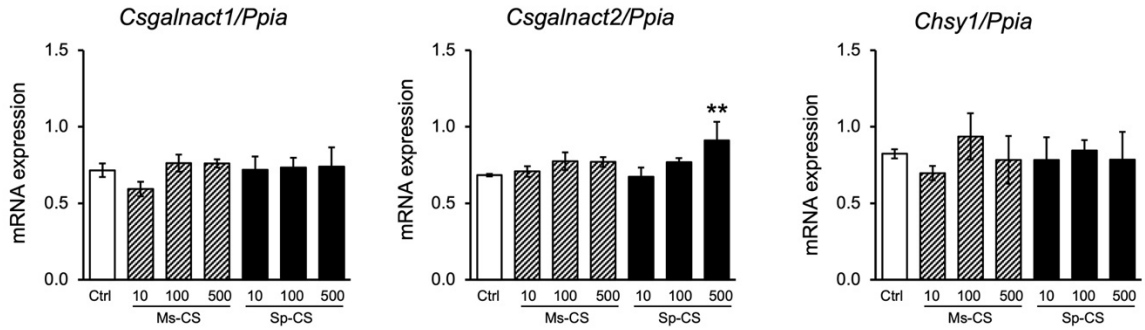

Figure 3.5 Effect of the exogenous CS treatment, Ms-CS and Sp-CS, on the expression of genes that encode CS biosynthesis enzymes, *Csgalnact1*, *Csgalnact2*, and *Chsy1*. Ms-CS, mako shark-derived CS; Sp-CS, sharpspine skate-derived CS. Data were obtained from triplicate of an independent experiment and analyzed with Dunnett's test. **P<0.01 compared to the control.

General Discussion

There has been a significant increase in studies on obesity (Coronado-Ferrer et al., 2022; Zhao et al., 2019). Many studies have been conducted to investigate the underlying mechanisms of adipogenesis as well as potential therapies for obesity. In addition, various cell lines for alternatives to the in vitro adipogenesis model have been established, with 3T3-L1 as the most widely used cell line (Dufau et al., 2021). Gene expression analysis is a crucial tool in the study of adipogenesis. This is because multiple molecular events take place during this process, making it essential to analyze gene expression. However, the normalization of the target genes against suitable reference genes should be considered for data reliability. The study described in this thesis revealed the validated reference genes, peptidylprolyl isomerase A (*Ppia*) and TATA box-binding protein (*Tbp*), for the adipogenesis study using the 3T3-L1 cell line. These findings support the notion that commonly used reference genes, such as beta-actin (*Actb*) and glyceraldehyde-3-phosphate dehydrogenase (*Gapdh*), are unstable across different tissues and experimental conditions (Adachi et al., 2015; Svingen et al., 2015), and should not be the choose in adipocyte differentiation studies without validation.

Considering the role of chondroitin sulfate/dermatan sulfate (CS/DS) in cell proliferation and differentiation, as described elsewhere (Haupt et al., 2009; Izumikawa et al., 2014; Mikael et al., 2019; Mikami et al., 2012; Nairn et al., 2007, 2012; Ogura et al., 2021; Sirko et al., 2007; Volpi et al., 1993), numerous studies on CS proteoglycan (CSPG) expression in adipose tissue and 3T3-L1 cells adipogenesis have been done (Calvo et al., 1991; Han et al., 2020; Musil et al., 1991; Zizola et al., 2007). The results described in this thesis add significant and novel findings on the CS/DS profile in adipocyte differentiation. The CS/DS compositional analyses described in the present study indicate that there was a

significant decrease in the amount of CS/DS in the differentiated (DI) group when compared to the non-differentiated (ND) group. Additionally, the GAGs in the DI group possess lower molecular weight than those in the ND group. Interestingly, the DI group also showed a lower expression of glycosyltransferase genes responsible for CS biosyntheses, such as chondroitin sulfate *N*-acetylgalactosaminyltransferase 1, chondroitin sulfate *N*-acetylgalactosaminyltransferase 2, and chondroitin polymerizing factor. The glycosyltransferases play a crucial role in the initiation and catalysis of chondroitin polymerization, which is essential for the formation of CS/DS (Gulberti et al., 2012; Izumikawa et al., 2007, 2008; Mikami and Kitagawa, 2013; Sato et al., 2003). Therefore, it is reasonable to assume that a decrease in these glycosyltransferases would lead to a reduction in the CS/DS content, as observed in the CS/DS compositional analyses. These findings suggest that there is a decrease in glycosyltransferase activity required for chondroitin sulfate biosynthesis during adipocyte differentiation. On day 10, the higher expression of *Hyal1* in the DI group compared to the ND group suggests that hyaluronidases, particularly HYAL1, may be involved in the reduction of the CS content in differentiating cells. It is known that hyaluronidases have the ability to degrade CS (Gushulak et al., 2012; Honda et al., 2012; Yamada and Mizumoto, 2022). It is believed that the decline in the production of glycosyltransferase has a more significant impact on the decrease in molecular weight and quantity of CS/DS than the change in Hyal1 expression. Hence, it is highly probable that the reduction in CS/DS biosynthesis is primarily caused by the decrease in glycosyltransferase production.

The composition of CS/DS unsaturated disaccharides varies among cell lines, and it is grouped into the three major disaccharides: ΔDi-0S, ΔDi-4S, or ΔDi-6S (Higashi, 2020). The study revealed that the A unit (ΔDi-4S) is the main disaccharide found in CS/DS from the 3T3-L1 cell line, whether in differentiated or non-differentiated cells. On day 10, the DI

group showed an increased expression of carbohydrate sulfotransferase 12 (*Chst12*). This may have contributed to the higher ratio of CS-A in the DI group. The *Chst12* gene encodes sulfotransferase C4ST-2, which is responsible for catalyzing the transfer of sulfate to position 4 of the GalNAc, which leads to the formation of CS-A and desulfated dermatan sulfate (Hiraoka et al., 2000). The absence of non-sulfated CS/DS in the DI group suggests sulfation occurred, forming different types of CS/DS. Increased *Chst12* expression facilitated the formation of non-sulfated CS/DS to A unit CS/DS. Therefore, the O unit of CS/DS from the DI group lacked both GlcA and IdoA residues, unlike the ND group. In addition, it has been observed that the absence of D4ST-1 activity, caused by a carbohydrate sulfotransferase 14 (CHST14) gene mutation, significantly reduces the number of IdoA residues (Miyake et al., 2010; Pacheco et al., 2009b). As a consequence, the DI group, which showed a significant decrease in *Chst14* expression, may experience a substantial reduction in IdoA residue, particularly DS-A.

Given the fact that the amount of CS/DS was reduced in cells undergoing differentiation, the effect of exogenous CS on the 3T3-L1 cell differentiation was evaluated. The present study used cartilaginous fish-derived CS polysaccharides isolated from different species: mako shark (*Isurus oxyrinchus*, spine part), blue shark (*Prionace glauca*, spine part), sharpspine skate (*Okamejei acutispina*, head and tail parts) and stingray (*Dasyatis akajei*, head part). Despite the origins, CS suppressed adipocyte differentiation by inhibiting lipid droplet formation, with Sp-CS showing the strongest inhibitory effect on lipid droplet accumulation among four different CS origins. It is suggested that the reduction of lipid accumulation in differentiated 3T3-L1 cells is due to the increased expression of *Csgalnact2*, a gene that encodes chondroitin GalNAc transferase-2 (ChGn-2), a glycosyltransferase responsible for CS chain initiation and elongation (Sato et al., 2003; Uyama et al., 2003).

In conclusion, the study's findings confirm that the biosynthesis of CS/DS is reduced in cells undergoing differentiation. However, it remains unclear whether the levels of CS/DS change along with adipocyte differentiation or whether the CS/DS biosynthesis controls adipocyte differentiation. Nevertheless, the changes in CS/DS and CS/DS-synthases/hydrolases observed before and after adipocyte differentiation provide valuable insights into the development of adipocytes, both qualitatively and quantitatively. Moreover, exogenous CS treatment can reduce the lipid droplet accumulation in the differentiated 3T3-L1 adipocytes, regardless of the degree of suppression.

Acknowledgments

Alhamdu lillāhi Rabbil'ālamīn. This thesis acknowledgment pays tribute to those who made my academic journey meaningful, and the completion of my Ph.D. thesis would not have been possible without their support.

I am deeply grateful to my supervisor, Dr. Katsuhiko Warita, Professor at the Laboratory of Veterinary Anatomy, Joint Graduate School of Veterinary Sciences, Tottori University, Japan, for his invaluable guidance and mentorship during my Ph.D. journey. His constant support, encouragement, and expert advice were instrumental to my success. I would also like to express my sincerest appreciation to Dr. Yoshinao Hosaka, my former supervisor and Professor at Tottori University. He gave me unwavering support, guidance, and constructive feedback throughout my research. He continued to mentor me despite being appointed Professor at the Laboratory of Functional Anatomy, Department of Bioresource Sciences, Faculty of Agriculture, Kyushu University, Japan. I am truly grateful to both of them for their exceptional mentorship and expertise.

I want to express my most profound appreciation to my co-supervisors at the Joint Graduate School of Veterinary Sciences, Dr. Takehito Morita, Professor at the Laboratory of Veterinary Pathology, Tottori University, and Dr. Shouichiro Saito, Professor at the Laboratory of Veterinary Anatomy, Gifu University, Japan. Their invaluable supervision, insightful suggestions, and comments on my research work have been appreciated. I would like to extend my appreciation to Dr. Takahiko Shiina, Professor at the Laboratory of Pathological Physiology, Gifu University, and Dr. Yukiko Tomioka, Associate Professor at the Laboratory of Laboratory Animal Science, Tottori University for their thoughtful feedback and recommendations during the review of this doctoral thesis.

I am immensely grateful to my collaborators who have contributed to my research work. I want to thank Dr. Jun-ichi Tamura, Professor at the Department of Agricultural, Life and Environmental Sciences, Faculty of Agriculture, Tottori University, and Dr. Naoko Takeda-Okuda, a fellow researcher in his laboratory, for their invaluable support, expertise, and technical guidance, especially on the glycosaminoglycan research. I also extend my deepest gratitude to Dr. Tomoko Warita from the Department of Biomedical Sciences, School of Biological and Environmental Sciences, Kwansei Gakuin University, Japan, for her invaluable contributions and expertise in completing my research work.

I am also grateful to all members of the Laboratory of Veterinary Anatomy, Department of Veterinary Medicine, Tottori University, and especially to Mr. Jiro Tashiro, Mr. Akihiro Sugiura. Thanks should also go to the former laboratory members, Dr. Takuro Ishikawa and Dr. Rattanatrai Chaiyasing. I appreciate their assistance and willingness to share their knowledge since the beginning of my Ph.D. study.

Furthermore, I am grateful to Japan's Ministry of Education, Culture, Sports, Science, and Technology (MEXT) for providing scholarships during my studies in Japan.

I am grateful for my family, especially my wife, Nurida Dessalma Syahrania, and our sons, Hamiz Yusuf Kawakibi and Hestama Yusuf Musaffa. I thank my parents, Bapak Arif Suharyanto and Ibu Sudarmini, and my brother Nur Fitrianto for their unwavering love and support. I appreciate the Indonesian Students Association and the Muslim Community in Tottori for their friendship during my stay in Japan. Last but not least, thanks to my seniors and colleagues at the School of Veterinary Medicine and Biomedical Sciences, IPB University, Indonesia, especially to the members of the Laboratory of Anatomy, for their continuous support in shaping my academic career.

Danang Dwi Cahyadi
Laboratory of Veterinary Anatomy, Tottori University, Japan

References

Achur, R. N., Valiyaveettil, M., Alkhalil, A., Ockenhouse, C. F., Gowda, D. C. (2000). Characterization of proteoglycans of human placenta and identification of unique chondroitin sulfate proteoglycans of the intervillous spaces that mediate the adherence of *Plasmodium falciparum*-infected erythrocytes to the placenta. *Journal of Biological Chemistry*, *275*(51), 40344–40356.

Adachi, H., Tominaga, H., Maruyama, Y., Yoneda, K., Maruyama, K., Yoshii, K., Kinoshita, S., Nakano, M., Tashiro, K. (2015). Stage-specific reference genes significant for quantitative PCR during mouse retinal development. *Genes to Cells*, *20*(8), 625–635.

Akatsu, C., Mizumoto, S., Kaneiwa, T., Maccarana, M., Malmström, A., Yamada, S., Sugahara, K. (2011). Dermatan sulfate epimerase 2 is the predominant isozyme in the formation of the chondroitin sulfate/dermatan sulfate hybrid structure in postnatal developing mouse brain. *Glycobiology*, *21*(5), 565–574.

Albrecht, E., Kuzinski, J., Komolka, K., Gotoh, T., Maak, S. (2015). Localization and abundance of early markers of fat cell differentiation in the skeletal muscle of cattle during growth--are DLK1-positive cells the origin of marbling flecks? *Meat Science*, *100*, 237–245.

Alexander, M. C., Lomanto, M., Nasrin, N., Ramaika, C. (1988). Insulin stimulates glyceraldehyde-3-phosphate dehydrogenase gene expression through cis-acting DNA sequences. *Proceedings of the National Academy of Sciences of the United States of America*, *85*(14), 5092–5096.

Alexander, M., Curtis, G., Avruch, J., Goodman, H. M. (1985). Insulin regulation of protein biosynthesis in differentiated 3T3 adipocytes. Regulation of glyceraldehyde-3-phosphate dehydrogenase. *Journal of Biological Chemistry*, *260*(22), 11978–11985.

Ambele, M. A., Dessels, C., Durandt, C., Pepper, M. S. (2016). Genome-wide analysis of

gene expression during adipogenesis in human adipose-derived stromal cells reveals novel patterns of gene expression during adipocyte differentiation. *Stem Cell Research*, *16*(3), 725–734.

Amendum, P. C., Khan, S., Yamaguchi, S., Kobayashi, H., Ago, Y., Suzuki, Y., Celik, B., Rintz, E., Hossain, J., Xiao, W., Tomatsu, S. (2021). Glycosaminoglycans as biomarkers for mucopolysaccharidoses and other disorders. *Diagnostics (Basel, Switzerland)*, *11*(9), 1563.

Anandacoomarasamy, A., Caterson, I., Sambrook, P., Fransen, M., March, L. (2008). The impact of obesity on the musculoskeletal system. *International Journal of Obesity*, *32*(2), 211–222.

Anbazhagan, A., Sridharan, P., Pratheesh, P. (2019). Validation of suitable housekeeping genes for 3T3-L1 derived adipocytes cultured in obesity mimicking conditions and RAW 264.7 macrophage cells lines in hypoxic and normoxic conditions. *Biocatalysis and Agricultural Biotechnology, 17*, 620–627.

Andersen, C. L., Jensen, J. L., Ørntoft, T. F. (2004). Normalization of real-time quantitative reverse transcription-PCR data: a model-based variance estimation approach to identify genes suited for normalization, applied to bladder and colon cancer data sets. *Cancer Research*, *64*(15), 5245–5250.

Arner, E., Westermark, P.O., Spalding, K.L., Britton, T., Ryden, M., Frisen, J., Bernard, S., Arner, P. (2010). Adipocyte turnover: relevance to human adipose tissue morphology. *Diabetes, 59*, 105-109.

Arsenijevic, T., Grégoire, F., Delforge, V., Delporte, C., Perret, J. (2012). Murine 3T3-L1 adipocyte cell differentiation model: validated reference genes for qPCR gene expression analysis. *PloS One*, *7*(5), e37517.

Asano, H., Kanamori, Y., Higurashi, S., Nara, T., Kato, K., Matsui, T., Funaba, M. (2014).

Induction of beige-like adipocytes in 3T3-L1 cells. *The Journal of Veterinary Medical Science*, *76*(1), 57–64.

Babicki, S., Arndt, D., Marcu, A., Liang, Y., Grant, J. R., Maciejewski, A., Wishart, D. S. (2016). Heatmapper: web-enabled heat mapping for all. *Nucleic Acids Research*, *44*(W1), W147–W153.

Barroso, I., Benito, B., Garcí-Jiménez, C., Hernández, A., Obregón, M. J., Santisteban, P. (1999). Norepinephrine, tri-iodothyronine and insulin upregulate glyceraldehyde-3-phosphate dehydrogenase mRNA during brown adipocyte differentiation. *European Journal of Endocrinology*, *141*(2), 169–179.

Bergefall, K., Trybala, E., Johansson, M., Uyama, T., Naito, S., Yamada, S., Kitagawa, H., Sugahara, K., Bergström, T. (2005). Chondroitin sulfate characterized by the E-disaccharide unit is a potent inhibitor of herpes simplex virus infectivity and provides the virus binding sites on gro2C cells. *Journal of Biological Chemistry*, *280*(37), 32193–32199.

Berry, R., Rodeheffer, M. (2013). Characterization of the adipocyte cellular lineage *in vivo*. *Nature Cell Biology*, *15*, 302–308.

Bieback, K., Ha, V. A., Hecker, A., Grassl, M., Kinzebach, S., Solz, H., Sticht, C., Klüter, H., Bugert, P. (2010). Altered gene expression in human adipose stem cells cultured with fetal bovine serum compared to human supplements. *Tissue Engineering Part A*, *16*(11), 3467–3484.

Blüher, M. (2019). Obesity: global epidemiology and pathogenesis. *Nature Reviews Endocrinology*, *15*(5), 288–298.

Braissant, O., Foufelle, F., Scotto, C., Dauça, M., Wahli, W. (1996). Differential expression of peroxisome proliferator-activated receptors (PPARs): tissue distribution of PPAR-alpha, -beta, and -gamma in the adult rat. *Endocrinology*, *137*(1), 354–366.

Broeders, S., Huber, I., Grohmann, L., Berben, G., Taverniers, I., Mazzara, M., Roosens, N., Morisset, D. (2014). Guidelines for validation of qualitative real-time PCR methods. *Trends in Food Science & Technology*, *37*(2), 115–126.

Brun, R. P., Kim, J. B., Hu, E., Altiok, S., Spiegelman, B. M. (1996). Adipocyte differentiation: a transcriptional regulatory cascade. *Current Opinion in Cell Biology*, *8*(6), 826–832.

Brzeszczyńska, J., Brzeszczyński, F., Samuel, K., Morgan, K., Morley, S. D., Plevris, J. N., Hayes, P. C. (2020). Validation of reference genes for gene expression studies by RT-qPCR in HepaRG cells during toxicity testing and disease modelling. *Cells*, *9*(3), 770.

Bustin, S. A. (2000). Absolute quantification of mRNA using real-time reverse transcription polymerase chain reaction assays. *Journal of Molecular Endocrinology*, *25*(2), 169–193.

Bustin, S. A., Benes, V., Garson, J. A., Hellemans, J., Huggett, J., Kubista, M., Mueller, R., Nolan, T., Pfaffl, M. W., Shipley, G. L., Vandesompele, J., Wittwer, C. T. (2009). The MIQE guidelines: minimum information for publication of quantitative real-time PCR experiments. *Clinical Chemistry*, *55*(4), 611–622.

Butterwith, S. C. (1994). Molecular events in adipocyte development. *Pharmacology & Therapeutics*, *61*(3), 399–411.

Cahyadi, D. D., Okamoto, M., Warita, K., Takeda-Okuda, N., Tamura, J. I., Hosaka, Y. Z. (2022). Compositional analysis of chondroitin/dermatan sulfate in rhesus monkeys (*Macaca mulatta*). *Bioscience, Biotechnology, and Biochemistry*, *86*(7), 811–818.

Cahyadi, D. D., Warita, T., Irie, N., Mizoguchi, K., Tashiro, J., Hosaka, Y. Z., Warita, K. (2023). Housekeeping gene expression variability in differentiating and non-differentiating 3T3-L1 cells. *Adipocyte*, *12*(1), 2235081.

Calvo, J. C., Rodbard, D., Katki, A., Chernick, S., Yanagishita, M. (1991). Differentiation

of 3T3-L1 preadipocytes with 3-isobutyl-1-methylxanthine and dexamethasone stimulates cell-associated and soluble chondroitin 4-sulfate proteoglycans. *Journal of Biological Chemistry*, *266*(17), 11237–11244.

Chang-Liu, C. M., Woloschak, G. E. (1997). Effect of passage number on cellular response to DNA-damaging agents: cell survival and gene expression. *Cancer Letters*, *113*(1-2), 77–86.

Chapman, J. R., Waldenström, J. (2015). With reference to reference genes: a systematic review of endogenous controls in gene expression studies. *PLoS One*, *10*(11), e0141853.

Chawla, A., Lazar, M. A. (1994). Peroxisome proliferator and retinoid signaling pathways co-regulate preadipocyte phenotype and survival. *Proceedings of the National Academy of Sciences of the United States of America*, *91*(5), 1786–1790.

Choi, B. H., Ahn, I. S., Kim, Y. H., Park, J. W., Lee, S. Y., Hyun, C. K., Do, M. S. (2006). Berberine reduces the expression of adipogenic enzymes and inflammatory molecules of 3T3-L1 adipocyte. *Experimental & Molecular Medicine*, *38*(6), 599–605.

Clement, A. M., Nadanaka, S., Masayama, K., Mandl, C., Sugahara, K., Faissner, A. (1998). The DSD-1 carbohydrate epitope depends on sulfation, correlates with chondroitin sulfate D motifs, and is sufficient to promote neurite outgrowth. *Journal of Biological Chemistry*, *273*(43), 28444–28453.

Clement, A. M., Sugahara, K., Faissner, A. (1999). Chondroitin sulfate E promotes neurite outgrowth of rat embryonic day 18 hippocampal neurons. *Neuroscience Letters*, *269*(3), 125–128.

Coronado-Ferrer, S., Ferrer-Sapena, A., Aleixandre-Benavent, R., Valderrama Zurián, J. C., Cogollos, L. C. (2022). Global Trends in Scientific Research on Pediatric Obesity. *International Journal of Environmental Research and Public Health*, *19*(3), 1251.

Czernichow, S., Kengne, A. P., Stamatakis, E., Hamer, M., Batty, G. D. (2011). Body mass index, waist circumference and waist-hip ratio: which is the better discriminator of cardiovascular disease mortality risk?: evidence from an individual-participant meta-analysis of 82 864 participants from nine cohort studies. *Obesity Reviews*, *12*(9), 680–687.

Derks, N. M., Müller, M., Gaszner, B., Tilburg-Ouwens, D. T., Roubos, E. W., Kozicz, L. T. (2008). Housekeeping genes revisited: different expressions depending on gender, brain area and stressor. *Neuroscience*, *156*(2), 305–309.

Diament A.L., Fisler J.S., Warden C.H. (2003). Obesity alleles in mice and humans. *Obesity Reviews, 4*, 249–255.

Doi, H., Masaki, N., Takahashi, H., Komatsu, H., Fujimori, K., Satomi, S. (2005). A new preadipocyte cell line, AP-18, established from adult mouse adipose tissue. *The Tohoku Journal of Experimental Medicine*, *207*(3), 209–216.

Dufau, J., Shen, J. X., Couchet, M., De Castro Barbosa, T., Mejhert, N., Massier, L., Griseti, E., Mouisel, E., Amri, E. Z., Lauschke, V. M., Rydén, M., Langin, D. (2021). In vitro and ex vivo models of adipocytes. *American Journal of Physiology*, *Cell Physiology*, *320*(5), C822–C841.

El-Jack, A. K., Hamm, J. K., Pilch, P. F., Farmer, S. R. (1999). Reconstitution of insulin-sensitive glucose transport in fibroblasts requires expression of both PPARgamma and C/EBPalpha. *Journal of Biological Chemistry*, *274*(12), 7946–7951.

Emam, M., Thompson-Crispi, K., Mallard, B. (2015). The effect of immunological status, in-vitro treatment and culture time on expression of eleven candidate reference genes in bovine blood mononuclear cells. *BMC Immunology*, *16*, 33.

Esteve Ràfols, M. (2014). Adipose tissue: cell heterogeneity and functional diversity. *Endocrinologia y Nutricion, 61*(2), 100–112.

Etherton, T.D. (2000). The biology of somatotropin in adipose tissue growth and nutrient partitioning. *The Journal of Nutrition*, *130*(11), 2623–2625.

Evans, R. M., Barish, G. D., Wang, Y. X. (2004). PPARs and the complex journey to obesity. *Nature Medicine*, *10*(4), 355–361.

Farmer, S. R. (2006). Transcriptional control of adipocyte formation. *Cell Metabolism*, *4*(4), 263–273.

Ferguson, B. S., Nam, H., Hopkins, R. G., Morrison, R. F. (2010). Impact of reference gene selection for target gene normalization on experimental outcome using real-time qRT-PCR in adipocytes. *PloS One*, *5*(12), e15208.

Gandhi, N. S., Mancera, R. L. (2008). The structure of glycosaminoglycans and their interactions with proteins. *Chemical Biology & Drug Design*, *72*(6), 455–482.

Gavva, C., Patel, K., Kudre, T., Sharan, K., Chilkunda, D. N. (2020). Glycosaminoglycans from fresh water fish processing discard - Isolation, structural characterization, and osteogenic activity. *International Journal of Biological Macromolecules*, *145*, 558–567.

Gowda D. C. (2006). Role of chondroitin-4-sulfate in pregnancy-associated malaria. *Advances in Pharmacology (San Diego, Calif.)*, *53*, 375–400.

Green, H., Kehinde, O. (1976). Spontaneous heritable changes leading to increased adipose conversion in 3T3 cells. *Cell*, *7*(1), 105–113.

Green, H., Meuth, M. (1974). An established pre-adipose cell line and its differentiation in culture. *Cell*, *3*(2), 127–133.

Guan, L., Hu, X., Liu, L., Xing, Y., Zhou, Z., Liang, X., Yang, Q., Jin, S., Bao, J., Gao, H., Du, M., Li, J., Zhang, L. (2017). bta-miR-23a involves in adipogenesis of progenitor cells derived from fetal bovine skeletal muscle. *Scientific Reports*, *7*, 43716.

Gulberti, S., Jacquinet, J. C., Chabel, M., Ramalanjaona, N., Magdalou, J., Netter, P.,

Coughtrie, M. W. H., Ouzzine, M., Fournel-Gigleux, S. (2012). Chondroitin sulfate *N*-acetylgalactosaminyltransferase-1 (CSGalNAcT-1) involved in chondroitin sulfate initiation: Impact of sulfation on activity and specificity. *Glycobiology, 22*(4), 561–571.

Gushulak, L., Hemming, R., Martin, D., Seyrantepe, V., Pshezhetsky, A., Triggs-Raine, B. (2012). Hyaluronidase 1 and β-hexosaminidase have redundant functions in hyaluronan and chondroitin sulfate degradation. *Journal of Biological Chemistry*, *287*(20), 16689–16697.

Han, C. Y., Kang, I., Harten, I. A., Gebe, J. A., Chan, C. K., Omer, M., Alonge, K. M., den Hartigh, L. J., Gomes Kjerulf, D., Goodspeed, L., Subramanian, S., Wang, S., Kim, F., Birk, D. E., Wight, T. N., Chait, A. (2020). Adipocyte-derived versican and macrophage-derived biglycan control adipose tissue inflammation in obesity. *Cell Reports*, *31*(13), 107818.

Han, L. K., Sumiyoshi, M., Takeda, T., Chihara, H., Nishikiori, T., Tsujita, T., Kimura, Y., Okuda, H. (2000). Inhibitory effects of chondroitin sulfate prepared from salmon nasal cartilage on fat storage in mice fed a high-fat diet. *International Journal of Obesity*, *24*(9), 1131–1138.

Hashiguchi, T., Kobayashi, T., Fongmoon, D., Shetty, A. K., Mizumoto, S., Miyamoto, N., Nakamura, T., Yamada, S., Sugahara, K. (2011). Demonstration of the hepatocyte growth factor signaling pathway in the in vitro neuritogenic activity of chondroitin sulfate from ray fish cartilage. *Biochimica et Biophysica Acta*, *1810*(4), 406–413.

Haupt, L.M., Murali, S., Mun, F.K., Teplyuk, N., Mei, L.F., Stein, G.S., van Wijnen, A.J., Nurcombe, V., Cool, S.M. (2009). The heparan sulfate proteoglycan (HSPG) glypican-3 mediates commitment of MC3T3-E1 cells toward osteogenesis. *Journal of Cellular Physiology*, *220*(3), 780-791.

Haylock-Jacobs, S., Keough, M. B., Lau, L., Yong, V. W. (2011). Chondroitin sulphate proteoglycans: extracellular matrix proteins that regulate immunity of the central nervous system. *Autoimmunity Reviews*, *10*(12), 766–772.

Henrotin, Y., Mathy, M., Sanchez, C., Lambert, C. (2010). Chondroitin sulfate in the treatment of osteoarthritis: from in vitro studies to clinical recommendations. *Therapeutic Advances in Musculoskeletal Disease*, *2*(6), 335–348.

Higashi, K. (2020). Expression of glycosaminoglycan-related genes and the role of polyamines in the glycosaminoglycan biosynthetic pathways. *Trends in Glycoscience and Glycotechnology, 32*(189), E167–E175.

Higashi, K., Takeuchi, Y., Mukuno, A., Tomitori, H., Miya, M., Linhardt, R. J., Toida, T. (2015). Composition of glycosaminoglycans in elasmobranchs including several deep-sea sharks: Identification of chondroitin/dermatan sulfate from the dried fins of *Isurus oxyrinchus* and *Prionace glauca*. *PLoS One*, *10*(3), 1–15.

Hiraoka, N., Nakagawa, H., Ong, E., Akama, T. O., Fukuda, M. N., Fukuda, M. (2000). Molecular cloning and expression of two distinct human chondroitin 4-*O*-sulfotransferases that belong to the HNK-1 sulfotransferase gene family. *Journal of Biological Chemistry*, *275*(26), 20188–20196.

Hjerpe, A., Aantonopoulos, C. A., Engfeldt, B. (1982). Determination of hyaluronic acid using high-performance liquid chromatography of chondroitinase digests. *Journal of Chromatography A*, *245*(3), 365–368.

Honda, T., Kaneiwa, T., Mizumoto, S., Sugahara, K., Yamada, S. (2012). Hyaluronidases have strong hydrolytic activity toward chondroitin 4-sulfate comparable to that for hyaluronan. *Biomolecules*, *2*(4), 549–563.

Hosaka, Y. Z., Washie, S., Warita, K. (2022). Preliminary study of the gene expression of sulfation and degradation enzymes for chondroitin sulfate in glycerol-treated C2C12

myoblast cells. *The Journal of Veterinary Medical Science*, *84*(3), 306–309.

Huang, E., Bi, Y., Jiang, W., Luo, X., Yang, K., Gao, J. L., Gao, Y., Luo, Q., Shi, Q., Kim, S. H., Liu, X., Li, M., Hu, N., Liu, H., Cui, J., Zhang, W., Li, R., Chen, X., Shen, J., Kong, Y., Zhang, J., Wang, J., Luo, J., He, B. C., Wang, H., Reid, R. R., Luu, H. H., Haydon, R. C., Yang, L., He, T. C. (2012). Conditionally immortalized mouse embryonic fibroblasts retain proliferative activity without compromising multipotent differentiation potential. *PloS One*, *7*(2), e32428.

Huggett, J., Dheda, K., Bustin, S., Zumla, A. (2005). Real-time RT-PCR normalisation; strategies and considerations. *Genes and Immunity*, *6*(4), 279–284.

Im, A. R., Park, Y., Kim, Y. S. (2010). Isolation and characterization of chondroitin sulfates from sturgeon (*Acipenser sinensis*) and their effects on growth of fibroblasts. *Biological & Pharmaceutical Bulletin*, *33*(8), 1268–1273.

Ito, Y., Habuchi, O. (2000). Purification and characterization of *N*-acetylgalactosamine 4-sulfate 6-*O*-sulfotransferase from the squid cartilage. *Journal of Biological Chemistry*, *275*(44), 34728–34736.

Izumikawa, T., Koike, T., Shiozawa, S., Sugahara, K., Tamura, J. I., Kitagawa, H. (2008). Identification of chondroitin sulfate glucuronyltransferase as chondroitin synthase-3 involved in chondroitin polymerization: Chondroitin polymerization is achieved by multiple enzyme complexes consisting of chondroitin synthase family members. *Journal of Biological Chemistry*, *283*(17), 11396–11406.

Izumikawa, T., Sato, B., Kitagawa, H. (2014). Chondroitin sulfate is indispensable for pluripotency and differentiation of mouse embryonic stem cells. *Scientific Reports*, *4*, 3701.

Izumikawa, T., Uyama, T., Okuura, Y., Sugahara, K., Kitagawa, H. (2007). Involvement of chondroitin sulfate synthase-3 (chondroitin synthase-2) in chondroitin polymerization

through its interaction with chondroitin synthase-1 or chondroitin-polymerizing factor. *Biochemical Journal*, *403*(3), 545–552.

Jadin, L., Wu, X., Ding, H., Frost, G. I., Onclinx, C., Triggs-Raine, B., Flamion, B. (2008). Skeletal and hematological anomalies in HYAL2-deficient mice: A second type of mucopolysaccharidosis IX?. *The FASEB Journal*, *22*(12), 4316–4326.

Kanda, T., Brown, J. D., Orasanu, G., Vogel, S., Gonzalez, F. J., Sartoretto, J., Michel, T., Plutzky, J. (2009). PPARγ in the endothelium regulates metabolic responses to high-fat diet in mice. *Journal of Clinical Investigation*, *119*(1), 110–124.

Kato, D., Era, S., Watanabe, I., Arihara, M., Sugiura, N., Kimata, K., Suzuki, Y., Morita, K., Hidari, K. I., Suzuki, T. (2010). Antiviral activity of chondroitin sulphate E targeting dengue virus envelope protein. *Antiviral Research*, *88*(2), 236–243.

Kitagawa, H., Izumikawa, T., Uyama, T., Sugahara, K. (2003). Molecular cloning of a chondroitin polymerizing factor that cooperates with chondroitin synthase for chondroitin polymerization. *Journal of Biological Chemistry*, *278*(26), 23666–23671.

Kobayashi, M., Sugumaran, G., Liu, J., Shworak, N. W., Silbert, J. E., Rosenberg, R. D. (1999). Molecular cloning and characterization of a human uronyl 2-sulfotransferase that sulfates iduronyl and glucuronyl residues in dermatan/chondroitin sulfate. *Journal of Biological Chemistry*, *274*(15), 10474–10480.

Koike, T., Izumikawa, T., Tamura, J., Kitagawa, H. (2012). Chondroitin sulfate-E fine-tunes osteoblast differentiation via ERK1/2, Smad3 and Smad1/5/8 signaling by binding to N-cadherin and cadherin-11. *Biochemical and Biophysical Research Communications*, *420*(3), 523–529.

Koike, T., Mikami, T., Shida, M., Habuchi, O., Kitagawa, H. (2015). Chondroitin sulfate-E mediates estrogen-induced osteoanabolism. *Scientific Reports*, *5*, 8994.

Kolset, S. O., Ivhed, I., Øvervatn, A., Nilsson, K. (1988). Differentiation-associated changes

in the expression of chondroitin sulfate proteoglycan in induced U-937 cells. *Cancer Research*, *48*(21), 6103–6108.

Kwon, D., Kim, J. S., Cha, B. H., Park, K. S., Han, I., Park, K. S., Bae, H., Han, M. K., Kim, K. S., Lee, S. H. (2016). The effect of fetal bovine serum (FBS) on efficacy of cellular reprogramming for induced pluripotent stem cell (iPSC) generation. *Cell Transplantation*, *25*(6), 1025–1042.

Laskin, J. D., Dokidis, A., Sirak, A. A., Laskin, D. L. (1991). Distinct patterns of sulfated proteoglycan biosynthesis in human monocytes, granulocytes and myeloid leukemic cells. *Leukimia Research*, *15*(6), 515–523.

Leal, A.F., Benincore-Flórez, E., Rintz, E., Herreño-Pachón, A.M., Celik, B., Ago, Y., Alméciga-Díaz, C.J., Tomatsu, S. (2023). Mucopolysaccharidoses: Cellular consequences of glycosaminoglycans accumulation and potential targets. *International Journal of Molecular Sciences*, *24*(1), 477.

Lee, A., Langer, R. (1983). Shark cartilage contains inhibitors of tumor angiogenesis. *Science (New York)*, *221*(4616), 1185–1187.

Lemma, S., Avnet, S., Meade, M. J., Chano, T., Baldini, N. (2018). Validation of suitable housekeeping genes for the normalization of mRNA expression for studying tumor acidosis. *International Journal of Molecular Sciences*, *19*(10), 2930.

Li, F., Ten Dam, G. B., Murugan, S., Yamada, S., Hashiguchi, T., Mizumoto, S., Oguri, K., Okayama, M., van Kuppevelt, T. H., Sugahara, K. (2008). Involvement of highly sulfated chondroitin sulfate in the metastasis of the Lewis lung carcinoma cells. *Journal of Biological Chemistry*, *283*(49), 34294–34304.

Li, J., Gong, L., Liu, S., Zhang, Y., Zhang, C., Tian, M., Lu, H., Bu, P., Yang, J., Ouyang, C., Jiang, X., Wu, J., Zhang, Y., Min, Q., Zhang, C., Zhang, W. (2019). Adipose HuR protects against diet-induced obesity and insulin resistance. *Nature Communications*,

10(1), 2375.

Li, W., Kobayashi, T., Moroi, S., Kotake, H., Ikoma, T., Saeki, H., Ura, K., Takagi, Y. (2019). Anti-obesity effects of chondroitin sulfate oligosaccharides from the skate *Raja pulchra*. *Carbohydrate Polymers*, *214*, 303–310.

Lyu, Z., Da, Y., Liu, H., Wang, Z., Zhu, Y., Tian, J. (2022). Chsy1 deficiency reduces extracellular matrix productions and aggravates cartilage injury in osteoarthritis. *Gene*, *827*, 146466.

Maccarana, M., Kalamajski, S., Kongsgaard, M., Magnusson, S. P., Oldberg, Å., Malmström, A. (2009). Dermatan sulfate epimerase 1-deficient mice have reduced content and changed distribution of iduronic acids in dermatan sulfate and an altered collagen structure in skin. *Molecular and Cellular Biology*, *29*(20), 5517–5528.

Madsen, M. S., Siersbæk, R., Boergesen, M., Nielsen, R., Mandrup, S. (2014). Peroxisome proliferator-activated receptor γ and C/EBPα synergistically activate key metabolic adipocyte genes by assisted loading. *Molecular and Cellular Biology*, *34*(6), 939–954.

Martel-Pelletier, J., Farran, A., Montell, E., Vergés, J., Pelletier, J. P. (2015). Discrepancies in composition and biological effects of different formulations of chondroitin sulfate. *Molecules (Basel, Switzerland)*, *20*(3), 4277–4289.

Mikael, P. E., Willard, C., Koyee, A., Barlao, C. G., Liu, X., Han, X., Ouyang, Y., Xia, K., Linhardt, R. J., Dordick, J. S. (2019). Remodeling of glycosaminoglycans during differentiation of adult human bone mesenchymal stromal cells toward hepatocytes. *Stem Cells and Development, 28*(4), 278–289.

Mikami, T., Kitagawa, H. (2013). Biosynthesis and function of chondroitin sulfate. *Biochimica et Biophysica Acta (BBA) - General Subjects*, *1830*(10), 4719–4733.

Mikami, T., Kitagawa, H. (2017). Sulfated glycosaminoglycans: their distinct roles in stem cell biology. *Glycoconjugate Journal*, *34*(6), 725–735.

Mikami, T., Koyama, S., Yabuta, Y., Kitagawa, H. (2012). Chondroitin sulfate is a crucial determinant for skeletal muscle development/regeneration and improvement of muscular dystrophies. *Journal of Biological Chemistry*, *287*(46), 38531–38542.

Miyachi, K., Wakao, M., Suda, Y. (2015). Syntheses of chondroitin sulfate tetrasaccharide structures containing 4,6-disulfate patterns and analysis of their interaction with glycosaminoglycan-binding protein. *Bioorganic & Medicinal Chemistry Letters*, *25*(7), 1552–1555.

Miyake, N., Kosho, T., Mizumoto, S., Furuichi, T., Hatamochi, A., Nagashima, Y., Arai, E., Takahashi, K., Kawamura, R., Wakui, K., Takahashi, J., Kato, H., Yasui, H., Ishida, T., Ohashi, H., Nishimura, G., Shiina, M., Saitsu, H., Tsurusaki, Y., Doi, H., Fukushima, Y., Ikegawa, S., Yamada, S., Sugahara, K., Matsumoto, N. (2010). Loss-of-function mutations of CHST14 in a new type of Ehlers-Danlos syndrome. *Human Mutation*, *31*(8), 966–974.

Miyata, S., Komatsu, Y., Yoshimura, Y., Taya, C., Kitagawa, H. (2012). Persistent cortical plasticity by upregulation of chondroitin 6-sulfation. *Nature Neuroscience*, *15*(3), 414–422.

Mizumoto, S., Watanabe, M., Yamada, S., Sugahara, K. (2013). Expression of *N*-acetylgalactosamine 4-sulfate 6-*O*-sulfotransferase involved in chondroitin sulfate synthesis is responsible for pulmonary metastasis. *BioMed Research International*, *2013*, 656319.

Mizumoto, S., Yamada, S. (2021). An overview of in vivo functions of chondroitin sulfate and dermatan sulfate revealed by their deficient mice. *Frontiers in Cell and Developmental Biology*, *9*, 764781.

Mizumoto, S., Yamada, S. (2022). The specific role of dermatan sulfate as an instructive glycosaminoglycan in tissue development. *International Journal of Molecular*

Sciences, *23*, 7485.

Mizumoto, S., Yamada, S., Sugahara, K. (2015). Molecular interactions between chondroitin-dermatan sulfate and growth factors/receptors/matrix proteins. *Current Opinion in Structural Biology*, *34*, 35–42.

Mohammadi-Farani, A., Ghazi-Khansari, M., Sahebgharani, M. (2014). Glucose concentration in culture medium affects mRNA expression of TRPV1 and CB1 receptors and changes capsaicin toxicity in PC12 cells. *Iranian Journal of Basic Medical Sciences*, *17*(9), 673–378.

Mueller, E., Drori, S., Aiyer, A., Yie, J., Sarraf, P., Chen, H., Hauser, S., Rosen, E. D., Ge, K., Roeder, R. G., Spiegelman, B. M. (2002). Genetic analysis of adipogenesis through peroxisome proliferator-activated receptor gamma isoforms. *Journal of Biological Chemistry*, *277*(44), 41925–41930.

Mukhitov, N., Adablah, J. E., Roper, M. G. (2019). Gene expression patterns in synchronized islet populations. *Islets*, *11*(2), 21–32.

Muñoz, J. J., Anauate, A. C., Amaral, A. G., Ferreira, F. M., Watanabe, E. H., Meca, R., Ormanji, M. S., Boim, M. A., Onuchic, L. F., Heilberg, I. P. (2021). *Ppia* is the most stable housekeeping gene for qRT-PCR normalization in kidneys of three *Pkd1*-deficient mouse models. *Scientific Reports*, *11*(1), 19798.

Musil, K. J., Malmström, A., Donnér, J. (1991). Alteration of proteoglycan metabolism during the differentiation of 3T3-L1 fibroblasts into adipocytes. *Journal of Cell Biology*, *114*(4), 821–826.

Muthusamy, A., Achur, R. N., Valiyaveettil, M., Madhunapantula, S. V., Kakizaki, I., Bhavanandan, V. P., Gowda, C. D. (2004). Structural characterization of the bovine tracheal chondroitin sulfate chains and binding of *Plasmodium falciparum*-infected erythrocytes. *Glycobiology*, *14*(7), 635–645.

Myung, D.-B., Han, H.-S., Shin, J.-S., Park, J. Y., Hwang, H. J., Kim, H. J., Ahn, H. S., Lee, S. H., Lee, K.-T. (2019). Hydrangenol isolated from the leaves of *Hydrangea serrata* attenuates wrinkle formation and repairs skin moisture in UVB-irradiated hairless mice. *Nutrients*, *11*(10), 2354.

Nadanaka, S., Clement, A., Masayama, K., Faissner, A., Sugahara, K. (1998). Characteristic hexasaccharide sequences in octasaccharides derived from shark cartilage chondroitin sulfate D with a neurite outgrowth promoting activity. *Journal of Biological Chemistry*, *273*(6), 3296–3307.

Nairn, A. V., Aoki, K., dela Rosa, M., Porterfield, M., Lim, J. M., Kulik, M., Pierce, J. M., Wells, L., Dalton, S., Tiemeyer, M., Moremen, K. W. (2012). Regulation of glycan structures in murine embryonic stem cells: Combined transcript profiling of glycan-related genes and glycan structural analysis. *Journal of Biological Chemistry*, *287*(45), 37835-37856.

Nairn, A. V., Kinoshita-Toyoda, A., Toyoda, H., Xie, J., Harris, K., Dalton, S., Kulik, M., Pierce, J. M., Toida, T., Moremen, K. W., Linhardt, R. J. (2007). Glycomics of proteoglycan biosynthesis in murine embryonic stem cell differentiation. *Journal of Proteome Research*, *6*(11), 4374–4387.

Négrel, R., Grimaldi, P., Ailhaud, G. (1978). Establishment of preadipocyte clonal line from epididymal fat pad of ob/ob mouse that responds to insulin and to lipolytic hormones. *Proceedings of the National Academy of Sciences of the United States of America*, *75*(12), 6054–6058.

Nishitani, K., Hayakawa, K., Tanaka, S. (2019). Extracellular glucose levels in cultures of undifferentiated mouse trophoblast stem cells affect gene expression during subsequent differentiation with replicable cell line-dependent variation. *The Journal of Reproduction and Development*, *65*(1), 19–27.

Novoa-Carballal, R., Pérez-Martín, R., Blanco, M., Sotelo, C. G., Fassini, D., Nunes, C., Coimbra, M. A., Silva, T. H., Reis, R. L., Vázquez, J. A. (2017). By-products of *Scyliorhinus canicula*, *Prionace glauca* and *Raja clavata*: a valuable source of predominantly 6S sulfated chondroitin sulfate. *Carbohydrate Polymers*, *157*, 31–37.

O'Driscoll, L., Gammell, P., McKiernan, E., Ryan, E., Jeppesen, P. B., Rani, S., Clynes, M. (2006). Phenotypic and global gene expression profile changes between low passage and high passage MIN-6 cells. *The Journal of Endocrinology*, *191*(3), 665–676.

Ogawa, H., Hatano, S., Sugiura, N., Nagai, N., Sato, T., Shimizu, K., Kimata, K., Narimatsu, H., Watanabe, H. (2012). Chondroitin sulfate synthase-2 is necessary for chain extension of chondroitin sulfate but not critical for skeletal development. *PLoS One*, *7*(8) e43806.

Ogura, C., Hirano, K., Mizumoto, S., Yamada, S., Nishihara, S. (2021). Dermatan sulphate promotes neuronal differentiation in mouse and human stem cells. *Journal of Biochemistry*, *169*(1), 55–64.

Ohtake, S., Kimata, K., Habuchi, O. (2003). A unique nonreducing terminal modification of chondroitin sulfate by *N*-acetylgalactosamine 4-sulfate 6-*O*-sulfotransferase. *Journal of Biological Chemistry*, *278*(40), 38443–38452.

Okazaki, J., Kamada, A., Gonda, Y., Sakaki, T. (1992). Analysis of chondroitin sulfate isomers in the periodontium of the monkey using high-performance liquid chromatography. *Journal of Periodontal Research*, *27*(5), 484–488.

Pacheco, B., Malmström, A., Maccarana, M. (2009a). Two dermatan sulfate epimerases form iduronic acid domains in dermatan sulfate. *Journal of Biological Chemistry*, *284*(15), 9788–9795.

Pacheco, B., Maccarana, M., Malmström, A. (2009b). Dermatan 4-*O*-sulfotransferase 1 is pivotal in the formation of iduronic acid blocks in dermatan sulfate. *Glycobiology*,

19(11), 1197–1203.

Pairault, J., Green, H. (1979). A study of the adipose conversion of suspended 3T3 cells by using glycerophosphate dehydrogenase as differentiation marker. *Proceedings of the National Academy of Sciences of the United States of America, 76*, 5138–5142.

Pfaffl, M. W., Tichopad, A., Prgomet, C., Neuvians, T. P. (2004). Determination of stable housekeeping genes, differentially regulated target genes and sample integrity: BestKeeper--Excel-based tool using pair-wise correlations. *Biotechnology Letters*, *26*(6), 509–515.

Puri, S., Coulson-Thomas, Y. M., Gesteira, T. F., Coulson-Thomas, V. J. (2020). Distribution and function of glycosaminoglycans and proteoglycans in the development, homeostasis and pathology of the ocular surface. *Frontiers in Cell and Developmental Biology*, *8*, 731.

Rauschner, M., Lange, L., Hüsing, T., Reime, S., Nolze, A., Maschek, M., Thews, O., Riemann, A. (2021). Impact of the acidic environment on gene expression and functional parameters of tumors in vitro and in vivo. *Journal of Experimental & Clinical Cancer Research*, *40*(1), 10.

Reiss, M., Maniglia, C. A., Sartorelli, A. C. (1985). Reversible effects of retinoic acid on glycosaminoglycan synthesis during differentiation of HL-60 leukemia cells. *Cancer Research*, *45*(5), 2092–2097.

Rosen, E. D., Hsu, C. H., Wang, X., Sakai, S., Freeman, M. W., Gonzalez, F. J., Spiegelman, B. M. (2002). C/EBPalpha induces adipogenesis through PPARgamma: a unified pathway. *Genes & Development*, *16*(1), 22–26.

Rosen, E. D., MacDougald, O. A. (2006). Adipocyte differentiation from the inside out. *Nature Reviews Molecular Cell Biology*, *7*(12), 885–896.

Sarma, S., Sockalingam, S., Dash, S. (2021). Obesity as a multisystem disease: Trends in

obesity rates and obesity-related complications. *Diabetes, Obesity & Metabolism*, *23*(S1), 3–16.

Sato, T., Gotoh, M., Kiyohara, K., Akashima, T., Iwasaki, H., Kameyama, A., Mochizuki, H., Yada, T., Inaba, N., Togayachi, A., Kudo, T., Asada, M., Watanabe, H., Imamura, T., Kimata, K., Narimatsu, H. (2003). Differential roles of two *N*-acetylgalactosaminyltransferases, CSGalNAcT-1, and a novel enzyme, CSGalNAcT-2. Initiation and elongation in synthesis of chondroitin sulfate. *Journal of Biological Chemistry*, *278*(5), 3063–3071.

Sato, Y., Nakanishi, K., Tokita, Y., Kakizawa, H., Ida, M., Maeda, H., Matsui, F., Aono, S., Saito, A., Kuroda, Y., Hayakawa, M., Kojima, S., Oohira, A. (2008). A highly sulfated chondroitin sulfate preparation, CS-E, prevents excitatory amino acid-induced neuronal cell death. *Journal of Neurochemistry*, *104*(6), 1565–1576.

Schiraldi, C., Cimini, D., De Rosa, M. (2010). Production of chondroitin sulfate and chondroitin. *Applied Microbiology and Biotechnology*, *87*(4), 1209–1220.

Schneider, C., Rasband, W., Eliceiri, K. (2012). NIH Image to ImageJ: 25 years of image analysis. *Nature Methods, 9*, 671–675.

Schreiber, I., Dörpholz, G., Ott, C. E., Kragesteen, B., Schanze, N., Lee, C. T., Köhrle, J., Mundlos, S., Ruschke, K., Knaus, P. (2017). BMPs as new insulin sensitizers: enhanced glucose uptake in mature 3T3-L1 adipocytes via PPARγ and GLUT4 upregulation. *Scientific Reports*, *7*(1), 17192.

Shida, M., Mikami, T., Tamura, J. I., Kitagawa, H. (2019). Chondroitin sulfate-D promotes neurite outgrowth by acting as an extracellular ligand for neuronal integrin αVβ3. *Biochimica et Biophysica Acta General subjects*, *1863*(9), 1319–1331.

Silver, N., Best, S., Jiang, J., Thein, S. L. (2006). Selection of housekeeping genes for gene expression studies in human reticulocytes using real-time PCR. *BMC Molecular*

Biology, *7*, 33.

Sirko, S., Von Holst, A., Wizenmann, A., Götz, M., Faissner, A. (2007). Chondroitin sulfate glycosaminoglycans control proliferation, radial glia cell differentiation and neurogenesis in neural stem/progenitor cells. *Development*, *134*(15), 2727–2738.

Smith, C. J., Osborn, A. M. (2009). Advantages and limitations of quantitative PCR (Q-PCR)-based approaches in microbial ecology. *FEMS Microbiology Ecology*, *67*(1), 6–20.

Stachtea, X. N., Tykesson, E., Van Kuppevelt, T. H., Feinstein, R., Malmström, A., Reijmers, R. M., Maccarana, M. (2015). Dermatan sulfate-free mice display embryological defects and are neonatal lethal despite normal lymphoid and non-lymphoid organogenesis. *PLoS One*, *10*(10), e0140279.

Sugahara, K., Mikami, T. (2007). Chondroitin/dermatan sulfate in the central nervous system. *Current Opinion in Structural Biology*, *17*(5), 536–545.

Sugiura, N., Shioiri, T., Chiba, M., Sato, T., Narimatsu, H., Kimata, K., Watanabe, H. (2012). Construction of a chondroitin sulfate library with defined structures and analysis of molecular interactions. *Journal of Biological Chemistry*, *287*(52), 43390–43400.

Sundaresan, G., Abraham, R. J. J., Appa Rao, V., Narendra Babu, R., Govind, V., Meti, M. F. (2018). Established method of chondroitin sulphate extraction from buffalo (*Bubalus bubalis*) cartilages and its identification by FTIR. *Journal of Food Science and Technology*, *55*(9), 3439–3445.

Suzuki, Y., Kerever, A., Tanaka, T., Higashi, K., Arikawa-Hirasawa, E. (2019). The structural and compositional changes of chondroitin sulfate chains in the aged mouse hippocampus. *Juntendo Medical Journal*, *65*(1), 64–70.

Svingen, T., Letting, H., Hadrup, N., Hass, U., Vinggaard, A. M. (2015). Selection of reference genes for quantitative RT-PCR (RT-qPCR) analysis of rat tissues under

physiological and toxicological conditions. *PeerJ*, *3*, e855.

Takeda-Okuda, N., Mizumoto, S., Zhang, Z., Kim, S. K., Lee, C. H., Jeon, B. T., Hosaka, Y. Z., Kadomatsu, K., Yamada, S., Tamura, J. I. (2019). Compositional analysis of the glycosaminoglycan family in velvet antlers of sika deer (*Cervus nippon*) at different growing stages. *Glycoconjugate Journal*, *36*(2), 127–139.

Takeda, N., Horai, S., Tamura, J. I. (2016). Facile analysis of contents and compositions of the chondroitin sulfate/dermatan sulfate hybrid chain in shark and ray tissues. *Carbohydrate Research*, *424*, 54–58.

Tang, Q. Q., Lane, M. D. (2012). Adipogenesis: from stem cell to adipocyte. *Annual Review of Biochemistry*, *81*, 715–736.

Taylor, S. M., Jones, P. A. (1979). Multiple new phenotypes induced in 10T1/2 and 3T3 cells treated with 5-azacytidine. *Cell*, *17*(4):771–779.

Taylor, S., Wakem, M., Dijkman, G., Alsarraj, M., Nguyen, M. (2010). A practical approach to RT-qPCR-Publishing data that conform to the MIQE guidelines. *Methods*, *50*(4), S1–S5.

Thellin, O., Zorzi, W., Lakaye, B., De Borman, B., Coumans, B., Hennen, G., Grisar, T., Igout, A., Heinen, E. (1999). Housekeeping genes as internal standards: use and limits. *Journal of Biotechnology*, *75*(2-3), 291–295.

Toledo, O. M. S., Dietrich, C. P. (1977). Tissue specific distribution of sulfated mucopolysaccharides in mammals. *Biochimica et Biophysica Acta (BBA) - General Subjects*, *498*(1), 114–122.

Tontonoz, P., Hu, E., Graves, R. A., Budavari, A. I., Spiegelman, B. M. (1994). mPPAR gamma 2: tissue-specific regulator of an adipocyte enhancer. *Genes & Development*, *8*(10), 1224–1234.

Torres, M., Zúñiga, R., Gutierrez, M., Vergara, M., Collazo, N., Reyes, J., Berrios, J.,

Aguillon, J. C., Molina, M. C., Altamirano, C. (2018). Mild hypothermia upregulates myc and xbp1s expression and improves anti-TNFα production in CHO cells. *PloS One*, *13*(3), e0194510.

Uyama, T., Kitagawa, H., Tanaka, J., Tamura, J. I., Ogawa, T., Sugahara, K. (2003). Molecular cloning and expression of a second chondroitin *N*-acetylgalactosaminyltransferase involved in the initiation and elongation of chondroitin/dermatan sulfate. *Journal of Biological Chemistry*, *278*(5), 3072–3078.

Valcarcel, J., Novoa-Carballal, R., Pérez-Martín, R. I., Reis, R. L., Vázquez, J. A. (2017). Glycosaminoglycans from marine sources as therapeutic agents. *Biotechnology Advances*, *35*(6), 711–725.

Vandesompele, J., De Preter, K., Pattyn, F., Poppe, B., Van Roy, N., De Paepe, A., Speleman, F. (2002). Accurate normalization of real-time quantitative RT-PCR data by geometric averaging of multiple internal control genes. *Genome Biology*, *3*(7), research0034.1.

Vasan, N. S., Saporito, R. A., Jr, Saraswathi, S., Tesoriero, J. V., Manley, S. (1983). Alterations of renal cortex and medullary glycosaminoglycans in aging dog kidney. *Biochimica et Biophysica Acta (BBA) - General Subjects*, *760*(2), 197–205.

Vergara, M., Becerra, S., Berrios, J., Osses, N., Reyes, J., Rodríguez-Moyá, M., Gonzalez, R., Altamirano, C. (2014). Differential effect of culture temperature and specific growth rate on CHO cell behavior in chemostat culture. *PloS One*, *9*(4), e93865.

Volpi, N. (2004). Disaccharide mapping of chondroitin sulfate of different origins by high-performance capillary electrophoresis and high-performance liquid chromatography. *Carbohydrate Polymers*, *55*(3), 273–281.

Volpi, N. (2019). Chondroitin Sulfate Safety and Quality. *Molecules (Basel, Switzerland)*, *24*(8), 1447.

Volpi, N., Bolognani, L., Conte, A., Petrini, M. (1993). Effects of chondroitin sulfates with

different structures on leukemia cells: U-937 cell proliferation and differentiation. *Leukemia Research*, *17*(9), 789–798.

Voss, G., Ceder, Y. (2023). Two-tailed RT-qPCR for the quantification of A-to-I-edited microRNA isoforms. *Current Protocols*, *3*(1), e645.

Willis, C. M., Klüppel, M. (2014). Chondroitin sulfate-E is a negative regulator of a pro-tumorigenic Wnt/beta-catenin-Collagen 1 axis in breast cancer cells. *PloS One*, *9*(8), e103966.

Wolins, N. E., Quaynor, B. K., Skinner, J. R., Tzekov, A., Park, C., Choi, K., Bickel, P. E. (2006). OP9 mouse stromal cells rapidly differentiate into adipocytes: characterization of a useful new model of adipogenesis. *Journal of Lipid Research*, *47*(2), 450–460.

Wu, Z., Rosen, E. D., Brun, R., Hauser, S., Adelmant, G., Troy, A. E., McKeon, C., Darlington, G. J., Spiegelman, B. M. (1999). Cross-regulation of C/EBP alpha and PPAR gamma controls the transcriptional pathway of adipogenesis and insulin sensitivity. *Molecular Cell*, *3*(2), 151–158.

Xie, F., Xiao, P., Chen, D., Xu, L., Zhang, B. (2012). miRDeepFinder: a miRNA analysis tool for deep sequencing of plant small RNAs. *Plant Molecular Biology*, *80*, 75–84.

Xu, H., Wang, J., Zhang, X., Li, Z., Wang, Y., Xue, C. (2015). Inhibitory effect of fucosylated chondroitin sulfate from the sea cucumber *Acaudina molpadioides* on adipogenesis is dependent on Wnt/β-catenin pathway. *Journal of Bioscience and Bioengineering*, *119*(1), 85–91.

Yada, T., Sato, T., Kaseyama, H., Gotoh, M., Iwasaki, H., Kikuchi, N., Kwon, Y. D., Togayachi, A., Kudo, T., Watanabe, H., Narimatsu, H., Kimata, K. (2003). Chondroitin sulfate synthase-3: Molecular cloning and characterization. *Journal of Biological Chemistry*, *278*(41), 39711–39725.

Yamada, S., Mizumoto, S. (2022). Characterization of hyaluronidase 4 involved in the

catabolism of chondroitin sulfate. *Molecules*, *27*(18), 6103.

Yamada, S., Sugahara, K. (2008). Potential therapeutic application of chondroitin sulfate/dermatan sulfate. *Current Drug Discovery Technologies*, *5*(4), 289–301.

Yamada, S., Sugahara, K., Özbek, S. (2011). Evolution of glycosaminoglycans: comparative biochemical study. *Communicative & Integrative Biology*, *4*(2), 150–158.

Yang, Q., Doshi, U., Li, N., Li, A. P. (2012). Effects of culture duration on gene expression of P450 isoforms, uptake and efflux transporters in primary hepatocytes cultured in the absence and presence of interleukin-6: implications for experimental design for the evaluation of downregulatory effects of biotherapeutics. *Current Drug Metabolism*, *13*(7), 938–946.

Yang, S., Gigout, S., Molinaro, A., Naito-Matsui, Y., Hilton, S., Foscarin, S., Nieuwenhuis, B., Tan, C. L., Verhaagen, J., Pizzorusso, T., Saksida, L. M., Bussey, T. M., Kitagawa, H., Kwok, J. C. F., Fawcett, J. W. (2021). Chondroitin 6-sulphate is required for neuroplasticity and memory in ageing. *Molecular Psychiatry*, *26*(10), 5658–5668.

Yoshida, K., Miyauchi, S., Kikuchi, H., Tawada, A., Tokuyasu, K. (1989). Analysis of unsaturated disaccharides from glycosaminoglycuronan by high-performance liquid chromatography. *Analytical Biochemistry*, *177*(2), 327–332.

Yoshizawa, T., Mizumoto, S., Takahashi, Y., Shimada, S., Sugahara, K., Nakayama, J., Takeda, S., Nomura, Y., Nitahara-Kasahara, Y., Okada, T., Matsumoto, K., Yamada, S., Kosho, T. (2018). Vascular abnormalities in the placenta of *Chst14*$^{-/-}$ fetuses: Implications in the pathophysiology of perinatal lethality of the murine model and vascular lesions in human CHST14/D4ST1 deficiency. *Glycobiology*, *28*(2), 80–89.

Zeigerer, A., Rodeheffer, M. S., McGraw, T. E., Friedman, J. M. (2008). Insulin regulates leptin secretion from 3T3-L1 adipocytes by a PI 3 kinase independent mechanism. *Experimental Cell Research*, *314*(11–12), 2249–2256.

Zhang, J., Fu, M., Cui, T., Xiong, C., Xu, K., Zhong, W., Xiao, Y., Floyd, D., Liang, J., Li, E., Song, Q., Chen, Y. E. (2004). Selective disruption of PPARgamma 2 impairs the development of adipose tissue and insulin sensitivity. *Proceedings of the National Academy of Sciences of the United States of America*, *101*(29), 10703–10708.

Zhang, J., Tang, H., Zhang, Y., Deng, R., Shao, L., Liu, Y., Li, F., Wang, X., Zhou, L. (2014). Identification of suitable reference genes for quantitative RT-PCR during 3T3-L1 adipocyte differentiation. *International Journal of Molecular Medicine*, *33*(5), 1209–1218.

Zhang, X., Liu, H., Yao, W., Meng, X., Li, Z. (2019). Semisynthesis of chondroitin sulfate oligosaccharides based on the enzymatic degradation of chondroitin. *The Journal of Organic Chemistry*, *84*(11), 7418–7425.

Zhang, Y., Li, D., Sun, B. (2015). Do housekeeping genes exist?. *PloS One*, *10*(5), e0123691.

Zhao, N., Tao, K., Wang, G., Xia, Z. (2019). Global obesity research trends during 1999 to 2017: A bibliometric analysis. *Medicine*, *98*(4), e14132.

Zizola, C. F., Julianelli, V., Bertolesi, G., Yanagishita, M., Calvo, J. C. (2007). Role of versican and hyaluronan in the differentiation of 3T3-L1 cells into preadipocytes and mature adipocytes. *Matrix Biology*, *26*(6), 419–430.